Chapter 4
Analysis and Modelling for Seismic Design or Assessment of Concrete Buildings

As pointed out in the Preamble, analysis carried out within the framework of seismic design or assessment determines by calculation the effects of the design actions (including the seismic action) in terms of internal forces and deformations, for the purpose of dimensioning or assessing structural members. For concrete members, design action effects are used to verify the sizes of members and to dimension or assess the amount of reinforcement.

Chapter 4 does not pretend to be a treatise on seismic analysis methods. Its scope is limited to the essentials for the application of well-established analysis methods in the design or assessment of buildings for earthquake resistance according to current generation seismic codes. The reader is supposed to be fairly conversant with the fundamentals of Structural Dynamics and their application for the seismic analysis of buildings.

As in Chapters 1 and 2, emphasis is placed on the portfolio of seismic analysis methods provided in Parts 1 and 3 of EN-Eurocode 8 and their scope of applicability. Special attention is paid to nonlinear seismic response analysis and to practical modelling of concrete members and buildings for its purposes. Examples of nonlinear modelling of concrete members and buildings and nonlinear dynamic analysis are presented.

4.1 Scope of Analysis in Codified Seismic Design or Assessment

4.1.1 Analysis for the Purposes of Seismic Design

As pointed out in Section 1.2 and elsewhere in Chapter 1, seismic design of new buildings according to current codes is force-based. Its prime workhorse is linear-elastic analysis, based on the 5%-damped elastic spectrum divided by a factor that accounts mainly for ductility and energy dissipation capacity, but also for overstrength (see Section 4.2.2). In Europe this factor is denoted by q and called "behaviour factor". In North America it is termed "Force reduction factor" or "Response modification factor" and denoted by R.

M.N. Fardis, *Seismic Design, Assessment and Retrofitting of Concrete Buildings*, Geotechnical, Geological, and Earthquake Engineering 8, DOI 10.1007/978-1-4020-9842-0_4,

Most current generation codes for the seismic design of new buildings include two alternative methods of linear-elastic seismic analysis:

(a) Linear static analysis, termed "lateral force" method of analysis in Eurocode 8 (CEN 2004a) and in certain US codes (SEAOC 1999), or "equivalent lateral force" procedure in other US codes (BSSC 2003), but known also in practice as "equivalent static" analysis.
(b) Modal response spectrum analysis, as called in Eurocode 8 (CEN 2004a); US codes use the term "response spectrum" procedure (BSSC 2003) or "dynamic lateral force" (SEAOC 1999) procedure.

Differences between codes are not limited to terminology but extend to the general attitude towards the method of analysis. Most codes allow application of the "modal response spectrum" analysis for the design of all new buildings and make it mandatory for new buildings that are irregular in elevation, or tall and/or flexible (i.e., in which higher modes are important). Only Eurocode 8 adopts it as the reference method for the design of new buildings and fully respects its rules and results. US codes essentially consider the linear static ("equivalent lateral force") procedure as the reference method and adapt the results and rules of application of "modal" analysis to conform to it. Their reasoning is that linear analysis is of limited relevance and value in the framework of seismic design, as its results apply only for ground motions less than a small fraction ($1/q$ or $1/R$) of the design seismic action. It makes little sense therefore, according to that point of view, to apply a sophisticated, complex and computationally demanding analysis method, liable to misuse, misinterpretation or errors due to lack of experience and expertise. It makes more sense, instead, to select the structural layout so that the structure lies well within the scope of the time-tested and almost fool-proof linear static analysis procedure.

This concept of the role of analysis is reflected in the common view that the value of the "modal response spectrum" procedure is limited:

1. to furnishing a heightwise pattern of lateral inertia forces in buildings with heightwise irregular geometry, mass, stiffness or strength, or dominated by higher modes which is more representative of the expected dynamic response; and
2. to better accounting for the coupling of torsional and translational vibrations in buildings with strong irregularity in plan.

Consistent with point (1) above, some codes with this attitude suggest applying "modal response spectrum" analysis not directly (i.e., computing modal contributions to the seismic action effects from the mode shapes themselves and combining them according to the appropriate rules, see Section 4.4.3), but indirectly: by deriving storey modal lateral forces through modal analysis, applying them as static lateral loads and computing via linear static analysis the modal seismic action effects of interest. Moreover, in SEAOC (1999) all modal lateral forces are scaled

up so that their resultant (the base shear) matches fully the value computed from the design spectrum at the fundamental period, if the building is irregular, or 90% of that value, if it is regular. In BSSC (2003) scaling of these modal lateral forces aims at matching 85% of the base shear obtained from the design spectrum at a period of 1.4 to 1.7 times an empirical period estimate, depending on the magnitude of the design ground acceleration.

If both the lateral force method and modal response spectrum analysis are applicable to the design of a given new building, modal response spectrum analysis gives on average a slightly more even distribution of peak internal forces at different critical sections (e.g. at the two ends of the same beam or column), translated to some material savings. If its results are used for member dimensioning, the overall inelastic performance of the structure would be expected to be better, as peak inelastic deformations normally agree better with its predictions than to those of linear static analysis (see Section 4.11.2).

As its use is not subject to any constraints of applicability, the modal response spectrum method can be adopted as the single analysis tool for seismic design of new buildings in 3D, provided that the designer masters the method. It is more sound (e.g., unlike the linear static method, its results for concurrent application of the two horizontal seismic action components are independent of the choice of the directions, X and Y, of these components) and offers a better overall balance of safety and economy. Its predictions for displacements and deformations are closer to those of a nonlinear dynamic analysis (see Section 4.11.2), while, for the same column or beam shears it gives a more even balance of column or beam seismic moments on opposite faces of joints, which are anyway covered by the same longitudinal reinforcement. So, with today's availability of reliable and efficient computer programs for modal response spectrum analysis in 3D, and the establishment of Structural Dynamics as a main subject in structural engineering curricula in seismic regions, it is expected that the application of modal response spectrum analysis for the design of new buildings will grow and prevail in the long run. Even then, though, the intuitively appealing, practical and conceptually simple lateral force method is expected to stay in codes as an option for the seismic design of new buildings.

In the framework of Part 1 of Eurocode 8 (CEN 2004a):

i. nonlinear static analysis (commonly known as "pushover" analysis), and
ii. nonlinear dynamic (time-history or response-history) analysis.

have a certain role for the design of new buildings. This role is limited to:

- detailed evaluation of the expected seismic performance of a building that has been designed using linear analysis (including confirmation of the intended plastic mechanism and of the distribution and extent of damage);
- the design of buildings with seismic isolation, for which nonlinear analysis is the reference method and linear analysis is allowed only under certain very restrictive conditions.

Specifically for the nonlinear static method of analysis, Part 1 of Eurocode 8 (CEN 2004a) defines two additional possible uses in the framework of the design of new buildings:

- To verify or revise the value of the factor α_u/α_1 incorporated in the basic or reference value of the behaviour factor, q_o, of concrete etc. buildings, to account for overstrength due to redundancy of the structural system (see Section 1.4.3.1 and Fig. 1.12).
- To design buildings on the basis of a nonlinear static analysis followed by deformation-based verification of its ductile members, in lieu of force-based design with linear elastic analysis and a design spectrum incorporating the behaviour factor q. The use of "pushover" analysis for the direct design of new buildings is a novelty of Part 1 of Eurocode 8 without precedent in codified seismic design.

Internal forces for dimensioning are taken equal to those estimated from the linear analysis for the design response spectrum (i.e. the 5%-damped elastic spectrum divided by the behaviour factor q). Consistent with the equal displacement rule and the concept and use of the behaviour factor, displacements due to the seismic action are taken in Part 1 of Eurocode 8 as equal to those derived from the linear analysis times the behaviour factor q. By contrast, when nonlinear analysis is used, all seismic action effects (internal forces, displacements and deformations) are those derived from the nonlinear analysis.

4.1.2 Analysis for Seismic Assessment and Retrofitting

Unlike seismic design of new buildings, which is still (mainly) force-based, seismic assessment or retrofitting of existing ones is nowadays fully displacement-based. The underlying reason is practical: Force-based approaches entail capacity-demand comparisons in terms of internal forces, with seismic internal force demands computed from a design response spectrum incorporating a global behaviour or force reduction factor, q or R. Values of this factor given in seismic design codes for new buildings go hand-in-hand with a corresponding set of prescriptive rules or restrictions (on structural layout, member detailing, capacity design, etc.). For an existing building to be entitled a q-factor larger than the value attributed to overstrength alone ($q = 1.5$ in Eurocode 8), the structure as a whole, as well as every single member considered to contribute to earthquake resistance (a "primary seismic" one, in Eurocode 8 terminology, see Section 4.12) should meet all the rules pertaining to one of the discrete ductility classes for which (higher) values of q are given in the code for new buildings (e.g., in Eurocode 8 for at least DC Medium). As the building most likely violates these rules in one way or another, it will be assigned at the end the value of the q-factor attributed to overstrength alone. In all likelihood, the force capacity of some members considered to contribute to earthquake resistance

will be less than the force demand resulting from such a low q-factor value. In this way any old concrete building, possibly except low-rise ones with large walls, will be assessed as seismically inadequate and will need retrofitting. Moreover, if it is decided to retrofit the building and the designer wants to use the (higher) q value of one of the discrete ductility classes in a code for new buildings, every single member considered to contribute to earthquake resistance should be retrofitted to meet all detailing, capacity design, etc. rules of that ductility class. This may increase the cost of retrofitting so much, that demolition or the "do-nothing" alternative may be the most likely outcome.

The only way out of the predicament created by the prescriptive rules of current force-based seismic design codes for new buildings, is to abandon the concept of a global q-factor that reduces the overall elastic seismic forces. Instead, each member should be assessed and retrofitted individually, on the basis of its own capacity determined by its own features and peculiarities. The capacity which is important for a member's seismic performance (including failure) is not its force-, but its deformation-capacity. One should keep in mind that, unlike gravity or wind actions, the seismic action is not a set of given forces to be resisted by the structure, but a given dynamic displacement or energy input to be accommodated. Therefore structural displacements and their derivatives, i.e., member deformations, should be the basis of seismic assessment, instead of forces. After all, structures collapse not because of the seismic lateral loads per se, but owing to gravity loads acting through the lateral displacements induced by the earthquake (P-Δ effects).

The prime objective of an analysis for the purposes of displacement-based seismic assessment or retrofitting is the calculation of deformation demands in structural members. Codes or standards that have recently emerged for (displacement-based) seismic assessment and retrofitting of buildings (ASCE 2007, CEN 2005a) provide to this end the full menu of analysis options mentioned in Section 4.1.1:

- the two linear-elastic options: (a) linear static analysis and (b) modal response spectrum analysis, and
- the two nonlinear ones: (i) nonlinear static or "pushover" analysis and (ii) nonlinear dynamic analysis.

Unlike linear analysis carried out for design purposes, which uses the design response spectrum, incorporating the behaviour factor q, linear analysis for displacement-based assessment and retrofitting employs the 5%-damped elastic response spectrum. Member inelastic deformation demands (e.g., chord-rotations) may be derived directly from such an analysis, essentially employing the equal-displacement rule at the member level. Of course, this simplification can be made only when the estimated chord-rotation ductility demands meet certain fairly restrictive conditions. In ASCE (2007) these conditions comprise upper limits on the absolute magnitude of these demands, as well as on their difference between storeys or at opposite sides of the building. By contrast, in CEN (2005a) only non-uniformity of the chord-rotation ductility ratio demands throughout the building restricts the

application of linear analysis for the estimation of member inelastic deformation demands. If the applicability conditions of linear-elastic analysis are not met, one should resort to nonlinear analysis. So, nonlinear analysis, being always applicable, is the reference method for displacement-based seismic assessment and retrofitting. Note that in seismic assessment all information necessary for the calculation of the yield moment, the secant stiffness to the yield-point, and all other member properties needed as input to nonlinear analysis, is readily available. In design of new structures, by contrast, the reinforcement is not known a-priori and (several) cycles of design-analysis iterations are needed, at the expense of design effort and convenience.

To be assessed on the basis of inelastic deformations, members (or, in general, mechanisms of behaviour) should have a minimum of ductility. As brittle mechanisms of behaviour, such as shear in concrete members, exhibit practically no ductility, they are more conveniently and reliably assessed on the basis of forces. Linear-elastic analysis is of no use for the estimation of internal force demands in the inelastic regime, even when its applicability conditions for the estimation of member inelastic deformation demands are met. When these conditions are met and member inelastic deformation demands are indeed estimated for simplicity from linear analysis, one has to resort to other means (notably, to capacity design calculations) to establish the internal force demands on members entering in the inelastic range.

4.2 The Seismic Action for the Analysis

4.2.1 Elastic Spectra

4.2.1.1 Elastic Response Spectra and Peak Ground Accelerations

The most common representation of the seismic action in codes is through the response spectrum of an elastic Single-Degree-of-Freedom (SDOF) oscillator with 5% viscous damping ratio. Any other alternative representation of the seismic action (e.g. in the form of acceleration time-histories) should conform to the 5%-damped elastic response spectrum.

Because:

- earthquake ground motions are traditionally recorded as acceleration time-histories, and
- seismic design is still based on forces, conveniently derived from accelerations,

the pseudo-acceleration response spectrum, $S_a(T)$, is normally used. If spectral displacements, $S_d(T)$, are of interest (notably for displacement-based assessment or design), they can be obtained from $S_a(T)$ assuming simple harmonic oscillation: $S_d(T) = (T/2\pi)^2 S_a(T)$. Spectral pseudo-velocities can also be obtained from $S_a(T)$ as $S_v(T) = (T/2\pi)S_a(T)$. Note that pseudo-values do not correspond to the real peak

spectral velocity or acceleration. For damping ratio up to 10% and for natural period T between 0.2 and 1.0 s, the pseudo-velocity spectrum closely approximates the actual relative velocity spectrum.

The Eurocode 8 spectra include ranges of:

- constant spectral pseudo-acceleration for natural periods between T_B and T_C;
- constant spectral pseudo-velocity between periods T_C and T_D; and
- constant spectral displacement, for periods longer than T_D.

In Eurocode 8 the elastic response spectrum is taken as proportional ("anchored") to the peak acceleration of the ground:

- the horizontal peak acceleration, a_g, for the horizontal component(s) of the seismic action, or
- the vertical peak acceleration, a_{vg}, for the vertical component.

The basis of the seismic design of new structures in Eurocode 8 is the "design seismic action", for which the no-(local-)collapse requirement should be met. It is specified through the "design ground acceleration" in the horizontal direction, a_g, which is equal to the "reference peak ground acceleration" on rock from national zonation maps,[1] times the importance factor, γ_I, of the building (see Section 1.1.1); for ordinary importance, by definition $\gamma_I = 1.0$. The "reference peak ground acceleration" corresponds to the reference return period, T_{NCR}, of the "design seismic action" for structures of ordinary importance.[2] Values of the importance factor greater or shorter than 1.0 correspond to mean return periods longer or shorter, respectively, than T_{NCR}. It is in the authority of each country to select the value of T_{NCR} that gives the appropriate trade-off between economy and public safety in its territory, as well as the importance factors for building other than ordinary, taking into account the specific regional features of the seismic hazard. Part 1 of Eurocode 8 (CEN 2004a) recommends the value T_{NCR}.= 475 years.

Eurocode 8 adopts the same spectral shape for the different seismic actions to be used for different performance levels or Limit States. The difference in the hazard level is reflected only through the peak ground acceleration to which the spectrum is anchored. Recall from Section 1.1.3 that Part 1 of Eurocode 8 recommends for the "damage limitation seismic action" of new buildings one having probability 10% of being exceeded in 10 years (i.e., mean return period: 95 years). Recall

[1] Data from Europe available at the time of drafting Eurocode 8 could not support dependence of the elastic spectrum on additional parameters.

[2] Under the Poisson assumption of earthquake occurrence (i.e. that the number of earthquakes in an interval of time depends only on the length of the interval in a time-invariant way), the return period, T_R, of seismic events exceeding a certain threshold is related to the probability this threshold will be exceeded, P, in T_L years as: $T_R = -T_L/\ln(1-P)$. So, for given T_L (e.g., the conventional design life of $T_L = 50$ years) the seismic action may equivalently be specified either via its mean return period, T_R, or its probability of exceedance in T_L years, P_R.

also from Section 1.1.3 that Part 3 of Eurocode 8 does not make a recommendation to countries or owners/designers for the hazard levels associated with the three "Limit States" ("Damage Limitation", "Significant Damage" and "Near Collapse") in performance-based seismic assessment and retrofitting.

The mean return period, $T_R(a_g)$, of a peak ground acceleration exceeding a value a_g is the inverse of the annual rate, $\lambda_a(a_g)$, of exceedance of this acceleration level: $T_R(a_g) = 1/\lambda_a(a_g)$. A functional form commonly used for $\lambda_a(a_g)$ is: $\lambda_a(a_g) = K_o(a_g)^{-k}$. If the exponent k (: slope of the "hazard curve" $\lambda_a(a_g)$ in a log-log plot) is about constant, two peak ground acceleration levels a_{g1}, a_{g2}, corresponding to two different mean return periods, $T_R(a_{g1})$, $T_R(a_{g2})$, are related as:

$$\frac{a_{g1}}{a_{g2}} = \left(\frac{T_R(a_{g1})}{T_R(a_{g2})}\right)^{1/k} \tag{4.1}$$

The value of k characterises the seismicity of the site. Regions where the difference in peak ground acceleration of frequent and very rare seismic excitations is very large, have low k values (around 2). For such regions full performance-based design or assessment at several performance levels with widely different hazard levels is very meaningful. Large values of k ($k > 4$) are typical of regions where high ground acceleration levels are almost as frequent as smaller ones. One performance level (normally the one associated with the lowest among the hazard levels) would always govern there; performance-based design or assessment at the other levels may be redundant.

For buildings Eurocode 8 does not have provisions for near-source effects on the seismic action. It provides, though, for topographic amplification (ridge effect, etc.) of the seismic action for all types of structures. Such effects have been identified in past earthquakes in Italy (Faccioli et al. 2002, Paolluci 2002, 2006) and along the Chelidonou ravine during the 1999 Athens earthquake. According to Eurocode 8, topographic amplification is mandatory for structures of importance above ordinary. An Informative Annex in Part 5 of Eurocode 8 (CEN 2004c) recommends amplification factors of the seismic action equal to 1.2 over isolated cliffs or long ridges with slope (to the horizontal) less than 30°, or to 1.4 at ridges steeper than 30°.

4.2.1.2 Elastic Spectra of the Horizontal Components in Eurocode 8

The elastic response spectral acceleration for the horizontal components of the seismic action in Eurocode 8 is described by the following expressions (Fig. 4.1):

$$0 \le T \le T_B \; : S_a(T) = a_g S \left[1 + \frac{T}{T_B}(2.5\eta - 1)\right] \tag{4.2a}$$

Constant spectral pseudo-acceleration range:

$$T_B \le T \le T_C \; : S_a(T) = a_g S \cdot 2.5\eta \tag{4.2b}$$

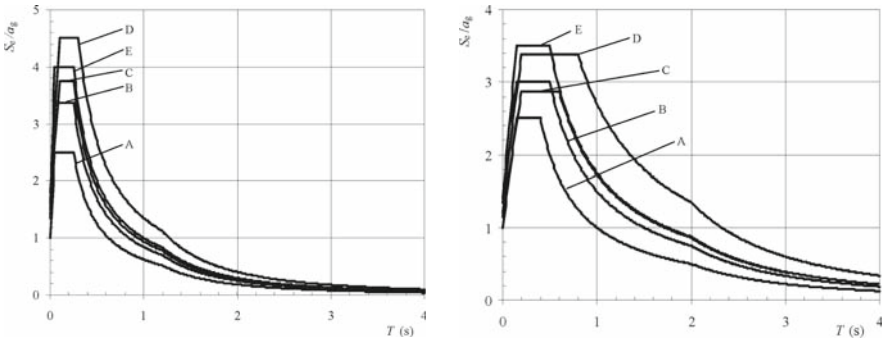

Fig. 4.1 Elastic response spectra of Type 1 (*left*) and 2 (*right*) recommended in EC8, for PGA on rock equal to 1 g and for 5% damping

Constant spectral pseudo-velocity range:

$$T_C \leq T \leq T_D \; : S_a(T) = a_g S \cdot 2.5\eta \left[\frac{T_C}{T} \right] \tag{4.2c}$$

Constant spectral displacement range:

$$T_D \leq T \leq 4 \; sec : S_a(T) = a_g S \cdot 2.5\eta \left[\frac{T_C T_D}{T^2} \right] \tag{4.2d}$$

where:

a_g is the design ground acceleration on rock;
S is the "soil factor";
$\eta = \sqrt{10/(5+\zeta)} \geq 0.55$ is a correction factor for viscous damping ratio, ζ, other than the reference value of 5% (Bommer and Elnashai 1999).

Witness the uniform amplification of the entire spectrum by the "soil factor" S over the spectrum for rock. By definition $S = 1$ over rock. The value $a_g S$ plays the role of "effective ground acceleration", as the spectral acceleration at the constant spectral acceleration plateau is always equal to $2.5 a_g S$.

The values of the periods T_B, T_C and T_D (i.e., the extent of the ranges of constant spectral pseudo-acceleration, pseudo-velocity and displacement) and of the soil factor, S, are taken to depend mainly on "ground type". In the Eurocodes the term ground includes any type of soil and rock. Eurocode 8 recognises five standard ground types, over which it recommends values for T_B, T_C, T_D and S, and two special ones, as listed in Table 4.1. The characterisation of the ground is based on the average value of shear wave velocity, $v_{s,30}$, at the top 30 m:

Table 4.1 Ground types in Eurocode 8 for the definition of the seismic action

	Description	$v_{s,30}$ (m/s)	N_{SPT}	c_u (kPa)
A	Rock outcrop, with less than 5 m cover of weaker material	>800	–	–
B	Very dense sand or gravel, or very stiff clay, several tens of metres deep; mechanical properties gradually increase with depth	360–800	>50	>250
C	Dense to medium-dense sand or gravel, or stiff clay, several tens to many hundreds metres deep	180–360	15–50	70–250
D	Loose-to-medium sand or gravel, or soft-to-firm clay	<180	<15	<70
E	5–20 m surface alluvium layer with $v_s < 360$ m/s underlain by rock (with $v_s > 800$ m/s)			
S_1	≥10 m thick soft clay or silt with plasticity index > 40 and high water content	<100	–	10–20
S_2	Liquefiable soils; sensitive clays; any soil not of type A to E or S_1			

$$v_{s,30} = \frac{30}{\sum_{i=1,N} \frac{h_i}{v_i}} \tag{4.3}$$

where h_i and v_i are the thickness (in m) and the shear wave velocity at small shear strains (less than 10^{-6}) of the i-th layer in N layers. If the value of $v_{s,30}$ is not known, the SPT (Standard Penetration Test) blow-count number may be used for soil types B, C or D, according to the correspondence of SPT to $v_{s,30}$ in Ohta and Goto (1976). If neither the SPT nor $v_{s,30}$ are available, the undrained cohesive resistance (c_u) may used to characterise the soil.

The two special ground types, S1 and S2, deserve carrying out special site-specific studies to define the seismic action. For ground type S1 the special study should take into account the thickness and the v_s-value of the soft clay or silt layer and the difference with the underlying materials and should quantify their effects on the elastic response spectrum. Note that soils of type S1 may have low internal damping and exhibit linear behaviour over a large range of strains, producing peculiar amplification of the bedrock motion and unusual or abnormal soil-structure interaction effects. The scope of the site-specific study should also address the possibility of soil failure under the design seismic action (especially at ground type S2 deposits with liquefiable soils or sensitive clays).

The values of T_B, T_C, T_D and S for the five standard ground types A to E, are meant to be defined by each country in the National Annex to Eurocode 8, depending on the magnitude of earthquakes contributing most to the hazard. The geological conditions at the site may also be taken into account in addition to determine these values. In principle, S factors may be introduced that decrease with increasing spectral value because of the soil nonlinearity effect. Instead of spectral amplification factors that decrease with increasing design acceleration (spectral or ground) as in US codes, e.g., BSSC (2003) and ASCE (2007), the non-binding recommendation of a note in Eurocode 8 is for two types of spectra:

Table 4.2 Recommended parameter values for the standard horizontal elastic response spectra in Eurocode 8 (Fig. 4.1)

Ground type	Spectrum type 1				Spectrum type 2			
	S	T_B (s)	T_C (s)	T_D (s)	S	T_B (s)	T_C (s)	T_D (s)
A	1.00	0.15	0.4	2.0	1.0	0.05	0.25	1.2
B	1.20	0.15	0.5	2.0	1.35	0.05	0.25	1.2
C	1.15	0.20	0.6	2.0	1.50	0.10	0.25	1.2
D	1.35	0.20	0.8	2.0	1.80	0.10	0.30	1.2
E	1.40	0.15	0.5	2.0	1.60	0.05	0.25	1.2

- Type 1: for moderate to large magnitude earthquakes;
- Type 2: for low magnitude ones (e.g. with surface magnitude less than 5.5) at close distance, producing over soft soils motions rich in high frequencies.

The values of T_B, T_C, T_D and S recommended in a non-binding note of Eurocode 8 for the five standard ground types A to E are given in Table 4.2. They are based on Rey et al. (2002) and European strong motion data. There are certain regions in Europe (e.g., where the hazard is contributed mainly by strong, intermediate depth earthquakes, as in the part of the eastern Balkans affected by the Vrancea region) where the two recommended spectral shapes may not be suitable. The lower S-values of Type 1 spectra are due to the larger soil non-linearity in the stronger ground motions produced by moderate to large magnitude earthquakes. The recommended values of the period T_D at the outset of the constant spectral displacement region seems rather low. For flexible structures (e.g., those with seismic isolation) they may not lead to safe-sided designs. A safeguard against the rapid decay of the elastic spectrum for $T > T_D$, is provided by the lower bound of 20% of $a_g S$ recommended in Eurocode 8 for the design spectral accelerations (see Eqs. (4.5c) and (4.5d) in Section 4.2.2).

4.2.1.3 Elastic Spectra of the Vertical Component

The vertical component of the seismic action needs to be taken into account in design only in few very well prescribed situations (see Section 4.5.1). Therefore, the practical importance of the vertical spectrum is limited. Eurocode 8 gives nevertheless a fairly detailed description of the vertical elastic response spectrum:

$$0 \le T \le T_B \; : \; S_{a,vert}(T) = a_{vg}\left[1 + \frac{T}{T_B}(3\eta - 1)\right] \tag{4.4a}$$

$$T_B \le T \le T_C \; : S_{a,vert}(T) = a_{vg} \cdot 3\eta \tag{4.4b}$$

$$T_C \le T \le T_D \; : S_{a,vert}(T) = a_{vg} \cdot 3\eta \left[\frac{T_C}{T}\right] \tag{4.4c}$$

$$T_{\mathrm{D}} \leq T \leq 4\,\mathrm{sec} \; : S_{\mathrm{a,vert}}(T) = a_{\mathrm{vg}} \cdot 3\eta \left[\frac{T_{\mathrm{C}} T_{\mathrm{D}}}{T^2} \right] \tag{4.4d}$$

The main differences between the horizontal and the vertical spectra lie:

- in the value of the amplification factor in the constant spectral pseudo-acceleration plateau, which is 3 instead of 2.5, and
- in the lack of a uniform amplification of the entire spectrum due to the type of soil.

Eurocode 8 recommends in a note the following non-binding values of T_{B}, T_{C}, T_{D} and of the design ground acceleration in the vertical direction, a_{vg}:

- $T_{\mathrm{B}} = 0.05$ s.
- $T_{\mathrm{C}} = 0.15$ s.
- $T_{\mathrm{D}} = 1.0$ s.
- $a_{\mathrm{vg}} = 0.9 a_{\mathrm{g}}$, if the Type 1 spectrum is considered as appropriate for the site;
- $a_{\mathrm{vg}} = 0.45 a_{\mathrm{g}}$, if the Type 2 spectrum is chosen.

The vertical response spectrum recommended in Eurocode 8 is based on work and data specific to Europe (Ambraseys and Simpson 1996, Elnashai and Papazoglou 1997). The ratio $a_{\mathrm{vg}}/a_{\mathrm{g}}$ is known to be higher at short distances (epicentral or to causative fault). However, as distance does not enter as a parameter in the definition of the seismic action in Eurocode 8, the type of spectrum has been chosen as the parameter determining this ratio, on the basis of the finding that $a_{\mathrm{vg}}/a_{\mathrm{g}}$ increases also with Magnitude (Ambraseys and Simpson 1996, Abrahamson and Litehiser 1989), which in turn determines the selection of the type of spectrum.

4.2.2 Design Spectrum for Forced-Based Design with Linear Analysis

For the horizontal components of the seismic action the design spectrum in Eurocode 8 for force-based design of new buildings is:

$$0 \leq T \leq T_B \; : \; S_{a,d}(T) = a_g S \left[\frac{2}{3} + \frac{T}{T_B} \left(\frac{2.5}{q} - \frac{2}{3} \right) \right] \tag{4.5a}$$

$$T_B \leq T \leq T_C \; : \; S_{a,d}(T) = a_g S \frac{2.5}{q} \tag{4.5b}$$

$$T_C \leq T \leq T_D \; : \; S_{a,d}(T) = a_g S \frac{2.5}{q} \left[\frac{T_C}{T} \right], \; S_{a,d}(T) \geq \beta a_g \tag{4.5c}$$

$$T_D \leq T : \; S_{a,d}(T) = a_g S \frac{2.5}{q} \left[\frac{T_C T_D}{T^2} \right], \; S_{a,d}(T) \geq \beta a_g \tag{4.5d}$$

The value 2/3 in Eq. (4.5a) is the inverse of the overstrength factor of 1.5 considered by Eurocode 8 to always be available even without any design measures for ductility and energy dissipation. Factor β in Eqs. (4.5c) and (4.5d) gives a lower bound for the horizontal design spectrum, acting as a safeguard against excessive reduction of the design forces due to flexibility of the system (real or presumed in the design). Its recommended value in Eurocode 8 is 0.2. Its practical implications may be particularly important, in view of the relatively low values recommended by Eurocode 8 for the corner period T_D at the outset of the constant spectral displacement range.

The design spectrum in the vertical direction is obtained by substituting in Eqs. (4.5) the design ground acceleration in the vertical direction, a_{vg}, for the "effective ground acceleration" $a_g S$. There is no clear, well-known energy dissipation mechanism for the response in the vertical direction. So, the "behaviour factor" q in that direction is attributed to overstrength alone and taken equal to 1.5, unless a higher value is supported by special studies and analyses.

4.3 Linear Static Analysis

4.3.1 Fundamentals and Conditions of Applicability

Linear static analysis is carried out under lateral forces applied separately in two orthogonal horizontal directions, X and Y. These forces are meant to simulate the peak inertia loads induced by the horizontal component of the seismic action in these directions, with the structure vibrating in its fundamental mode in the corresponding direction. As designers are familiar and conversant with elastic analysis for static loads (due to gravity or wind actions, etc.), this analysis is the workhorse of practical seismic design.

The fundamental assumptions of the method are:

1. The fundamental translational mode in the direction of the applied lateral forces governs the response.
2. The shape of the fundamental translational mode is known, without solving the eigenvalue problem.

Accordingly, design codes limit the application of this method to buildings with a heightwise distribution of mass and stiffness which is sufficiently regular for assumption 2 to be made with some confidence. Most codes, especially those adopting a standard 1st mode drift pattern independent of the value of the 1st natural period, e.g. (CEN 2004a), do not allow application of the method to tall flexible structures where higher modes dominate the response. Eurocode 8 in particular, allows applying linear static analysis only if both conditions (a) and (b) are met:

(a) The building is regular in elevation, according to the criteria in Section 2.1.7 which can be checked by inspection of the framing and the architectural drawings, without any structural calculations. The rationale for the exclusion of

heightwise irregular buildings is that their 1st mode shape may be far from the simple approximation assumed in linear static analysis. Moreover, higher mode effects may be locally significant (notably, around discontinuities or abrupt changes along the height), even though they may not be important for the global response (e.g., for the base shear and overturning moment).

(b) The fundamental period of the building is not longer than 2 s or four times the corner period T_C between the constant-spectral-pseudoacceleration and constant-spectral-pseudovelocity ranges of the elastic spectrum. Recall that at periods above 2 s or $4T_C$ spectral pseudoaccelerations are low and that, if the 1st mode is in that range, the 2nd and/or 3rd modes may be at, or close to, the range where spectral pseudo-accelerations are constant and highest. So, their contribution to the response may be comparable to that of the 1st mode, notwithstanding their normally lower participation mass and factors.

Conditions (a) and (b) should be met in both horizontal directions for linear static analysis to be applicable, as it is impractical to carry out this analysis in one horizontal direction and modal response spectrum analysis in the orthogonal one.

US codes (BSSC 2003, SEAOC 1999) allow using linear static analysis for low to moderate seismicity and ordinary importance of the building (notably, for "Seismic Design Categories" A to C in BSSC (2003), see Section 1.4.2.2), i.e., irrespective of its structural features. These aspects aside, the counterpart of regularity condition (a) of Eurocode 8 for the application of linear static analysis comprise all of the following:

i. regularity in plan: the maximum storey drift under the design seismic action should not exceed by 20% or more the mean drift of the storey;
ii. vertical regularity of mass: storey mass not exceeding by more than 50% that of an adjacent storey;
iii. vertical regularity of stiffness: storey stiffness not less than 70% of the storey above or 80% of the average stiffness of the three storeys above;
iv. vertical regularity of geometry: plan dimension of lateral-force-resisting system does not exceed by 30% or more the parallel dimension of an adjacent storey.

The counterpart of the Eurocode's flexibility condition (b) above for the applicability of linear static analysis is:

– In BSSC (2003): Fundamental period shorter than 3.5 times the transition period T_C between the constant-spectral-pseudoacceleration and constant-spectral-pseudovelocity ranges.
– In SEAOC (1999): Height less than 240 ft (73 m) for regular buildings meeting all criteria (i)–(iv) above, or less than 65 ft (20 m) or five storeys for irregular ones, according to any of the criteria (i)–(iv) above.

4.3.2 Fundamental Period and Base Shear

Linear static analysis is applied in Eurocode 8 in a way that gives similar results for storey shears – considered as the most important seismic action effect – as modal response spectrum analysis, at least for the type of buildings where both methods are applicable.

The seismic shear above the foundation or the top of a rigid basement ("base shear"), V_b, is determined separately in horizontal directions X and Y, on the basis of the 1st translational mode period, T_1, in the direction of interest:

$$V_b = m_{eff,1} S_{a,d}(T_1) \tag{4.6}$$

where $S_{a,d}(T_1)$ is the value of the design response spectrum from Eqs. (4.5) at the 1st mode and $m_{eff,1}$ is an estimate of the effective modal mass of that mode. Normally $m_{eff,1}$ is taken equal to the total mass, m, of the building above the foundation or the top of a rigid basement (BSSC 2003, SEAOC 1999). Eurocode 8 (CEN 2004a) allows a reduction to: $m_{eff,1} = 0.85m$, in buildings with more than two storeys above the foundation or the top of a rigid basement and a period $T_1 < 2T_C$ (where T_C is the corner period between the constant-spectral-acceleration and the constant-spectral-pseudovelocity ranges). This value is, on average, representative of heigthwise regular buildings with at least three storeys, while if $T_1 < 2T_C$ the 2nd and higher modes are normally below the plateau where spectral pseudo-accelerations are constant and highest. US codes (BSSC 2003, SEAOC 1999) take $m_{eff,1} = m$ but allow a reduction of the overturning moment (see last paragraph in Section 4.3.3).

Eurocode 8 promotes calculation of T_1 on the basis of mechanics, notably from the Rayleigh quotient:

$$T_1 = 2\pi \sqrt{\frac{\sum_i m_i \delta_i^2}{\sum F_i \delta_i}} \tag{4.7}$$

where:

- i indexes all the degrees-of-freedom (DoF) of the system in the horizontal direction, X or Y, where T_1 is calculated;
- m_i is the (translational) mass associated with degree-of-freedom i;
- F_i is the lateral force applied to degree-of-freedom i; and
- δ_i is the displacement of degree-of-freedom i, obtained from an elastic analysis of the structure for the set of lateral forces F_i.

For given relative magnitudes of the forces F_i (i.e., pattern over the DoFs i), the displacements δ_i are proportional to F_i. So, the value of T_1 from Eq. (4.7) does not depend on the absolute magnitudes of F_i. It is also rather insensitive to the relative magnitudes of F_i: any reasonable distribution of F_i to the DoFs i may be

adopted. It is very convenient and also quite accurate to use as F_i lateral forces proportional to the postulated distribution of V_b to the DoFs i in linear static analysis (see Eq. (4.8) in Section 4.3.3). Note that at the stage of the calculation of T_1 through Eq. (4.7) the base shear, V_b, is still unknown: the lateral forces F_i can be chosen such that their resultant is equal to the total weight of the structure (i.e., with $S_{a,d}(T_1) = 1.0$ g). Then a single linear static analysis per horizontal direction, X or Y, suffices in order both:

- to estimate T_1 from Eq. (4.7), and
- to determine the effects, E_X or E_Y, of the seismic action component in direction X or Y, as the seismic action effects from this analysis just need to be multiplied by $m_{eff,1}S_{a,d}(T_1)/m$, with $S_{a,d}(T_1)$ derived from the design spectrum at the – now known – value of T_1.

Codes (CEN 2004a, BSSC 2003, SEAOC 1999) give also empirical expressions for T_1, representing lower bounds (mean minus standard deviation) from measurements on buildings in California in moderate earthquakes. Such measurements reflect also the influence of non-structural elements on the response. So, the empirical expressions underestimate the period compared to Eq. (4.7). The empirical expressions may give values for T_1 that lie in the constant spectral acceleration region even for flexible buildings. So, they are sometimes used to obtain a safe-side estimate of $S_{a,d}(T_1)$ for force-based design. In the light of the upcoming displacement-based design and assessment, where realistic estimation of displacement demands is of prime importance, the empirical expressions for T_1 are not just inaccurate and misleading, but unsafe as well. So, given that Eq. (4.7) gives accurate estimates of T_1 at no additional effort, further use of the empirical period formulas in seismic design seems unwarranted.

Unlike Eurocode 8, which tries to emulate in linear static analysis a modal response spectrum one through a mechanics-based value of T_1 (e.g., from Eq. (4.7)) and a value of $m_{eff,1}$ in Eq. (4.6) which – under certain conditions – is less than the total mass m, US codes (BSSC 2003, SEAOC 1999) seem to have more confidence in the empirical expressions for T_1 than in Eq. (4.7). So, if the designer applies Eq. (4.7) or any alternative mechanics-based approach, he/she should respect a lower limit on the pseudo-acceleration $S_{a,d}(T_1)$ from the design spectrum. In SEAOC (1999) the limit is 80% of the $S_{a,d}(T_1)$ value determined from the spectrum at the empirical T_1-value. In BSSC (2003) a lower limit is set to the value of T_1 from Eq. (4.7) or other mechanics-based expressions: the T_1-value to be used cannot exceed the empirical period times 1.4–1.7.[3]

[3]Low values of the multiplicative factor are applied for high values of the design ground acceleration and large ones for lower design ground accelerations.

4.3.3 Pattern of Lateral Forces

The base shear of Eq. (4.6) is considered to be the resultant of a set of concurrent peak inertia forces on the masses m_i associated with DoF i in the horizontal direction of the component of the seismic action. In a single mode of vibration (in this case the 1st mode in the direction of the horizontal component) the peak lateral inertia force on DoF i is proportional to $\Phi_i m_i$, where Φ_i is the value of the 1st eigenmode at that DoF. Then, the base shear from Eq. (4.6) is distributed to the DoFs as:

$$F_i = V_b \frac{\Phi_i m_i}{\sum_j \Phi_j m_j} \tag{4.8}$$

with the summation in the denominator extending over all DoFs i.

If the building has rigid diaphragms, masses are often lumped there (at the floor centres of mass). Then the general formulation above, applying for any arrangement of masses and DoFs in space, is simplified to refer just to floors or storeys, with $i = 1$ at the lowest floor above the foundation or the top of a rigid basement and $i = n_{st}$ at the roof. The lateral forces F_i are then applied at the floor centres of mass.

Within the field of application of linear static analysis (regularity in elevation, higher modes unimportant), Eurocode 8 takes for simplicity the 1st mode shape as proportional to the elevation, z, from the base or above the top of a rigid basement: i.e. $\Phi_i = az_i$. Then Eq. (4.8) is commonly termed "inverted triangular" pattern of lateral forces, although it is only the assumed peak response accelerations that have "inverted triangular" distribution, while the force pattern depends also on the distribution of masses, m_i.

As US codes are more liberal than Eurocode 8 on the applicability of linear static analysis to taller, more flexible structures, their lateral force patterns attempt to capture higher-mode effects. So, for structures with $T_1 > 0.7$ s SEAOC (1999) assigns a fraction of the base shear equal to $0.07T_1$(s), but not exceeding one-quarter, to a concentrated force at the roof level and distributes the rest according to Eq. (4.8) with $\Phi_i = az_i$. In BSSC (2003) Φ_i is taken proportional to $z_i{}^k$ with $k = 0.75 + 0.5T_1 \leq 2$ and $k \geq 1$, giving $k = 1$ and $\Phi_i = az_i$ for $T_1 < 0.5$ s.

Interesting is the approach in AIJ (1992). The seismic shear at storey i is given directly as a fraction of the total building weight at storey i and above, a_i; the proportionality constant is equal to $1 + 2(1/\sqrt{a_i} - a_i)/(3 + 1/T_1)$ and empirically reflects higher-mode effects on long-period structures. For uniform distribution of the total weight to n_{st} levels, a_i is equal to $(1–(i+1)/n_{st})$ with $i = 1$ at the lowest storey. For flexible structures this dependence of seismic shears on storey level amount to a very nonlinear distribution of storey lateral loads with height and a strong concentration of lateral loads near the top.

Note that the lateral forces of Eq. (4.8) are meant to produce (by equilibrium) safe-side envelopes of storey seismic shears. Overturning moments, calculated also by equilibrium from these lateral forces, may significantly overestimate the actual peak values at some storeys. Accordingly, BSSC (2003) allows reducing by 25%

the overturning moment at the foundation level computed by equilibrium from the lateral forces of Eq. (4.8).

4.4 Modal Response Spectrum Analysis

4.4.1 Modal Analysis and Its Results

As a first step in a modal response spectrum analysis, the modal shapes (eigenmodes) in 3D and the natural frequencies (eigenvalues) are computed. Note that, even when the building may be sufficiently regular in plan for separate planar (2D) analyses to be allowed in two vertical planes, XZ and YZ, modal response spectrum analysis should be done on a full 3D structural model. Then, each modal shape, represented by vector $\boldsymbol{\Phi}_n$ for mode n, will in general have displacements and rotations in all three directions, X, Y and Z for all nodes i of the structural model (unless the solution of the eigenvalue problem is based on few DoFs, with the rest condensed out, see "indirect" approach at the end of this section).

An eigenmode-eigenvalue analysis gives for each normal mode, n:

1. The natural period, T_n , and the corresponding circular frequency, $\omega_n = 2\pi/T_n$.
2. The mode shape vector $\boldsymbol{\Phi}_n$.
3. Factors of modal participation to the response to the seismic action component in direction X, Y or Z, denoted as Γ_{Xn}, Γ_{Yn}, Γ_{Zn} and calculated as: $\Gamma_{Xn} = \boldsymbol{\Phi}_n{}^T\mathbf{M}\boldsymbol{I}_X/\boldsymbol{\Phi}_n{}^T\mathbf{M}\boldsymbol{\Phi}_n = \Sigma_i\varphi_{Xi,n}m_{Xi}/\Sigma_i(\varphi^2{}_{Xi,n}m_{Xi}+ \varphi^2{}_{Yi,n}m_{Yi}+\varphi^2{}_{Zi,n}m_{Zi})$, where i denotes nodes associated with dynamic DoFs, $\mathbf{M}$ is the mass matrix, $\boldsymbol{I}_X$ is a vector with elements equal to 1 for the translational DoFs parallel to direction X and all other elements equal to 0, $\varphi_{Xi,n}$ is the element of $\boldsymbol{\Phi}_n$ corresponding to the translational DoF of node i parallel to X and m_{Xi} the associated element of the mass matrix. Similarly for $\varphi_{Yi,n}$, $\varphi_{Zi,n}$, m_{Yi} and m_{Zi}. If $\mathbf{M}$ contains rotational mass moments of inertia, $I_{\theta Xi,n}$, $I_{\theta Yi,n}$, $I_{\theta Zi,n}$, the associated terms are included in the sum at the denominator of Γ_{Xn}. The definitions of Γ_{Yn}, Γ_{Zn} are similar.
4. The (base-shear-)effective modal masses in directions X, Y and Z, M_{Xn}, M_{Yn}, and M_{Zn}, respectively: $M_{Xn} = (\boldsymbol{\Phi}_n{}^T\mathbf{M}\boldsymbol{I}_X)^2/\boldsymbol{\Phi}_n{}^T\mathbf{M}\boldsymbol{\Phi}_n = (\Sigma_i\varphi_{Xi,n}m_{Xi})^2/\Sigma_i(\varphi^2{}_{Xi,n}m_{Xi}+ \varphi^2{}_{Yi,n}m_{Yi}+\varphi^2{}_{Zi,n}m_{Zi})$, and similarly for M_{Yn}, $M_{Zn.}$ They are important because they give the peak force resultants in mode n along direction X, Y or Z: $V_{bX,n} = S_a(T_n)M_{Xn}$, $V_{bY,n} = S_a(T_n)M_{Yn}$, $V_{bZ,n} = S_a(T_n)M_{Zn}$, respectively. The sum of the effective modal masses in X, Y or Z over all modes of the structure is equal to its total mass.

Participation factors and effective modal masses convey a certain physical meaning, essential for the understanding of the nature and relative importance of each mode. For example:

– the relative magnitude of the modal participation factors determines the predominant direction of the mode: its inclination to horizontal direction X is Γ_{Yn}/Γ_{Xn}, etc.;

- the predominant direction of the mode with the largest modal base shear is a good choice, together with the orthogonal direction, as a "principal" or "main" direction of the structure in plan, along which the horizontal seismic action components are taken to act.
- a good measure of the regularity in plan (irrespective of the qualitative criteria for regularity) is the lack of significant rotation about the vertical (and of global reaction torque with respect to that axis) in the (few) lower most modes.

Unfortunately, the presence and potential dominance of torsion about the vertical in a mode can only be detected from participation factors and modal masses for rotation about Z, normally not reported in computer output.[4] The importance of torsion in a mode can also be appreciated on the basis of modal reaction forces and moments.

Peak modal seismic action effects in the response to the seismic action component in direction X, Y or Z may be computed as follows:

I. For each normal mode n the spectral displacement, $S_{\mathrm{dX}}(T_{\mathrm{n}})$, is calculated from the pseudo-acceleration spectrum of the seismic action component, let's say X, as $S_{\mathrm{dX}}(T_{\mathrm{n}}) = (T_{\mathrm{n}}/2\pi)^2 S_{\mathrm{aX}}(T_{\mathrm{n}})$.
II. The nodal displacement vector of the structure in mode n due to the seismic action component of interest, let's say in direction X, $\boldsymbol{U}_{\mathrm{Xn}}$, is computed as: $\boldsymbol{U}_{\mathrm{Xn}} = S_{\mathrm{dX}}(T_{\mathrm{n}})\Gamma_{\mathrm{Xn}}\boldsymbol{\Phi}_{\mathrm{n}}$.
III. Peak modal values of the effects of the seismic action component of interest are computed from the modal displacement vector of Step II. Member modal deformations (e.g., chord rotations) or modal interstorey drifts are obtained directly from the nodal displacement vector of mode n. Modal member (end) forces are computed by multiplying the member modal deformations by the member stiffness matrix and modal storey shears, overturning moments, etc. by equilibrium from modal member shears, moments, axial forces, etc.

The so-computed peak modal responses are exact. However, they occur at different instances in the response and can be combined only approximately. Section 4.4.3 presents combination rules for peak modal responses. Rules to take into account in approximation the simultaneous occurrence of the seismic action components are given in Section 4.7.

Condensation of degrees of freedom (DoFs) is sometimes applied to buildings with rigid diaphragms to reduce the number of static DoFs into just three dynamic ones per floor (two horizontal translations, one rotation about the vertical). This is possible only if the vertical seismic action component, Z, is of no interest or importance. Dynamic condensation profits from the fact that horizontal seismic action components normally induce negligible vertical nodal inertia forces or nodal inertia

[4]The commonly reported modal participation factors and effective modal masses along X, Y and Z are not so informative about torsion about the vertical.

moments about the X and Y axes. This allows expressing nodal translations in Z and nodal rotations about X and Y in terms of the dynamic DoFs[5] and eliminating them from the equation of motion. If a diaphragm is rigid, the three in-plane DoFs (two horizontal translations and the rotation about the vertical axis) of each one of its nodes can be expressed through a kinematic constraint in terms of the corresponding DoFs of a single node of the diaphragm, termed master node. The master node is often taken to coincide with the storey centre of mass, where the storey's full translational mass, $m_{\mathrm{Xi}} = m_{\mathrm{Yi}}$, and floor rotational mass moment of inertia, $I_{\theta\mathrm{i}}$, are lumped. The reduced dynamic model has just $3n_{\mathrm{st}}$ modes in 3D (n_{st}: number of storeys). For each mode n the response spectrum in entered with the natural period T_{n} of the mode to read the spectral acceleration $S_{\mathrm{a}}(T_{\mathrm{n}})$. Then, for each one of the two horizontal components of the seismic action two horizontal forces and one torque with respect to the vertical are computed for mode n at each floor level i: $F_{\mathrm{Xi,n}}$, $F_{\mathrm{Yi,n}}$ and $M_{\mathrm{i,n}}$, where indexes X and Y denote now the direction of the two forces and not that of the seismic action component (which may be either X or Y). These forces and moments are computed as $S_{\mathrm{a}}(T_{\mathrm{n}})$ times:

- the participation factor of mode n to the response to the seismic action component of interest, let's say Γ_{Xn} for the one in direction X;
- the mass associated with the corresponding floor DoFs: floor mass $m_{\mathrm{Xi}} = m_{\mathrm{Yi}}$ and floor rotational mass moment of inertia, $I_{\theta\mathrm{i}}$; and
- the corresponding component of the modal eigenvector, $\varphi_{\mathrm{Xi,n}}$, $\varphi_{\mathrm{Yi,n}}$, $\varphi_{\theta\mathrm{i,n}}$.

For each mode n and separately for the two horizontal components of the seismic action, a static analysis of the full structural model in 3D is carried out then, under static forces and moments $F_{\mathrm{Xi,n}}$, $F_{\mathrm{Yi,n}}$ and $M_{\mathrm{i,n}}$, applied to the corresponding dynamic DoFs of each floor i. Peak modal response quantities (nodal displacements, member internal forces or deformations, e.g. chord rotations, interstorey drifts, etc.) are computed separately for each mode and combined for all modes according to the rules in Section 4.4.3 for each horizontal component X or Y of the seismic action.

As the "indirect" approach above computes internal forces and other response quantities by static analysis for specified (modal) forces at floor levels, resembling external loads, it is more intuitive and appealing to designers who are familiar with analysis for static actions, such as wind or gravity, but maybe not so conversant with modal response spectrum analysis. For this reason, despite its lack of generality and limitations in its use (rigid diaphragms, no vertical seismic action component) some codes (BSSC 2003) do suggest the "indirect" procedure for the calculation of peak dynamic response quantities in the framework of modal response spectrum analysis.

[5]Dynamic DoFs are those contributing to the equation of motion with inertia terms.

4.4.2 Minimum Number of Modes

Modal response spectrum analysis should take into account all modes contributing significantly to any response quantity of interest. This is difficult to achieve in practice, because the number of modes to be considered should be specified as input to the eigenvalue analysis. Codes (CEN 2004a, BSSC 2003, SEAOC 1999) focus on base shears as the prime response quantities of interest and use as a criterion the relevant measure(s) from the eigenvalue analysis. They require the N considered modes to provide together a total effective modal mass along any individual seismic action component, X, Y, or even Z, at least 90% of the total mass.

If the above criterion is hard to satisfy, Eurocode 8 (CEN 2004a) allows as alternative to take into account all modes which individually have effective modal mass along any one of the seismic action components, X, Y or Z, considered in design, at least 5% of the total mass. This criterion refers to modes that may have not been captured so far in the eigenvalue analysis; so it is difficult to apply. As a third alternative in case meeting any of the two criteria above is unfeasible (e.g. when torsional modes are important, or when the vertical seismic action component should be considered in design), Eurocode 8 is content if the eigenvalue analysis captures at least $3\sqrt{n_{st}}$ modes (where n_{st} is the number of storeys above the foundation or the top of a rigid basement) and at least one natural periods below 0.2 s.

The 1st and most commonly used of the above criteria (that of the sum of effective modal masses captured) addresses only the base shear reflected in the computed modes, and even that only partly. As modal shears are equal to the effective modal mass times the spectral acceleration at the mode's period, if the 1st mode period is fairly long and higher mode periods are in the constant spectral acceleration plateau, the effective modal mass alone underestimates the contribution of higher modes to base shear. Other global response quantities, such as the overturning moment at the base and the top displacement, are less sensitive to the number of modes than the base shear. However, response quantities used in local verifications (interstorey drifts, member chord rotations or internal forces, etc.) may be more sensitive to the number of modes included. So, these modes would preferably account for much more than 90% of the total mass (close to 100%), to approximate well the peak values of these quantities.

There exist techniques to approximately account for the missing mass due to truncation of higher modes (e.g. by adding static response). However, Eurocode 8 does not require such measures for buildings.

Modal overturning moments from modal analysis reflect realistically the distribution of modal inertia forces along the height. So, their final combination via the rules of Section 4.4.3 into peak dynamic storey overturning moments can be considered as free of the conservatism associated with calculation of storey "static" or "equivalent lateral" forces by equilibrium. BSSC (2003) allows up to 10% reduction of the value of the overturning moment at the foundation level as computed from modal contributions according to Section 4.4.3.

4.4.3 Combination of Modal Results

In modal response spectrum analysis it is convenient to take the elastic response to two different modes as independent of each other. In reality this is just an approximation. The magnitude of the actual correlation between modes *i* and *j* is estimated through a correlation coefficient of the two modes, ρ_{ij}. The following approximation has been proposed in (Rosenblueth and Elorduy 1969):

$$\rho_{ij} = \frac{\zeta^2(1+\lambda)^2}{(1-\lambda)^2 + 4\zeta^2\lambda} \tag{4.9a}$$

Nowadays the approximation proposed in Wilson et al. (1981) and Der Kiureghian (1981) is more widely accepted and used:

$$\rho_{ij} = \frac{8\sqrt{\zeta_i\zeta_j}(\zeta_i + \lambda\zeta_j)\lambda^{3/2}}{(1-\lambda^2)^2 + 4\zeta_i\zeta_j\lambda(1+\lambda^2) + 4(\zeta_i^2 + \zeta_j^2)\lambda^2} \tag{4.9b}$$

In Eqs. (4.9) ζ_i, ζ_j are the viscous damping ratios in modes *i* and *j*, respectively (taken as equal in Eq. (4.9a) and denoted by ζ), while $\lambda = T_i/T_j$. If two modes have closely spaced natural periods ($\lambda \approx 1.0$), ρ_{ij} is close to 1.0 and the responses in the two modes cannot be considered independent of each other. For buildings Eurocode 8 (CEN 2004a) considers that modes *i* and *j* cannot be taken as independent, if λ is between 0.9 and 1/0.9. At the two extremes of this range of λ and for $\zeta_i = \zeta_j = 0.05$, Eq. (4.9b) gives $\rho_{ij} = 0.47$. Part 2 of Eurocode 8 for bridges (CEN 2005b) is more restrictive, considering that modes *i* and *j* are not independent if λ is between $[0.1 + \sqrt{(\zeta_i\zeta_j)}]$ and $0.1/[0.1 + \sqrt{(\zeta_i\zeta_j)}]$; if $\zeta_i = \zeta_j = 0.05$ and λ is equal to these limit values, Eq. (4.9b) gives indeed a low value: $\rho_{ij} = 0.05$. Note that buildings with about the same lateral stiffness in horizontal directions X and Y have pairs of modes with very similar periods at about right angles in plan (albeit not necessarily in the two direction, X and Y). The modes of each pair are closely correlated.

When all relevant modal responses can be taken as independent of each other, random vibration theory gives the expected value of the maximum, E_E, of a seismic action effect as the Square Root of the Sum of Squares of the modal responses – SRSS rule (Rosenblueth 1951):

$$E_E = \sqrt{\sum_N E_{Ei}^2} \tag{4.10}$$

where the summation extends over the *N* modes taken into account and E_{Ei} is the peak value of the seismic action effect in mode *i*. If the response in any two vibration modes *i* and *j* cannot be taken as independent of each other, the SRSS rule is unconservative. Then more accurate procedures for the combination of peak modal responses should be used (CEN 2004a). Random vibration theory gives

the Complete Quadratic Combination – CQC rule (Wilson et al. 1981) quoted in Eurocode 8 for the expected value of the maximum, E_{E}, of a seismic action effect due to correlated modes:

$$E_E = \sqrt{\sum_{i=1}^{N} \sum_{j=1}^{N} \rho_{\mathrm{ij}} E_{Ei} E_{Ej}} \tag{4.11}$$

In Eq. (4.11) E_{Ei}, E_{Ej} are the peak values of the seismic action effect in modes i and j. The correlation coefficient of modes i and j, ρ_{ij}, may be taken from the approximation of Eqs. (4.9). Comparison with the results of response-history analyses has demonstrated good average accuracy of the CQC rule. Note that the CQC includes the SRSS rule, Eq. (4.10), as a special case for $\rho_{\mathrm{ij}} = 0$ if $i \neq j$ (for $i = j$ we have $\rho_{\mathrm{ij}} = 1$).

The SRSS and the CQC give only the absolute value of the peak response estimate, which should be considered and combined with non-seismic action effects (e.g., due to gravity loads) as both negative and positive. So, although modal internal forces satisfy equilibrium at any level, member end force values from the SRSS or CQC rules do not satisfy equilibrium at the level of the individual member or node. So, envelopes of moments along members cannot be constructed from the member end forces and equilibrium. They may be constructed, instead, point-by-point, by SRSS or CQC combination of the modal moments at the generic point x along the member. Such envelopes do not have a point of inflection and do not show whether the member is in single or in double curvature bending when its peak end moments take place. This can be judged from the peak shear forces computed through the same mode combination rules. The member may be considered to be in double or single curvature; if the product of the member's peak shear force and the member length is closer to the sum of the (positive) member end moments, or to their difference, respectively.

4.5 Linear Analysis for the Vertical Seismic Action Component

4.5.1 When is the Vertical Component Important and Should Be Taken Into Account?

In buildings the vertical seismic action component may in general be neglected, because:

- its effects are normally covered by the design for factored gravity loads;
- except in buildings having long span beams with significant mass distributed along them, the fundamental period of the building in the vertical direction is governed by the axial stiffness of vertical members and is very short; so, spectral amplification of the vertical ground motion is low.

Seismic design codes require to take into account the vertical seismic action component only when its effects are likely to be significant (in view of the arguments above). Eurocode 8 considers this to be the case only if the design ground acceleration in the vertical direction, a_{vg}, exceeds 0.25 g, and even then only in the following cases:

- in base-isolated buildings; or
- for (nearly) horizontal members (beams, girders, or slabs) which:
  - have a span of at least 20 m; or
  - cantilever over at least 5 m; or
  - support directly columns; or
  - are prestressed.

4.5.2 Special Linear Static Analysis Approach for the Vertical Component

The analysis provisions of current seismic design codes pertain primarily (essentially only) to the horizontal components of the seismic action. At most they include very limited special guidance for the analysis under the vertical component. The modal response spectrum and the nonlinear dynamic methods of analysis are, of course, applicable for the analysis of the response to the vertical component, provided that floor masses are not lumped only at nodes of vertical and horizontal elements, but at several intermediate points of the horizontal elements as well. However, a very large number of modes may need to be determined in modal analysis to capture 90% of the participating mass in the vertical direction, or, in general, to accurately estimate the seismic action effects due to the vertical component.

Although not described in codes, an "equivalent static" linear analysis can be used for the vertical component. This is a modification of the "lateral force procedure" to address the vertical direction instead of the horizontal. For convenience, it may employ the same structural model as the analysis for the horizontal components. In this approach the fundamental period of vibration in the vertical direction, T_1, may be estimated via Eq. (4.7), using as F_i the weights of the masses m_i and as δ_i the vertical nodal displacements from the analysis for the loads F_i. As these forces are the gravity loads concurrent with the design seismic action, a linear static analysis for them is done anyway and its results are already available. A total vertical seismic force can then be computed from Eq. (4.6) with $m_{eff,1} = m$, on the basis of the spectral acceleration, $S_{av}(T_1)$, derived from the vertical design spectrum (see last paragraph in Section 4.2.2). For the purposes of the static analysis for the vertical seismic action component, this total vertical force can be distributed to all nodes of the structure in proportion to the product of their mass, m_i, times their vertical displacement, δ_i, under the weights of the masses m_i.

In those horizontal members for which the vertical component needs to be taken into account, the relevant dynamic response is often of local nature. It involves these members and their immediately adjacent or supporting ones, but not the entire structure. So, Eurocode 8 considers sufficient to carry out an analysis on a partial structural model capturing the important aspects of the response in the vertical direction, without irrelevant and unimportant influences that may confuse or obscure the important results. The partial model includes fully the horizontal members on which the vertical component is considered to act, as well as the elements (or systems of elements) directly supporting them. All other adjacent elements (e.g. adjacent spans) may be included only with their stiffness. More specifically:

(a) the partial structural model should include all (nearly) horizontal members for which the vertical component needs to be taken into account, each discretised into a few (e.g. about five) beam elements with masses lumped at the intermediate nodes;
(b) directly supporting elements or systems of elements may also be included, up to their supports by the ground or at another vertically stiff element or system of elements; for example, columns directly supporting the members on which the vertical component is taken to act may be included with their full length down to the foundation;
(c) adjacent spans continuous to the member(s) on which the vertical component is taken to act may be included up to their next support, with appropriate boundary conditions there (e.g. pinned or fixed against rotation, fixed vertically, etc.);
(d) the partial structural model should include those beams, girders or other horizontal elements which are connected at an angle (often at right angles) to the members on which the vertical component is taken to act; these transverse or oblique elements should be included in the model with their full connectivity and the appropriate boundary conditions at their supports, but without intermediate nodes for lumped masses;

The members on which the vertical component is considered to act (those listed in (a) above) and their directly associated supporting elements or systems of elements (e.g. those listed in (b) or (d)) are the only ones to be dimensioned on the basis of the computed action effects of the vertical component.

The designer may find it inconvenient to develop the partial structural model just for the purposes of the analysis for the vertical component. He/she may prefer to keep instead the overall structural model of the analysis for gravity loads and the horizontal components of the seismic action, but use a partial model only to calculate T_1 from Eq. (4.7) and distribute to the individual masses the total vertical seismic force derived from T_1 and from the vertical design spectrum. Such a partial model may be developed from the overall structural model, by considering all nodes of vertical elements as fixed against vertical displacement. These vertical DoFs are released in the subsequent static analysis for the calculation of the effects of the

vertical seismic action component. This latter analysis is carried out on the overall structural model under vertical nodal loads proportional to $m_i\delta_i$ and applied only to the vertically active DoFs of the partial structural model. In this way the action effects of the vertical component, E_Z, can be realistically computed, not only in the horizontal members included in the partial model, but also in their supporting or adjacent elements and the whole structure.

4.6 Nonlinear Analysis

4.6.1 Nonlinear Static ("Pushover") Analysis

4.6.1.1 Introduction

The prime use of nonlinear analysis is for assessment of existing or retrofitted buildings, for which, as pointed out in Section 4.1.3, nonlinear analysis is the reference method, or for evaluation of the seismic performance of new designs.

Unlike linear analysis, which has long been the basis of practical seismic design of new buildings, and nonlinear dynamic analysis, which has been extensively used since the 1970s for research, code-calibration or other special tasks, nonlinear static analysis (commonly called "pushover" analysis) was not widely known or used until the first new-generation guidelines for seismic rehabilitation of existing buildings (ATC 1997) adopted it as the reference method. Since then, its appealing simplicity and intuitiveness and the wide availability of reliable and user-friendly analysis software have made it the analysis method of choice for seismic assessment and retrofitting of buildings.

"Pushover" analysis is essentially the extension of the "lateral force procedure" of static analysis into the nonlinear regime. It is carried out under constant gravity loads and monotonically increasing lateral loading applied on the masses of the structural model. This loading is meant to simulate inertia forces due to a horizontal component of the seismic action (the vertical component is not addressed). While the applied lateral forces increase in the course of the analysis, the engineer can follow the gradual emergence of plastic hinges, the evolution of the plastic mechanism and damage, as a function of the magnitude of the imposed lateral loads and of the resulting displacements.

4.6.1.2 Lateral Load Vector

Pushover analysis was initially developed, and still mainly applied, for 2D analyses. Even when applied on 3D structural models the lateral loading simulates the inertia due to a single horizontal seismic action component. In the fundamental and most commonly used version of the method, the forces F_i incrementally applied on the masses m_i remain proportional to an invariant pattern of horizontal displacements Φ_i:

$$F_i = \alpha m_i \Phi_i \tag{4.12}$$

as if the entire response were in a single invariant mode with horizontal modal displacements Φ_i.

According to Eurocode 8 (CEN 2004a, 2005a), pushover analyses should be applied to buildings using both of the following lateral load patterns:

1. A "modal pattern", simulating the inertia forces of the 1st mode in the horizontal direction in which the analysis is carried out. This pattern is meant to apply in the elastic regime and during the initial stages of the plastic mechanism development, as well as in a full-fledged beam-sway mechanism (see Fig. 1.3(b)–(e)). The precise pattern depends on the type of linear analysis applicable:
   - If the building meets the applicability conditions of linear static analysis, an "inverted triangular" unidirectional lateral load pattern is applied, like the one used in a linear static analysis (i.e. with $\Phi_i = z_i$ in Eq. (4.12));
   - When the building does not fulfil the conditions for the application of linear static analysis, Φ_i in Eq. (4.12) is the 1st mode shape from modal analysis. If the 1st mode is not purely translational, the patterns of Φ_i and F_i are not unidirectional: they may have horizontal components orthogonal to that of the seismic action component in question.
2. A "uniform pattern", corresponding to uniform unidirectional lateral accelerations, i.e. to $\Phi_i = 1$ in Eq. (4.12). It attempts to simulate the inertia forces in a potential soft-storey mechanism, limited in all likelihood to the bottom storey, with the lateral drifts concentrated there and the storeys above moving laterally almost as a rigid body (Fig. 1.3(a)).

The most unfavourable result of the pushover analyses with the two standard lateral force patterns, 1 or 2, should be used. Unless the structure is symmetric about an axis at right angles to the seismic action component considered, the lateral forces should be applied in both the positive and the negative direction (sense).

More sophisticated versions of pushover analysis (Bracci et al. 1997, Elnashai 2001, Gupta and Kunnath 2000) do not use a fixed pattern of applied lateral loads, Eq. (4.12), but "adapt" it to the evolution of nonlinearity, as this affects the dynamic properties of the structure. However, any increase in accuracy is at the expense of the most attractive feature of pushover analysis, namely its simplicity. So, here we stay with the original and simplest version of pushover analysis, as in the N2 procedure (Fajfar 2000) adopted in Eurocode 8 (CEN 2004a, 2005a).

4.6.1.3 Capacity Curve and Equivalent SDOF System

It is convenient and common to present the results of a "pushover" analysis in the form of a nonlinear force-displacement curve (Fig. 4.2). Although it depicts a certain aspect of the building's nonlinear response and has little to do with its capacity

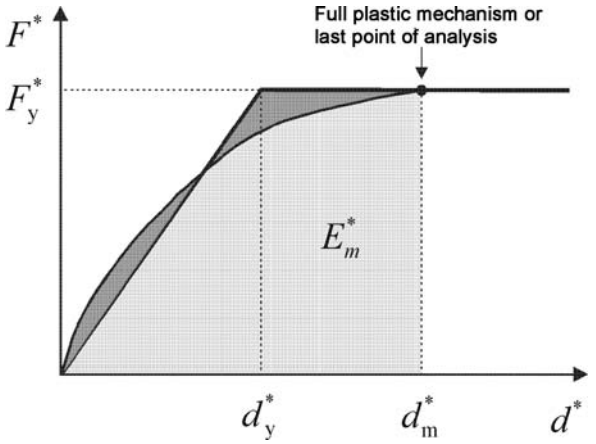

Fig. 4.2 Elastic-perfectly plastic idealisation of capacity curve of equivalent SDOF system in pushover analysis (Fajfar 2000, CEN 2004a)

to withstand the seismic action, the curve is commonly referred to as "capacity curve". This differentiates it from the "demand" curve, which relates the spectral displacement to the product of the mass and the spectral acceleration (Acceleration-Displacement-Response-Spectrum, ADRS, Fig. 4.3). The proximity of the "capacity curve" to the results of a series of nonlinear dynamic (response-history) analysis, considered as the benchmark, is often taken as a measure of the accuracy of a "pushover" analysis.

An obvious force quantity for the vertical axis of the "capacity curve" is the base shear, V_b, as it represents the total force resistance in the horizontal direction considered at an instant of the displacement response. The lateral displacement on the horizontal axis, d_n, is often taken at a certain node n of the structural model, termed "control node". That node is normally at the centre of mass of the roof. A mathematically better choice, relating very well to the definition of the seismic demand in terms of spectral quantities, are the lateral force and displacement of an equivalent Single-Degree-of-Freedom (SDOF) system. In the N2 procedure (Fajfar 2000) adopted in Eurocode 8 the equivalent SDOF system is defined as follows:

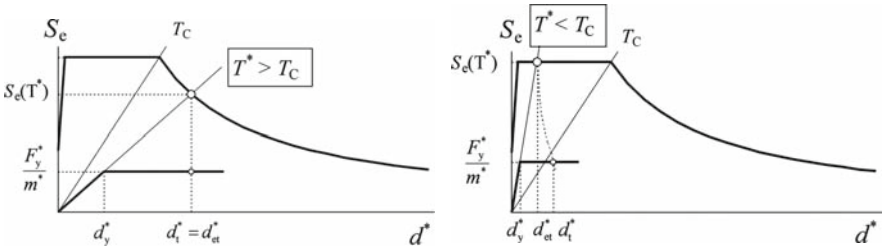

Fig. 4.3 "Target displacement" of equivalent SDOF system in "pushover" analysis (Fajfar 2000, CEN 2004a): (**a**) long and intermediate period ranges; (**b**) short period range

- The horizontal displacements Φ_i in Eq. (4.12) are normalised so that $\Phi_n = 1$ at the control node.
- The mass of the equivalent SDOF system m^* is:

$$m^* = \sum m_i \Phi_i \tag{4.13}$$

- Its force, F^* and displacement d^* are:

$$F^* = \frac{V_b}{\Gamma},\ d^* = \frac{d_n}{\Gamma} \tag{4.14}$$

where:

$$\Gamma = \frac{m^*}{\sum m_i \Phi_i^2} \tag{4.15}$$

Note that in the "modal pattern" of lateral loads, where Φ_i emulates a mode shape, Γ is the participation factor of that mode in the direction of the lateral forces (point 3 in Section 4.4.1).

To determine the seismic demand (see Section 4.6.1.4) we need to estimate the period T^* of the equivalent SDOF system. According to Fajfar (2000) and CEN (2004a) T^* can be determined on the basis of the mass from Eq. (4.13) and of the elastic stiffness of an elastic-perfectly plastic idealisation of the "capacity curve" of the SDOF system. The yield force, $F_y{}^*$, of the elastic-perfectly plastic curve, taken as the ultimate strength of the SDOF system, is the value of F^* when a complete plastic mechanism forms (or at the terminal point of the "capacity curve", if a full plastic mechanism does not develop by then). The yield displacement, $d_y{}^*$, is chosen so that the deformation energy of the elastic-perfectly plastic idealisation at the displacement of the equivalent SDOF system when the plastic mechanism forms or at the terminal point, $d_m{}^*$, is equal to that of the actual "capacity curve" at the same point, $E_m{}^*$ (Fig. 4.2):

$$d_y^* = 2\left(d_m^* - \frac{E_m^*}{F_y^*}\right) \tag{4.16}$$

The elastic stiffness of the SDOF system is $F_y{}^*/d_y{}^*$ and its period T^* is (Fajfar 2000, CEN 2004a):

$$T^* = 2\pi\sqrt{\frac{m^* d_y^*}{F_y^*}} \tag{4.17}$$

If the structure is almost linear until the "yield point" of the elastic-perfectly plastic SDOF system, the period from Eq. (4.17) is the same as the one computed

from Eq. (4.7) on the basis of the results of a linear analysis under lateral forces with the pattern of Eq. (4.12).

4.6.1.4 Definition of the Seismic Demand Through the "Target Displacement"

Unlike linear or nonlinear dynamic analysis, which both give directly all peak seismic demands under a given earthquake, a pushover analysis per se gives only the "capacity curve". The demand is estimated separately. This is normally done in terms of the maximum displacement induced by the earthquake, either to the equivalent SDOF system or at the "control node" of the full structure. This is called "target displacement". In the N2 method (Fajfar 2000, CEN 2004a) the "target displacement" is determined on the basis of the "equal displacement rule", modified for short period systems according to Eqs. (1.1) and (1.2) (Vidic et al. 1994). As shown in Fig. 4.3, if T^* is longer than the transition period, T_C, between the constant pseudo-acceleration and the constant pseudo-velocity parts of the elastic spectrum, the target displacement of the equivalent SDOF system is taken equal to the spectral displacement from the 5%-damped elastic spectrum at period T^*:

$$d_t^* = S_d(T^*) = \left[\frac{T^*}{2\pi}\right]^2 S_a(T^*) \qquad \text{if } T \geq T_C \tag{4.18a}$$

Otherwise, the spectral displacement is corrected according to the q-μ-T relation in (Vidic et al. 1994):

$$d_t^* = \frac{S_d(T^*)}{q_u}\left(1 + (q_u - 1)\frac{T_C}{T^*}\right) \geq S_d(T^*) \qquad \text{if } T < T_C \tag{4.18b}$$

where $q_u = m^* S_a(T^*)/F_y{}^*$. Equation (4.14) can then be inverted for the displacement at the control node, d_n, corresponding to the "target displacement" of the SDOF system.

The "target displacement" may be determined more accurately (especially if the seismic action is given in terms of one or more acceleration time-histories instead of a smooth, 5%-damped elastic spectrum) as the peak displacement from a nonlinear dynamic analysis of a SDOF system with the mass m^* of the equivalent SDOF system and an elastic-perfectly plastic force-deformation monotonic law with the yield force, $F_y{}^*$, and the yield displacement, $d_y{}^*$, of the equivalent SDOF system of Section 4.6.1.3. This analysis may be carried out according to Section 4.6.2, using a hysteresis model, such those in Section 4.10.1.6.

The demands at the local level (inelastic deformations and forces) due to the horizontal component of the seismic action in the direction of the pushover analysis are those corresponding to the "target displacement". Codes (ATC 1997, CEN 2004a, 2005a, ASCE 2007) require carrying out the pushover until a terminal point at 1.5 times the "target displacement".

4.6.1.5 Torsional Effects

The original development of pushover analysis and the N2 method (Fajfar 2000) are for 2D analysis under a single component of the seismic action. The question arises to what extent the standard pushover analysis may be applied, if the response is significantly affected by torsion in 3D and what corrections may be needed in that case.

If the 1st mode along, or close to, each one of the two orthogonal horizontal directions in which the pushover analysis is carried out includes a significant torsional component, the "modal pattern" of lateral loads should be applied to individual nodes (not to the floor centres of mass), with the displacements Φ_i in Eq. (4.12) taken according to the shape of the corresponding 1st mode in 3D. However, if the 1st or 2nd mode in one of the two orthogonal horizontal directions is primarily torsional, such a pushover analysis may overestimate horizontal displacements on the flexible/weak side in plan (the one developing larger horizontal displacements along the direction of lateral forces than the opposite side), i.e., is on the safe side and the difference may be ignored. By contrast, the displacements of the stiff/strong side are underestimated. This difference in the prediction is on the unsafe side and should be taken into account (CEN 2004a). This may be done as follows (Peruš and Fajfar 2005, Marušić and Fajfar 2005, Fajfar et al. 2004, 2005):

1. The standard pushover analysis is carried out on the 3D structure, with the unidirectional pattern of lateral forces, "uniform" or "modal", applied to the floor centres of mass.
2. The equivalent SDOF system is established, along with the elastic-perfectly plastic idealisation of its "capacity curve". Its "target displacement" is determined and translated to a displacement at the control node n at the centre of mass of the roof by inverting Eq. (4.14).
3. A modal response spectrum analysis of the same 3D structural model is carried out. The displacement in the horizontal direction of the pushover analysis is computed at all nodes of the roof (including the control node at the centre of mass) through the CQC rule, Eq. (4.11) and divided by the corresponding value of the control node at the centre of mass, to give an "amplification factor" reflecting the effect of torsion on roof displacements.
4. At all points where the "amplification factor" derived in 3 above is greater than 1.0, it multiplies the displacements of all nodes along the same vertical line, as these are obtained from the standard pushover analysis in 1 and 2 above. These products are taken as the outcome of the analysis, reflecting on one hand the global inelastic response and its heightwise distribution as captured by standard pushover analysis, and on the other the effect of global torsion on the planwise distribution of inelasticity. Eurocode 8 limits the "amplification factor" to values not less than 1.0 and does not allow de-amplification due to the effects of torsion.

Nonlinear dynamic analyses show that the larger the extent and magnitude of inelasticity, the less are the effects of torsion on local response.

4.6.1.6 Higher Mode Effects

Pushover analysis with a force pattern from Eq. (4.12) captures only the effects of a single mode, and, as a matter of fact, only to the extent that the modal shape is fairly well approximated by the displacement pattern(s) used in Eq. (4.12). To capture the effects of higher modes, "Modal Pushover Analysis" has been proposed in Chopra and Goel (2002, 2004). In it a pushover analysis is fully carried out separately for each mode of interest, with gravity loads considered concurrently with every single mode. The horizontal displacement pattern Φ_i in Eq. (4.12) follows the modal shape. For each mode an equivalent SDOF system is defined through Eqs. (4.13), (4.14), (4.15), (4.16) and (4.17) and the seismic demand is determined from Eqs. (4.18) in terms of a "target displacement". A pushover analysis is carried out for each mode up to its own "target displacement"; modal displacements (accounting for the modal participation factors) at the modal target displacement are combined, e.g., via the CQC rule, Eq. (4.11). Recognising that in most cases inelasticity is limited to the 1st mode, a "Modified Modal Pushover Analysis" has been proposed in Chopra et al. (2004), in which higher mode contributions are considered as elastic.

Application of the method to flexible multistorey steel frames, regular or not, suggests that three modes may provide good agreement with the peak storey displacements from nonlinear dynamic analysis. However, element deformations (e.g., plastic hinge or chord rotations) are not estimated equally well. So, they are determined not by combining modal deformations via the CQC rule but from the computed global displacements, using case-dependent transformations from them to local deformations (e.g. via interstorey drifts). Element forces are computed in the end from local element deformations, via the element's nonlinear constitutive relation used in the pushover analysis.

Part 3 of Eurocode 8 limits the application of pushover analysis with the two standard lateral force patterns of Section 4.6.1.2 to buildings meeting condition (b) in Section 4.3.1 for the applicability of linear static analysis (1st mode period not longer than 2 s or four times the transition period T_C between the constant-spectral-acceleration and the constant-spectral-pseudovelocity regions of the spectrum). For buildings violating this condition, reference is made to either "modal pushover" or nonlinear dynamic analysis.

4.6.2 Nonlinear Dynamic (Response- or Time-History) Analysis

4.6.2.1 Scope of Application

Nonlinear dynamic analysis was developed as a method in the 1970s for research, code-calibration, or special applications. Since then, with the availability of several reliable and numerically stable computer codes with nonlinear dynamic analysis capabilities, it has gained its place in engineering practice for the evaluation of structural designs carried out using other approaches (e.g., by conventional force-based design with the q-factor and linear analysis) or cycles of analysis and design evaluation. Its application in design is greatest in buildings with base isolation, as their

response is governed by a few elements (the isolation devices) with strongly nonlinear force-deformation law that depends on the specific devices and does not follow a standard pattern. Moreover, as isolation normally shields the superstructure from seismic damage, residual displacements of the isolation system are of great interest. They can be estimated only through nonlinear dynamic analysis.

The main practical application of nonlinear dynamic analysis, currently and in the foreseeable future, is for seismic assessment of existing structures, where, as pointed out in Section 4.1.3, nonlinear analysis is the reference method. Professionals practicing seismic assessment and retrofitting are fewer and more specialised than in every-day seismic design. So they often master nonlinear dynamic analysis and its special software tools.

4.6.2.2 The Seismic Input Motions

If the analysis is linear or nonlinear static, the seismic action can be defined through its 5%-damped elastic response spectrum. For a nonlinear dynamic (response-history) analysis, time-histories of the ground motion are needed. These time-histories should conform on average with the 5%-damped elastic response spectrum defining the seismic action.

Current seismic codes (CEN 2004a, BSSC 2003, SEAOC 1999, ASCE 2007) require as input for a response-history analysis an ensemble of at least three records (or pairs or triplets of different records, for analysis under two or three concurrent components of the action). Eurocode 8 accepts artificial, historic or simulated records, but US codes (BSSC 2003, SEAOC 1999) only recorded, or simulated ones. Artificial (or "synthetic") records can be mathematically produced using random vibration theory to match almost perfectly the response spectrum defining the seismic action (Gasparini and Vanmarcke 1976). It is fairly straightforward to adjust the phases of the various sinusoidal components of the artificial waveform, as well as the time-evolution of their amplitudes ("envelope function"), so that the artificial record resembles a specific recorded motion. Note, however, that records which are equally rich in all frequencies are not realistic. Moreover, an excitation with a smooth response spectrum without peaks or troughs introduces a conservative bias in the response, as it does not let inelastic response help the structure escape from a spectral peak to a trough at a longer period. Therefore, historic records are favoured also in CEN (2004a). Records simulated from mathematical source models, including rupture, propagation of the motion through the bedrock to the site and, finally, through the subsoil to the surface, are also preferred over artificial ones (CEN 2004a), as the final records resemble natural ones and are physically appealing. Obviously, an equally good average fitting of the target spectrum requires more – appropriately selected – historic or simulated records than artificial ones. Individual recorded or simulated records should be "adequately qualified with regard to the seismogenetic features of the sources and to the soil conditions appropriate to the site" (CEN 2004a). In more plain language, they should come from events with magnitude, fault distance and mechanism of rupture at the source consistent with those of the design seismic action (BSSC 2003, SEAOC 1999, ASCE 2007). The travel

path and the subsoil conditions should preferably resemble those of the site. These requirements are not only hard to meet, but may also conflict with conformity (in the mean) to the target spectrum of the design seismic action. The requirement of CEN (2004a) to scale individual historic or simulated records so that their peak ground acceleration (PGA) matches on average the value of $a_g S$ of the design seismic action may also be considered against physical reality. It is more meaningful, instead, to use individual historic or simulated records with PGA values already conforming to the target value of $a_g S$. Note also that the PGA alone may be artificially increased or reduced, without affecting at all the structural response. So, it is more meaningful to select the records on the basis of conformity of spectral values alone, as described below.

If pairs or triplets of different records are used as input for analysis under two or three concurrent seismic action components, conformity to the target 5%-damped elastic response spectrum may be achieved by scaling the amplitude of the individual records as follows:

- For each earthquake consisting of a triplet of translational components, the records of horizontal components are checked for conformity separately from the vertical one (CEN 2005b).
- The records of the vertical component, if considereded, are scaled so that the average 5%-damped elastic spectra of their ensemble is at least 90% of the 5%-damped vertical spectrum at all periods between $0.2T_v$ and $2T_v$, where T_v is the period of the lowest mode with participation factor of the vertical component higher than those of both horizontal ones (CEN 2005b).
- For analysis in 3D under both horizontal components, the 5%-damped elastic spectra of the two horizontal components in each pair are combined by applying the SRSS rule at each period value. The average of the "SRSS spectra" of the two horizontal components of the individual earthquakes in the ensemble should be at least $0.9\sqrt{2} \approx 1.3$ times ($\sqrt{2} \approx 1.4$ times in (SEAOC 1999, ASCE 2007)) the target 5%-damped horizontal elastic spectrum at all periods from $0.2T_1$ up to $2T_1$ in CEN (2004a) or $1.5T_1$ in BSSC (2003), SEAOC (1999) and ASCE (2007), where T_1 is the lowest natural period of the structure in any horizontal direction. If it isn't, all individual horizontal components are scaled up, so that their final average "SRSS spectrum" exceeds by a factor of 1.3 (or 1.4 in (SEAOC 1999, ASCE 2007)) the target 5%-damped horizontal elastic spectrum everywhere between $0.2T_1$ and $2T_1$ in CEN (2004a) or $1.5T_1$ in BSSC (2003), SEAOC (1999) and ASCE (2007).

For analysis under a single horizontal component, Eurocode 8 (CEN 2004a) requires the mean 5%-damped elastic spectrum of the applied motions not to fall below 90% of that of the design seismic action at any period from $0.2T_1$ to $2T_1$. In BSSC (2003) the lower limit is 100% of the spectrum of the design seismic action at all periods from $0.2T_1$ to $1.5T_1$ (T_1 is the fundamental period in the horizontal direction along which the motion is applied).

If the response is obtained from at least seven nonlinear time-history analyses with (triplets or pairs of) ground motions chosen in accordance with the previous paragraphs, the relevant verifications may use the average of the response quantities from all these analyses as action effect. Otherwise, is should use the most unfavourable value of the response quantity among the analyses.

4.6.2.3 Damping

If the response is indeed elastic, nonlinear and linear response-history analysis should give identical results, even when they are carried out using different algorithms and software tools. Linear response-history analysis should, in turn, produce the same peak SDOF response as given by the elastic response spectrum, normally associated in design codes with viscous damping ratio 5% of critical. Therefore, for consistency across methods as well as with the elastic spectrum to which the input time-histories conform, nonlinear dynamic analysis should have a built-in 5% viscous damping ratio associated with elastic response. Recall that in a design context the upper limit of the elastic regime is defined by yielding of members. So, the 5% viscous damping ratio is considered to encompass all sources of damping up to member yielding, including any structural damping of hysteretic nature, e.g., due to cracking of concrete members and energy dissipation during pre-yield cycles. Hysteretic damping after member yielding should be reflected just by the nonlinear force-deformation laws describing the post-yield behaviour of members in cyclic loading.

Recall that the forces due to viscous damping enter in the equations of motion as $\mathbf{C}\dot{\boldsymbol{U}}$. For convenience of the numerical integration of the nonlinear equations of motion, the damping matrix, $\mathbf{C}$, is typically taken to be of the Rayleigh type,

$$\mathbf{C} = \alpha_{\mathrm{o}}\mathbf{M} + \alpha_1\mathbf{K} \tag{4.19}$$

Rayleigh damping gives a viscous damping ratio ζ at a circular frequency ω equal to:

$$\zeta = \frac{1}{2}\left(\frac{\alpha_o}{\omega} + \alpha_1\omega\right) \tag{4.20}$$

So, the mass-proportional part damps out lower-frequency components and the stiffness-proportional part high-frequency ones. To achieve values of the damping ratio as close as possible to the target value $\zeta = \zeta_{\mathrm{o}} = 0.05$ within the predominant frequency range of the response, one may specify $\zeta = \zeta_{\mathrm{o}}$ at two circular frequencies, ω_1 and ω_2, straddling that range and solve for α_{o} and α_1 to get:

$$\zeta = \frac{\zeta_o}{\omega_1 + \omega_2}\left(\frac{\omega_1\omega_2}{\omega} + \omega\right) \tag{4.20a}$$

For analysis under a single component of the seismic action a good choice for ω_1 is the circular frequency of the mode with the highest modal base shear in the

elastic structure.[6] For concurrent application of the two horizontal components, the average circular frequency in the two modes with the highest modal base shears in two nearly orthogonal horizontal directions may be appropriate. The value of ω_2 may be chosen two to three times ω_1, bracketing the range of the 1st and 2nd modes in both horizontal directions. The resulting viscous damping ratio is lower than $\zeta = \zeta_o = 0.05$ at frequencies between ω_1 and ω_2 and higher outside that range (Chopra 2007). The further away the values of ω_1 and ω_2, the larger is the dip in damping ratio in-between. The minimum damping occurs at $\omega_{min} = \sqrt{(\omega_1 \omega_2)}$ and is equal to $\zeta_{min} = 2\zeta_o \omega_{min}/(\omega_1 + \omega_2)$. However, the closer together ω_1 and ω_2 are, the steeper the increase of damping at higher frequencies.

Hysteretic damping depends on the unloading and reloading rules ("hysteresis rules") adopted for the behaviour of the members after their yielding (see Section 4.10.1.7).

4.6.2.4 Numerical Integration of the Equation of Motion

Nonlinear response-history analysis entails numerical integration of the equation of motion:

$$\boldsymbol{M}\left(\ddot{\boldsymbol{U}} + \sum_j \alpha_{gj} \boldsymbol{e}_j\right) + \boldsymbol{C}\dot{\boldsymbol{U}} + \boldsymbol{F_R} = 0 \tag{4.21}$$

where **M** is the mass matrix (usually diagonal, with masses lumped at the nodes), $\boldsymbol{U}$ is the vector of nodal DoFs relative to the ground, a_{gj} are the acceleration time-histories in the three directions, with $j = 1, 2, 3$ denoting translation along directions X, Y, Z, **C** is the damping matrix, $\boldsymbol{F}_{\mathbf{R}}$ is the vector of resisting forces and vectors $\boldsymbol{e}_j$ have the value 1 at DoF j of each node and 0 at all others. Usually the time-step for the numerical integration, $\Delta t = t_{i+1} - t_i$, is chosen the same as the discretisation interval of the ground acceleration $a_{gj}(t)$ (typically 0.01 s), or one-half of it. Only implicit integration schemes, which are unconditionally stable for linear systems, are appropriate for such a long Δt. For the same stability performance the simpler and computationally efficient explicit schemes, like the central difference method, require a much shorter time-step. They are more appropriate for the analysis of fast transients or wave propagation problems, whose accurate description requires anyway a very short Δt.

Although the engine for the integration of the equation of motion is normally a black box for the user of nonlinear analysis software, the choice among numerical integration schemes and/or of their parameters is often left to him/her. As numerical instabilities in nonlinear response-history analyses are not rare (especially when the number of DoFs is very large and the analysis is carried out for many

[6] An eigenvalue analysis of the elastic structure should precede the nonlinear dynamic one anyway, for insight into the predominant features of the expected response.

ground motions), the user should pay special attention to the choice of numerical integration scheme.

Two widely used schemes, both unconditionally stable for linear systems, are (Chopra 2007):

- Newmark's average acceleration method (Newmark 1959), and
- Wilson's ϑ method.

In Newmark's average acceleration method $\ddot{\boldsymbol{U}}$ is taken constant within Δt : $\ddot{\boldsymbol{U}} = \ddot{\boldsymbol{U}}_{\mathrm{i}} + 0.5\Delta\ddot{\boldsymbol{U}}_{\mathrm{i}}$ giving velocity and displacement at $t_{\mathrm{i+1}}$: $\dot{\boldsymbol{U}}_{i+1} = \dot{\boldsymbol{U}}_i + (\ddot{\boldsymbol{U}}_i + 0.5\Delta\ddot{\boldsymbol{U}}_i)\Delta\boldsymbol{t}$, $\boldsymbol{U}_{i+1} = \boldsymbol{U}_i + (\dot{\boldsymbol{U}}_i + 0.5(\ddot{\boldsymbol{U}}_i + 0.5\Delta\dot{\boldsymbol{U}}_i)\Delta\boldsymbol{t})\Delta\boldsymbol{t}$. Substituting in the incremental equation of motion between t_{i} and $t_{\mathrm{i+1}}$, one obtains for $\Delta\boldsymbol{U}_{\mathrm{i}} = \boldsymbol{U}_{\mathrm{i+1}} - \boldsymbol{U}_{\mathrm{i}}$:

$$\mathbf{K}_{\mathrm{i}}^{*}\Delta\boldsymbol{U}_{\mathrm{i}} = \Delta\boldsymbol{F}_{\mathrm{i}}^{*} \tag{4.22}$$

with:

$$\boldsymbol{K}_i^{*} = \boldsymbol{K}_i + \frac{2}{\Delta\boldsymbol{t}}\left(\boldsymbol{C} + 2\frac{\boldsymbol{M}}{\Delta\boldsymbol{t}}\right),\ \Delta\boldsymbol{F}_i^{*} = 2\left(\boldsymbol{C} + 2\frac{\boldsymbol{M}}{\Delta\boldsymbol{t}}\right)\dot{\boldsymbol{U}}_i + 2\boldsymbol{M}\ddot{\boldsymbol{U}}_i - \boldsymbol{M}\sum_j \Delta\alpha_{gj}\boldsymbol{e}_j \tag{4.23a}$$

where $\mathbf{K}_{\mathrm{i}}$ is the tangent stiffness matrix at time t_{i}. Equation (4.22) is solved with equilibrium iterations, until the unbalanced load vector (i.e., the difference between the generalised external nodal forces and the internal ones calculated from member deformations) becomes less than a specified tolerance. During iterations and after convergence $\boldsymbol{U}_{\mathrm{i+1}}$, $\dot{\boldsymbol{U}}_{i+1}$ and $\ddot{\boldsymbol{U}}_{\mathrm{i+1}}$ are computed (for use in the next step) by adding $\Delta\boldsymbol{U}_{\mathrm{i}}$, $\Delta\dot{\boldsymbol{U}}_i = 2(\Delta\boldsymbol{U}_i/\Delta\boldsymbol{t} - \dot{\boldsymbol{U}}_i)$, $\Delta\ddot{\boldsymbol{U}}_{i+1} = 2\left(2\left(\Delta\boldsymbol{U}_i/\Delta\boldsymbol{t} - \dot{\boldsymbol{U}}_i\right)/\Delta\boldsymbol{t} - \ddot{\boldsymbol{U}}_i\right)$ to $\boldsymbol{U}_{\mathrm{i}}$, $\dot{\boldsymbol{U}}_i$ and $\ddot{\boldsymbol{U}}_{\mathrm{i}}$, respectively.

In Wilson's ϑ-method the nodal acceleration, $\Delta\ddot{\boldsymbol{U}} = \ddot{\boldsymbol{U}} - \ddot{\boldsymbol{U}}_{\mathrm{i+1}}$ and the input accelerations, $\Delta a_{\mathrm{gj}}(t)$ are taken linear functions of $t - t_{\mathrm{i}}$ up to time $t_{\mathrm{i}} + \vartheta\Delta t > t_{\mathrm{i+1}}$ (with $\vartheta > 1$). Then $\mathbf{K}_{\mathrm{i}}{}^{*}$ and $\delta\boldsymbol{F}_{\mathrm{i}}{}^{*}$ (which refers to $\delta\boldsymbol{U}_{\mathrm{i}}$, from t_{i} to $t_{\mathrm{i}} + \vartheta\Delta t$) become:

$$\begin{aligned}
&\boldsymbol{K}_i^{*} = \boldsymbol{K}_i + \frac{3}{\vartheta\Delta\boldsymbol{t}}\left(\boldsymbol{C} + 2\frac{\boldsymbol{M}}{\vartheta\Delta\boldsymbol{t}}\right),\\
&\delta\boldsymbol{F}_i^{*} = 3\left(\boldsymbol{C} + 2\frac{\boldsymbol{M}}{\vartheta\Delta\boldsymbol{t}}\right)\dot{\boldsymbol{U}}_i + \left(3\boldsymbol{M} + \frac{\vartheta\Delta\boldsymbol{t}}{2}\boldsymbol{C}\right)\ddot{\boldsymbol{U}}_i - \vartheta\boldsymbol{M}\sum_j \Delta\ddot{\boldsymbol{u}}_{gj}\alpha_j
\end{aligned} \tag{4.23b}$$

After solving $\mathbf{K}_{\mathrm{i}}{}^{*}\delta\boldsymbol{U}_{\mathrm{i}} = \delta\boldsymbol{F}_{\mathrm{i}}{}^{*}$ for $\delta\boldsymbol{U}_{\mathrm{i}}$, the expression for $\delta\boldsymbol{U}_{\mathrm{i}}$ in terms of $\delta\ddot{\boldsymbol{U}}_{\mathrm{i}}$ is solved for $\delta\ddot{\boldsymbol{U}}_i = 6(\delta\boldsymbol{U}_i/\vartheta\Delta\boldsymbol{t} - \dot{\boldsymbol{U}})/\vartheta\Delta\boldsymbol{t} - 3\ddot{\boldsymbol{U}}_i$, giving $\Delta\ddot{\boldsymbol{U}}_{\mathrm{i}} = \delta\ddot{\boldsymbol{U}}_{\mathrm{i}}/\vartheta$, and then $\Delta\dot{\boldsymbol{U}}_i = (\ddot{\boldsymbol{U}}_i + 0.5\Delta\ddot{\boldsymbol{U}}_i)\Delta t$, $\Delta\boldsymbol{U}_i = (\dot{\boldsymbol{U}}_i + 0.5(\ddot{\boldsymbol{U}}_i + \Delta\ddot{\boldsymbol{U}}_i/3)\Delta\boldsymbol{t})\Delta\boldsymbol{t}$, to be used to compute $\boldsymbol{U}_{\mathrm{i+1}}$, $\dot{\boldsymbol{U}}_{i+1}$, $\ddot{\boldsymbol{U}}_{\mathrm{i+1}}$.

Wilson's method introduces numerical damping which eliminates spurious high frequency response. For $\vartheta \geq 1.37$ it is unconditionally stable for linear systems and for $\vartheta = 1.42$ it gives optimal accuracy for them.

4.6.3 Concluding Remarks on the Nonlinear Analysis Methods

Thanks to its simplicity and intuitiveness and the wide availability of reliable and user-friendly analysis software, the standard form of pushover analysis, as described in Sections 4.6.1.2, 4.6.1.3 and 4.6.1.4 and in Fajfar (2000) (i.e., without the "adaptive" options for the lateral load pattern or higher mode and torsional effects, not even as highlighted in Sections 4.6.1.5 and 4.6.1.6), has become the workhorse of practical nonlinear seismic response analysis. It should be kept in mind, though, that it has been developed for 2D analysis under a single horizontal component of the seismic action and applies under such conditions alone, and even then only when the effects of higher modes are unimportant. This restricts its application to height-wise regular low-rise buildings, almost fully symmetric about an axis parallel to the seismic action component considered. The ways proposed to take into account 3D and torsional effects or higher modes, e.g., according to Sections 4.6.1.5 and 4.6.1.6, respectively, have not been sufficiently validated so far and are not widely accepted yet. The same applies for the concurrent application of both horizontal components of the seismic action (see last paragraph of Section 4.7.1). Last, but not least, there is certain ambiguity in the determination of the seismic demand. The approach in Section 4.6.1.3, Eqs. (4.18), is just one way to determine the "target displacement" for given elastic spectrum. There other approaches that may yield very different answers.

Unlike the static method of nonlinear analysis, the dynamic one does not require approximate a-priori determination of the global nonlinear seismic demand (like the "target displacement" of pushover analysis). Global displacement demands are determined in the course of the analysis of the response and are free of ambiguities, such as that about the "target displacement" in pushover analysis. Torsional, 3D and higher mode effects are fully accounted for, as well as concurrent application of two or three seismic action components. Note, also, that, unlike the modal response spectrum analysis, which provides only (statistically) best estimates of the peak response (via the SRSS or CQC rules), peak response quantities determined via nonlinear dynamic analysis are exact, even under concurrent seismic action components (within, of course, the limits of nonlinear modelling and of its capability to represent well the structure). Last, but not least, nonlinear dynamic analysis provides estimates not only of peak deformations, which are important for the overall safety and integrity of the structure, but of residual ones as well, which are the most meaningful measure of damage and, hence, very important for performance-based design or assessment.

Limitations of nonlinear dynamic analysis are:

- its sophistication and lack of familiarity among practitioners;
- the lack of simple and numerically stable, yet fairly accurate, models for vertical members in 3D analysis (see Section 4.10.1.8); and,
- certain sensitivity of the outcome to the choice of input ground motions, which is at the absolute discretion of the engineer.

The second drawback plagues static and dynamic nonlinear analysis alike (only that static nonlinear analysis does not apply well under 3D conditions, anyway). However, continuous progress in the state of the art and practice will reduce with time the importance of this and of the first drawback. The third limitation often raises doubts about the outcome of nonlinear dynamic analysis. It is possible (although not very likely, unless there is intention) to arrive at one conclusion using one ensemble of input motions meeting the requirements set out by codes and standards (see Section 4.6.2.2) and to another with a different set of equally legitimate motions. Standardisation of motions to resolve this question is too rigid a straitjacket, running, among others, against the continuous evolution of scientific knowledge and information on ground motion.

Despite its current limitations, nonlinear dynamic analysis is bound to become in the long run the technique of choice for practical nonlinear analysis, eclipsing the static version, which may end up being remembered as just an interlude that paved the way of nonlinear dynamic analysis into everyday practice.

4.7 Combination of the Maximum Effects of the Individual Seismic Action Components

4.7.1 The Two Options: The SRSS and the Linear Approximation

The two horizontal components of the seismic action, as well as the vertical component (when taken into account), are considered to act concurrently on the structure.

In planwise regular buildings with completely independent lateral-force-resisting systems along two orthogonal horizontal directions, the seismic action component in each one of these directions does not produce (significant) seismic action effects in the lateral-force-resisting systems of the orthogonal direction. For this reason, if in such buildings the independent lateral-force-resisting systems in the two horizontal directions consist solely of walls, Eurocode 8 (CEN 2004a) does not require combining the effects of the two horizontal components of the seismic action.

Simultaneous occurrence of more than one component can be handled rigourously only in time-history analysis (which is normally nonlinear). Such an analysis is carried out with the two horizontal components (and the vertical one, if taken into account) acting simultaneously. All other methods of analysis (i.e., the two linear approaches and nonlinear static analysis) give only estimates of the peak value of seismic action effects during the response to a single component. These estimates are denoted here as E_X and E_Y for the two horizontal components (considered to include also the effect of the associated accidental eccentricities, see Section 4.8) and E_Z for the vertical component. The peak values of the seismic action effects do not take place simultaneously. So, a combination of the type: $E = E_X + E_Y + E_Z$ is overly conservative for the expected value of the peak seismic action effect, E, under

three concurrent components. Design codes adopt more representative, probability-based combination rules for the estimation of E.

The reference rule for the combination of the peak values of seismic action effects, E_X, E_Y, E_Z, computed for separate action of the individual components is the SRSS rule in (Smebby and Der Kiureghian 1985):

$$E = \pm\sqrt{E_X^2 + E_Y^2 + E_Z^2} \tag{4.24}$$

If E_X, E_Y, E_Z are computed via the modal response spectrum method by combining modal contributions to each one of them via the CQC rule, Eq. (4.11), and, besides, the seismic action components in directions X, Y, Z are statistically independent, the outcome of Eq. (4.24) in an elastic structure is indeed the expected value of the peak seismic action effect, E, under concurrent seismic action components. Under these conditions, the result from Eq. (4.24) is also independent of the choice of horizontal directions X and Y. In other words, if a single modal response spectrum analysis is carried out covering all three components, X, Y, Z, at the same time and modal contributions for each component are combined via the CQC rule, Eq. (4.24) gives the expected value of the peak elastic seismic action effect, E, for all members of the structure, no matter the choice of directions X and Y. In this simple way Eq. (4.24) automatically fulfils an – at first sight – onerous requirement of Eurocode 8 for buildings with resisting elements not in two perpendicular directions (hence with no obvious choice for the two directions X and Y as main or principal ones): to apply the two horizontal components along all relevant horizontal directions, X, and the orthogonal direction, Y.

Eurocode 8 (CEN 2004a) adopts the combination rule of Eq. (4.24) as the reference, not only under the conditions for which it has been developed as an exact rule (namely for modal response spectrum analysis with modal contributions combined via the CQC rule), but also for linear static analysis (the lateral force method of Section 4.3 for the horizontal components and the method in Section 4.5.2 for the vertical component, if considered), modal response spectrum analysis with modal contributions combined via the SRSS rule, or even pushover analysis.

US codes (BSSC 2003, SEAOC 1999) have opted for the linear superposition rule:

$$E = \pm\{E_X + \lambda E_Y + \lambda E_Z\} \tag{4.25a}$$

$$E = \pm\{\lambda E_X + E_Y + \lambda E_Z\} \tag{4.25b}$$

$$E = \pm\{\lambda E_X + \lambda E_Y + E_Z\} \tag{4.25c}$$

A value $\lambda \approx 0.275$ provides the best average agreement with the result of Eq. (4.24) in the range of possible positive values of E_X, E_Y, E_Z. This optimal value has been rounded to $\lambda = 0.3$ in BSSC (2003) and SEAOC (1999). Equations (4.25)

may underestimate the result of Eq. (4.24) by less than 9% (when E_X, E_Y, E_Z are about equal) and may overestimate it by not more than 8% (when two of the three seismic action effects are an order of magnitude less than the third).

Eurocode 8 (CEN 2004a) accepts Eq. (4.25) with $\lambda = 0.3$ as alternative to the reference rule of Eq. (4.24).

If dimensioning is based on a single, one-component stress resultant, as, e.g., for beams in bending or shear, the outcome of Eq. (4.24), or the maximum value among the three alternatives in Eq. (4.25) should be added to, or subtracted from, the action effect of the gravity loads which are concurrent with the design seismic action. Then Eqs. (4.24) and (4.25) give approximately the same design.

Equations (4.24) and (4.25) can be applied also in nonlinear static (pushover) analysis, but only to combine peak displacement and deformation results due to the two horizontal components (the vertical component is irrelevant in that case). Peak internal forces may be combined in the same way only if they are still in the elastic range of the corresponding force-deformation relation. Otherwise, this relation should be used to determine the peak internal forces due to the two horizontal components from the corresponding peak deformation estimated through Eq. (4.24) or (4.25).

4.7.2 Combination of the Effects of the Seismic Action Components in Dimensioning for Vectorial Action Effects

Often dimensioning of a member section or region is carried out for two or three concurrent stress-resultants. Vertical members, for instance, are dimensioned for uniaxial or biaxial bending with axial force and for uniaxial shear with axial force (possibly depending also on the bending moment through the moment-to-shear ratio). It is convenient to consider the seismic action effects that enter such dimensioning as arranged in a vector (array) of dimension 3 for biaxial bending with axial force, 2 for shear with axial force or uniaxial bending with axial force, etc. One of the stress-resultants in that vector should be chosen as the main one, with the others considered as accompanying. For instance, when dimensioning in shear, the shear force may be the main stress-resultant and the axial force and the bending moment the accompanying ones. For uniaxial bending with axial force, the main component is always the moment. In columns under biaxial bending with axial force, the main component is one of the two components of bending moment, chosen as follows: the bending moments are normalised to a measure of the section's moment resistance so that they become independent of it size (e.g., to $A_c h$ with A_c being the cross-sectional area and h its depth for the bending moment considered); then the bending moment with the largest normalised value is the main component.

In dimensioning for multi-component action effects the application of Eqs. (4.24) and Eq. (4.25) may not be so straightforward and may lead to markedly different designs, depending on how the issues of signs and of simultaneity of peak values of

different stress-resultants are addressed. The following sections elaborate different cases and options for the application of Eqs. (4.24) or (4.25) in that case. The implications of the different options are exemplified at the end of each section for a column with centroidal axes y and z parallel to the horizontal components of the seismic action, X and Y, assuming that these components excite exclusively the 1st translational mode in each direction. To eliminate the effect of differences due to the analysis method and focus on the combination rule, it is also assumed that any analysis method produces the same values for the action effects and that we have nearly uniaxial bending, i.e.: $E_X = [M_{y,X}, M_{z,X}, N_X]^T$ with $M_{y,X} >> M_{z,X}$, $E_Y = [M_{y,Y}, M_{z,Y}, N_Y]^T$ with $M_{y,Y} << M_{z,Y}$. The vertical effect of the component of the seismic action is neglected in this illustration: $E_Z \approx [0, 0, 0]^T$.

4.7.2.1 The Linear Approximation with Linear Static Analysis

In each one of the three alternatives of Eq. (4.25), e.g. in $E_X + \lambda E_Y + \lambda E_Z$ for Eq. (4.25a), the seismic action components Y and Z are taken with a sense of action (positive or negative) such that, when component X acts in the positive sense, the contributions of λE_Y and λE_Z to the main component in the vector have the same sign as that of E_X. The signs of the three terms E_X, λE_Y, λE_Z in the sum $E_X + \lambda E_Y + \lambda E_Z$ for the accompanying components (elements of the vector) are controlled by the sense (positive or negative) of the corresponding component, X, Y, or Z, of the seismic action, as this sense is determined from the sign of E_X in the main component of the vector of seismic action effects. As a result, the vector of seismic action effects for $E_X + \lambda E_Y + \lambda E_Z$ assumes only two equal and opposite values. The same applies for Eqs. (4.25b) and (4.25c).

If the main component is the same in all three multi-component action effect vectors of the three versions of Eq. (4.25) (e.g., in dimensioning for shear with axial force and bending moment, or for uniaxial bending with axial force), then the vector to be used as E is normally the one of the three with the largest (absolute) value of the main component. So, there are just two cases for E. If the main component has about equally large values in two of the vectors, both of them are considered as potentially critical and we should consider $2 \times 2 = 4$ cases for E. If it has about equally large values in all three vectors, there are $2 \times 3 = 6$ cases for E.

If the main component is not the same in all three vectors of the three alternatives in Eq. (4.25) (e.g. in biaxial bending with axial force), then the two vectors where each of these two different main components clearly assumes its largest (absolute) value should be considered as potentially critical. Then we have $2 \times 2 = 4$ cases for E. If the choice is not clear, all three vectors of the three alternatives in Eq. (4.25) are potentially critical and there are $2 \times 3 = 6$ cases for E. If in a single one of the three vectors both of the two main components are clearly (absolutely) larger than in the two other vectors, that vector is the single possible choice for E and just two different cases are considered for E.

In the example case of the column, such an application of Eq. (4.25) gives the following four vectors $\boldsymbol{E}$:

$$\pm\,[M_{y,X} + \text{sign}(M_{y,X}M_{y,Y})\lambda M_{y,Y},\quad M_{z,X} + \text{sign}(M_{y,X}M_{y,Y})\lambda M_{z,Y},$$
$$N_X + \text{sign}(M_{y,X}M_{y,Y})\lambda N_Y]^T,$$

$$\pm\,[M_{y,Y} + \text{sign}(M_{z,X}M_{z,Y})\lambda M_{y,X},\quad M_{z,Y} + \text{sign}(M_{z,X}M_{z,Y})\lambda M_{z,X},$$
$$N_Y + \text{sign}(M_{z,X}M_{z,Y})\lambda N_X]^T,$$

where "sign($M_{y,X}M_{y,Y}$)" is the sign of the product of $M_{y,X}$ and $M_{y,Y}$ (similarly for "sign($M_{z,X}M_{z,Y}$)").

4.7.2.2 The Linear Approximation with Modal Response Spectrum Analysis

Modal response spectrum analysis gives positive peak values for all seismic action effects, without any correspondence between the peak value of a seismic action stress resultant and the concurrent values of the other two. The only possible way to combine these stress resultants is to consider their peak values as concurrent and combine them with the same sign in each one of the three alternatives of Eq. (4.25) – because that's how Eq. (4.25) is an approximation to Eq. (4.24) for $\lambda = 0.3$. This gives $3 \times 2^3 = 24$ combinations of signs for the three stress resultants in the vector $\boldsymbol{E}$, namely the following, for biaxial bending with normal force:

$$M_y = \pm\left(|M_{y,X}| + \lambda|M_{y,Y}| + \lambda|M_{y,Z}|\right),\ M_z = \pm\left(|M_{z,X}| + \lambda|M_{z,Y}| + \lambda|M_{z,Z}|\right),$$
$$N = \pm\left(|N_X| + \lambda|N_Y| + \lambda|N_Z|\right) \tag{4.26a}$$

$$M_y = \pm\left(\lambda|M_{y,X}| + |M_{y,Y}| + \lambda|M_{y,Z}|\right),\ M_z = \pm\left(\lambda|M_{z,X}| + |M_{z,Y}| + \lambda|M_{z,Z}|\right),$$
$$N = \pm\left(\lambda|N_X| + |N_Y| + \lambda|N_Z|\right) \tag{4.26b}$$

$$M_y = \pm\left(\lambda|M_{y,X}| + \lambda|M_{y,Y}| + |M_{y,Z}|\right),\ M_z = \pm\left(\lambda|M_{z,X}| + \lambda|M_{z,Y}| + |M_{z,Z}|\right),$$
$$N = \pm\left(\lambda|N_X| + \lambda|N_Y| + |N_Z|\right) \tag{4.26c}$$

For the example of the column this way of applying Eq. (4.25) gives the following 16 vectors $\boldsymbol{E}$:

$$[\pm(|M_{y,X}| + \lambda|M_{y,Y}|),\quad \pm(|M_{z,X}| + \lambda|M_{z,Y}|),\quad \pm(|N_X| + \lambda|N_Y|)]^T,$$
$$[\pm(|M_{y,Y}| + \lambda|M_{y,X}|),\quad \pm(|M_{z,Y}| + \lambda|M_{z,X}|),\quad \pm(|N_Y| + \lambda|N_X|)]^T.$$

The main difference with the approach in Section 4.7.2.1 is that we lose the correspondence between the signs of different stress resultants, notably of bending moments and axial forces in the same element or of the axial forces in different elements (see Sections 5.7.3.5 and 5.7.4.1 for the implications). This may be a more serious handicap of Eq. (4.25) when used with modal response spectrum analysis,

than the large number of different vectors taken in the dimensioning in order to consider all possible combinations of signs.

4.7.2.3 SRSS Rule with Modal Response Spectrum Analysis

When applied for the calculation of each stress-resultant in the vector of seismic action effects for the dimensioning of a member section or region, Eq. (4.24) gives the expected value of the peak stress-resultant during the response to the (three) simultaneous components of the seismic action. The peak values of the individual stress resultants do not take place concurrently. If it is assumed they do, the design is safe-sided but probably too conservative.

Eurocode 8 allows using more accurate rules for the estimation of the most probable value of the seismic action effect that takes place concurrently with the expected value of the maximum of each one of the two (or more) stress-resultants that enter the dimensioning of a member section or region. A rule of this type is described in this section, with reference to biaxial bending with moments M_y and M_z (defined with respect to the local axes y and z of the cross-section) and axial force N. This is a fairly general case, not only as far as the dimension of the vector of stress-resultants is concerned, but also in that either M_y or M_z may be the "main component" of this vector, depending on their (normalised) magnitude. Uniaxial bending with axial force, M_y-N, and uniaxial shear, V_y, with axial force and bending moment, N and M_z, are special cases, with only one of the stress-resultants (V_y and M_z, respectively) being the "main component" of the vector.

Equation (4.24), should be applied at the lowest possible level at which the verification is carried out. For biaxial bending with axial force, this means to the strains of the extreme concrete fibres in the section. This is not feasible, as seismic action effects are calculated through modal response spectrum analysis separately from the nonlinear plane-section analysis. So, extreme combinations of M_y, M_z and N should be sought (rather than extreme but separate values of M_y, M_z, N) which lead, in good approximation, to the SRSS result at the final, e.g., fibre strain, level. It has been shown in Gupta and Singh (1977) that, if the seismic action effect of interest is a scalar which is a linear function of M_y, M_z and N, then the M_y-M_z-N combinations that lead to the expected peak value of this effect under the (three) concurrent components of the seismic action satisfy the condition:

$$\mathbf{E}^{\mathbf{T}}\mathbf{C}^{-1}\,\mathbf{E} = \mathbf{I} \tag{4.27}$$

In Eq. (4.27) $\mathbf{I}$ is the identity matrix, $\boldsymbol{E}$ is the vector $[M_y\ M_z\ N\ ]^T$ and $\mathbf{C}$ is its covariance matrix:

$$\mathbf{C} = \begin{bmatrix} M_{y,\max}^2 & \mathrm{cov}(M_y, M_z) & \mathrm{cov}(M_y, N) \\ & M_{z,\max}^2 & \mathrm{cov}(M_z, N) \\ symmetric & & N_{\max}^2 \end{bmatrix} \tag{4.28}$$

with:

$$M_{y,\max}^2 = \sum_i \sum_j \rho_{ij}(M_{y,iX}M_{y,jX} + M_{y,iY}M_{y,jY} + M_{y,iZ}M_{y,jZ}) = M_{y,X}^2 + M_{y,Y}^2 + M_{y,Z}^2 \tag{4.29}$$

$$M_{z,\max}^2 = \sum_i \sum_j \rho_{ij}(M_{z,iX}M_{z,jX} + M_{z,iY}M_{z,jY} + M_{z,iZ}M_{z,jZ}) = M_{z,X}^2 + M_{z,Y}^2 + M_{z,Z}^2 \tag{4.30}$$

$$N_{\max}^2 = \sum_i \sum_j \rho_{ij}(N_{iX}N_{jX} + N_{iY}N_{jY} + N_{iZ}N_{jZ}) = N_X^2 + N_Y^2 + N_Z^2 \tag{4.31}$$

$$\operatorname{cov}(M_y, M_z) = \sum_i \sum_j \rho_{ij}(M_{y,iX}M_{z,jX} + M_{y,iY}M_{z,jY} + M_{y,iZ}M_{z,jZ}) \tag{4.32}$$

$$\operatorname{cov}(M_y, N) = \sum_i \sum_j \rho_{ij}(M_{y,iX}N_{jX} + M_{y,iY}N_{jY} + M_{y,iZ}N_{jZ}) \tag{4.33}$$

$$\operatorname{cov}(M_z, N) = \sum_i \sum_j \rho_{ij}(N_{iX}M_{z,jX} + N_{iY}M_{z,jY} + N_{iZ}M_{z,jZ}) \tag{4.34}$$

In Eqs. (4.29), (4.30), (4.31), (4.32), (4.33) and (4.34) X, Y or Z index the effects due to the seismic action component X, Y, or Z, respectively, i and j index normal modes, while ρ_{ij} is their correlation coefficient, as given, e.g. from Eqs. (4.9). Modal seismic effects $M_{y,iX}$, etc., are computed as the product of the participation factor of mode i for the seismic action component in direction X, times the stress resultant M_y in mode i from the eigenvector of the mode scaled to the corresponding spectral displacement. $M_{y,\max}$, $M_{z,\max}$ and $N_{\max}$ from Eqs. (4.29), (4.30) and (4.31) are the expected values of the peak stress resultants under the three-component seismic action according to Eq. (4.24).

Values of the vector $[M_y\ M_z\ N]^T$ satisfying Eq. (4.27) lie on an ellipsoidal surface in the space M_y-M_z-N. It is usually sufficient to consider only the six points on this surface corresponding to algebraically maximum and minimum values of one of the stress resultants, M_y, M_z, N, and to the corresponding concurrent values of the two others. With $M_{y,\max}$, $M_{z,\max}$ and $N_{\max}$ taken positive, these six triplets are:

$$\pm\left(M_{y,\max} = \sqrt{M_{y,X}^2 + M_{y,Y}^2 + M_{y,Z}^2},\ \frac{\operatorname{cov}(M_y, M_z)}{M_{y,\max}},\ \frac{\operatorname{cov}(M_y, N)}{M_{y,\max}}\right) \tag{4.35}$$

$$\pm\left(\frac{\operatorname{cov}(M_y, M_z)}{M_{z,\max}},\ M_{z,\max} = \sqrt{M_{z,X}^2 + M_{z,Y}^2 + M_{z,Y}^2},\ \frac{\operatorname{cov}(M_z, N)}{M_{z,\max}}\right) \tag{4.36}$$

$$\pm\left(\frac{\operatorname{cov}(M_y, N)}{N_{\max}},\ \frac{\operatorname{cov}(M_z, N)}{N_{\max}},\ N_{\max} = \sqrt{N_X^2 + N_Y^2 + N_Z^2}\right) \tag{4.37}$$

As $\operatorname{cov}(M_y, M_z)$, $\operatorname{cov}(M_y, N)$, and $\operatorname{cov}(M_z, N)$ have signs, the two stress resultants which take place concurrently with the maximum of the third one also have signs.

If:

- only the two bending moments, M_y and M_z, are taken as main components of $[M_y\ M_z\ N]^T$, and
- only the cases when the absolute value of a main component is maximum are of interest,

then only the four different values from Eqs. (4.35) and (4.36) need to be considered as the values of E from Eq. (4.24). This is the case in the column example, where this way of applying Eq. (4.24) gives the following four vectors $\boldsymbol{E}$:

$$\begin{aligned}
&\pm [\sqrt{(M_{y,X}^2 + M_{y,Y}^2)}, (M_{y,X}M_{z,X} + M_{y,Y}M_{z,Y})/\sqrt{(M_{y,X}^2 + M_{y,Y}^2)},\\
&\quad (M_{y,X}N_X + M_{y,Y}N_Y)/\sqrt{(M_{y,X}^2 + M_{y,Y}^2)}]^T\\
&\pm [(M_{y,X}M_{z,X} + M_{y,Y}M_{z,Y})/\sqrt{(M_{z,X}^2 + M_{z,Y}^2)}, \sqrt{(M_{z,X}^2 + M_{z,Y}^2)},\\
&\quad (M_{z,X}N_X + M_{z,Y}N_Y)/\sqrt{(M_{z,X}^2 + M_{z,Y}^2)}]^T
\end{aligned}$$

4.7.2.4 SRSS Rule with Linear Static Analysis

Calculation of E_X, E_Y, E_Z by linear static analysis corresponds to taking a single normal mode for each component of the seismic action, i.e. to using in Eqs. (4.29), (4.30), (4.31), (4.32), (4.33) and (4.34) i=1, j=2, ρ_{11}=1, ρ_{22}=1, ρ_{12}=0. Then Eqs. (4.35), (4.36) and (4.37) give the following six triplets (M_y, M_z, N):

$$\pm \left(M_{y,\max} = \sqrt{M_{y,X}^2 + M_{y,Z}^2 + M_{y,Z}^2},\ M_z = \frac{M_{y,X}M_{z,X} + M_{y,Y}M_{z,Y} + M_{y,Z}M_{z,Z}}{M_{y,\max}},\ N = \frac{M_{y,X}N_X + M_{y,Y}N_Y + M_{y,Z}N_Z}{M_{y,\max}} \right) \tag{4.38}$$

$$\pm \left(M_y = \frac{M_{y,X}M_{z,X} + M_{y,Y}M_{z,Y} + M_{y,Z}M_{z,Z}}{M_{z,\max}},\ M_{z,\max} = \sqrt{M_{z,X}^2 + M_{z,,Y}^2 + M_{z,Y}^2},\ N = \frac{M_{z,X}N_X + M_{z,Y}N_Y + M_{z,Z}N_Z}{M_{z,\max}} \right) \tag{4.39}$$

$$\pm \left(M_y = \frac{M_{y,X}N_X + M_{y,Y}N_Y + M_{y,Z}N_Z}{N_{\max}},\ M_z = \frac{M_{z,X}N_X + M_{z,Y}N_Y + M_{z,Z}N_Z}{N_{\max}},\ N_{\max} = \sqrt{N_X^2 + N_Y^2 + N_Z^2} \right) \tag{4.40}$$

If only M_y and M_z are taken as main components and just the cases where the absolute value of a main component is maximum are of interest, only the four triplets from Eqs. (4.38), (4.39) will be considered as values of $\boldsymbol{E}$ from Eq. (4.24).

In the column example Section 4.7.2.4 gives the same result as 4.7.2.3, if there are no differences due to the analysis method.

4.7.2.5 Concluding Remarks

The different values of $\boldsymbol{E}$ from any one of the four approaches above should be superimposed to the vector of stress-resultants due to gravity loads considered concurrent with the design seismic action. This gives the vector of stress-resultants for dimensioning. Apart from any difference between the seismic effects from a modal response spectrum analysis or a linear static one, the four approaches in Sections 4.7.2.1, 4.7.2.2, 4.7.2.3 and 4.7.2.4 do not lead normally to very different designs. So, the criteria for selecting which one to apply should be their computational convenience and soundness from the theoretical point of view.

If a modal response spectrum analysis is used, application of Eq. (4.24) the way proposed in Section 4.7.2.3 (which also entails combining modal responses through the CQC rule) is the most sound and computationally convenient approach and leads to economic designs. For this method of analysis, the straightforward application of Eq. (4.25) according to Section 4.7.2.2 is less sound. Besides, it gives many more combinations of stress resultants for dimensioning, some of which are physically meaningless. So, it is computationally inconvenient and may lead to less economic designs.

If linear static analysis is used, application of Eq. (4.24) according to Section 4.7.2.4 is sound and computationally convenient and leads to economic designs. Application of Eq. (4.25) as proposed in Section 4.7.2.1 is a plausible, computationally convenient and economic alternative. It is also physically appealing, as it preserves the correspondence of signs of stress resultants and retains the notion of separate seismic action components, with $E_X + \lambda E_Y + \lambda E_Z$ considered as governed by the horizontal component in direction X, $\lambda E_X + E_Y + \lambda E_Z$ by that in Y and $\lambda E_X + \lambda E_Y + E_Z$ by the vertical component.

The combination of the seismic action effects of the different components according to Section 4.7.2.3 should be integrated in the modal response spectrum analysis. In all other cases these seismic action effects may also be combined after the analysis, just before their use for member dimensioning or verification. This is very convenient, as it can be done with a post-processing module, independently of the analysis software.

The – unfortunately not uncommon in practice – application of Eq. (4.24) to all stress resultants, taking the computed peak response estimates as simultaneous, is overly conservative. For the case of column biaxial bending with normal force addressed in Sections 4.7.2.1, 4.7.2.2, 4.7.2.3 and 4.7.2.4, this would give the following eight values of $\boldsymbol{E}$:

$$\left(\pm M_{y,\max} = \pm\sqrt{M_{y,X}^2 + M_{y,Z}^2 + M_{y,Z}^2}, \pm M_{z,\max} = \pm\sqrt{M_{z,X}^2 + M_{z,Y}^2 + M_{z,Y}^2},\right.$$
$$\left.\pm N_{\max} = \pm\sqrt{N_X^2 + N_Y^2 + N_Z^2}\right)$$

with the individual seismic action effects computed by either a linear static or a modal response spectrum analysis. Such an approach is irrational – despite its presumption of soundness – and leads to very uneconomic designs.

4.8 Analysis for Accidental Torsional Effects

4.8.1 Accidental Eccentricity

When the planwise distribution of stiffness or mass is asymmetric, the response to the horizontal components of the seismic action includes torsional-translational coupling. Analysis in 3D for the horizontal components takes this coupling into account in a satisfactory way, especially in modal response spectrum or nonlinear dynamic analysis.

Some seismic design codes attempt to take into account amplification or de-amplification of the static or "natural" eccentricity between the centres of mass and stiffness during the dynamic response (see Figs. 2.22, 4.14 and 4.19 for examples of this eccentricity). This is very inconvenient for the analysis, as normally the storey stiffness centre cannot be uniquely defined (see Section 2.1.5). Locating a conventionally defined storey stiffness centre is not worth the effort of the tedious additional analyses required to achieve the accuracy and sophistication consistent with a dynamic amplification of static eccentricities.

In a building with full planwise symmetry of stiffness and nominal masses the analysis for the horizontal components of the seismic action produces no torsional response at all. However, a conventional seismic response analysis cannot capture possible variations in the stiffness or mass distribution from the nominal one, or a possible torsional component of the ground motion about the vertical. Such effects may produce torsional response even for a nominally fully symmetric building. To ensure a minimum of torsional resistance and stiffness and limit the consequences of unforeseen torsional response, most seismic design codes introduce accidental torsional effects by shifting the masses with respect to their nominal positions by an "accidental eccentricity". Examples of factors for which the "accidental eccentricity" attempts to account are:

- A planwise distribution of any "imposed" ("live" loads) present at the instant the earthquake occurs that differs from the uniform one assumed in design.
- Infill walls – considered as nonstructural elements and neglected in design calculations – with a distribution in plan that does not follow that of the elements of the lateral-load-resisting system.
- A planwise distribution of the effective stiffness of structural members different from that of the nominal ones used in design (based on the geometry of the cross-section alone, no matter the reinforcement). Recall that in design of new buildings the analysis is based on nominal member rigidities, $(EI)_n$, taken for convenience as a fixed fraction of the rigidity of the gross uncracked section, $(EI)_c$, e.g. $(EI)_n =$

$0.5(EI)_c$ (see Section 4.9.2). As pointed out in Section 3.2.3.3, for given cross-sectional dimensions the effective member rigidity after cracking, e.g. the secant rigidity to yield-point, $(EI)_{eff}$, depends on the shear span ratio and axial stress of the member, as well as on the amount and layout of reinforcement. So, the actual distribution in plan of structural stiffness may significantly differ from the nominal one considered in design.

The "accidental eccentricity" of each horizontal seismic action component is specified in codes as a fraction of the dimension of the storey at right angles to that of the seismic action component. In most codes (CEN 2004a, BSSC 2003, SEAOC 1999) this fraction is one-twentieth (5%). Eurocode 8 doubles that fraction to one-tenth (10%), if the effects of the "accidental eccentricity" are taken into account in the simplified way of Section 4.8.4 on a separate 2D model for each horizontal component of the seismic action,[7] instead of a full 3D model. Moreover, if there are masonry infills with a moderately irregular and asymmetric distribution in plan,[8] the "accidental eccentricity" is doubled further in Eurocode 8 (i.e., to 10% of the storey orthogonal dimension in the baseline case, or 20% if accidental torsional effects are evaluated in a simplified way when using two separate 2D models).

The "accidental eccentricity" is taken in both the positive and the negative sense along any horizontal direction, but practically along the two orthogonal directions of the horizontal seismic action components. It is taken also in the same horizontal direction and in the same sense (positive or negative) for the whole building at a time, which is simple and safe-sided for the global seismic action effects (but not always for local ones).

In a dynamic analysis (modal response spectrum analysis or nonlinear dynamic), the masses may be shifted from their nominal location by the "accidental eccentricity". This produces four dynamic models in total, with different dynamic characteristics (natural periods and mode shapes) and entails using the envelope of the seismic action effects from the four analyses. This is at the expense not only of convenience and computational effort, but also of our understanding of the dynamic response. So, it is done only in the framework of nonlinear analysis (dynamic and often for static, as well) for the assessment of existing buildings, but very rarely in modal response spectrum analysis for design. Seismic design codes normally allow replacing the "accidental eccentricity" of the masses from their nominal positions, by an "accidental eccentricity" of the horizontal seismic components with respect to the nominal position of the masses. The effects of the "accidental eccentricity" are determined then through static approaches (see Section 4.8.2).

In SEAOC (1999) and BSSC (2003) as well – but only for "Seismic Design Category" C and above, as defined in Section 1.4.2.2 – the "accidental eccentricity"

[7]This is allowed in Eurocode 8 for structures regular in plan. Note than in a 2D model all nodes of a floor that may belong to different 2D frames have the same horizontal displacement, regardless of any static eccentricity between the floor centres of stiffness and mass.

[8]Strongly irregular arrangements, such as infills mainly along two adjacent faces of the building, cannot be taken into account in this simplified way, see Section 2.1.13.2.

of 5% of the perpendicular floor plan dimension is multiplied by the following factor at each floor level i, to take into account dynamic amplification:

$$A_{xi} = \left(\frac{\delta_{\max,i}}{0.6(\delta_{\max,i} + \delta_{\min,i})} \right)^2 \tag{4.41}$$

In Eq. (4.41) $\delta_{\max,i}$ and $\delta_{\min,i}$ are the maximum and minimum, over the plan, lateral displacements in the direction of the horizontal seismic action component in question, under the combination of this component and its accidental eccentricity, which is taken initially as 5% of the perpendicular floor plan dimension, but then multiplied by A_{xi}. The accidental eccentricity of each horizontal component should be taken both in the positive and in the negative sense, giving two values of A_{xi}. If the maximum of these two values is greater than 1.0 in at least one floor level i, the analysis should be repeated, using the corresponding value of A_i (but not greater than 3.0) as amplification factor of the accidental eccentricity at the corresponding level(s). Values of A_{xi} for this horizontal seismic direction and sense (sign) of the corresponding eccentricities are recomputed, the analyses repeated, etc., until convergence of all values of A_{xi} which are greater than 1.0. However, considering the semi-empirical nature of the amplification factor A_{xi} and the arbitrary choice of the initial accidental eccentricity value as 5% of the structure's plan dimension, the iterative calculation may not be worthy. A single cycle of analysis under the combination of this horizontal component and its accidental eccentricity at 5% of the perpendicular floor plan dimension would seem sufficient for the calculation of A_{xi}. Note that each sense of action of the accidental eccentricity, positive or negative, is in principle associated with different values of A_{xi}, and should normally be considered as a different load case, uniquely associated to the corresponding direction and sense of action of the horizontal seismic action component.

4.8.2 Estimation of the Effects of Accidental Eccentricity Through Linear Static Analysis

In linear static analysis the action effects of the "accidental eccentricity" alone of a horizontal seismic action component are computed through a linear static analysis of a 3D structural model under storey torques about the vertical axis, taken all with the same sign and equal to the storey lateral loads due to the horizontal component in question times its "accidental eccentricity" at the storey. The lateral loads are those of Eq. (4.8) in Section 4.3.3. In the context of linear static analysis this is equivalent to shifting the masses, and hence exact. By analogy, if the modal response spectrum method is used in the analysis for the horizontal seismic action components, the static storey torques may be computed as: (a) the storey "accidental eccentricity" times (b) the floor mass times (c) the floor response acceleration in the direction of the considered horizontal component of the seismic action, from the CQC combination of modal contributions to floor response accelerations. Eurocode

8 allows taking, instead, the storey torques as the storey lateral loads of the linear static analysis from Eq. (4.8) times the "accidental eccentricity" at the storey. This is computationally simpler, especially if in both horizontal directions the storey "accidental eccentricity" is constant at all levels (i.e., if all floors have the same plan dimensions). Then it suffices to carry out a single static analysis for storey torques proportional to the storey lateral loads from Eq. (4.8) for $V_b = 1.0$. The effects of the "accidental eccentricity" of each horizontal seismic action component can be obtained then by multiplying the results of this single analysis by the base shear V_b from Eq. (4.6) corresponding to the 1st mode period in the horizontal direction of interest and by the (constant at all floors) eccentricity of this component of the seismic action.

If the floors are taken as rigid diaphragms, the total storey torque may be applied to a single floor node of the storey (the "master node"). If a diaphragm may not be considered as rigid and its in-plane flexibility is taken into account in the 3D structural model, it is more meaningful to replace the storey torque with nodal torques at each nodal mass m_i, equal to the product of the "accidental eccentricity" and that mass's lateral force from Eq. (4.8).

Action effects of "accidental eccentricities" produced from static analysis have signs. As the "accidental eccentricity" is meant to be taken in both the positive and the negative sense along the two directions of the horizontal seismic action components in order to produce the most unfavourable value for the seismic action effect of interest, the action effect of the accidental eccentricity of horizontal component X, symbolised here as e_X, is taken to have the same sign as that due to the horizontal component X itself and superimposed to it. The outcome is the total seismic action effect of horizontal component X, symbolised here as E_X. Note that it is these latter total 1st-order action effects that should be multiplied by $1/(1–\theta_i)$ to include a-posteriori P-Δ effects according to the approximate procedure of Section 4.9.7. The exact approaches of the three last paragraphs of Section 4.9.7 for 2nd-order effects apply to both analyses: for the horizontal component X itself and for its accidental eccentricity, if carried out separately. When the "accidental eccentricities" are modelled by shifting the masses from their nominal location, as often done in nonlinear dynamic analysis, 2nd-order effects are taken into account once and for all.

4.8.3 Combination of Accidental Eccentricity Effects Due to the Two Horizontal Components of the Seismic Action for Linear Analysis

An accidental eccentricity is associated to each direction of application of the translational component, X or Y, of the seismic action. The total action effect of horizontal component X, including the effect of accidental eccentricity e_X, is considered as E_X. It is this total effect that is combined according to Section 4.7 with the total action effect of horizontal component Y, E_Y, (that includes the effect of accidental eccentricity e_Y) and sometimes with the action effect of the vertical component Z.

If the action effects of the components X, Y, Z are combined linearly through Eq. (4.25) (cf. Sections 4.7.2.1 and 4.7.2.2), the action effects of the accidental eccentricity e_X of component X and those of the translational component X itself are added with the same sign. Similarly for horizontal component Y and e_Y. It is computationally straightforward to incorporate the effect of e_X or e_Y, into the total effect of horizontal component X or Y, respectively, as the combination of seismic action effects anyway takes place after the analysis for the individual seismic action components.

When action effects are computed through separate analyses for each components X, Y or Z and combined via the rigorous approach of Eq. (4.24) as in Sections 4.7.2.3 and 4.7.2.4, those due to the accidental eccentricity e_X from linear static analysis may be added (with the same sign) to the action effects of the horizontal component X, no matter whether the latter is computed by linear static or modal response spectrum analysis. Similarly for component Y and e_Y. These individual "sums" are considered as E_X and E_Y, respectively, and enter as such in Eq. (4.24). When, by contrast, the action effects due to the translational components X and Y are computed via a single modal response spectrum analysis for all three components, with an extension of the CQC combination module to include expressions like Eqs. (4.29)–(4.37) in Section 4.7.2.3, it is computationally inconvenient to include the effects of e_X or e_Y in the total effect of horizontal components X or Y through such an "addition". Moreover, such an "addition" destroys the beauty and rigour of the approach of Section 4.7.2.3 for the combination of the three seismic action components in a single step. A procedure like the following would be more consistent with the rigorous approach of Eq. (4.24):

1. Combine separately, via Eq. (4.24), and in a single-step the action effects of the translational components X, Y, (Z) from modal response spectrum analysis.
2. Carry out one static analysis to determine the effect of accidental eccentricity e_X, and another one to determine that of e_Y and combine their results using Eq. (4.24). It is convenient to substitute for these analyses a single one, with storey torques equal to the SRSS of those representing e_X and e_Y at that storey.
3. Add together the (positive) outcomes of the two calculations 1 and 2.

As a matter of fact, the outcome of this procedure is generally more safe-sided than the option given at the beginning of the previous paragraph, where the action effects of the accidental eccentricity of each component are "added" to those due to the horizontal component itself, and the two sums (for X and Y) combined via Eq. (4.24) in the end.

4.8.4 Simplified Estimation of Accidental Eccentricity Effects in Eurocode 8 for Planwise Symmetric Lateral Stiffness and Mass

In the spirit of simplification associated with linear static analysis, Eurocode 8 allows it to account for the effects of "accidental eccentricities" in buildings with

planwise symmetric distribution of lateral stiffness and mass in a way simpler than that in Sections 4.8.2 and 4.8.3. This may be done by amplifying the results of linear static analysis for each translational component of the seismic action by $(1 + 0.6x/L)$, where x is the distance of the member in question to the mass centre in plan and L is the plan dimension, both at right angles to the horizontal component of the seismic action. This factor is derived assuming that:

- torsional effects are fully resisted by the stiffness of the structural elements in the direction of the horizontal component in question, without any contribution from any element stiffness in the orthogonal horizontal direction; and
- the stiffness of the members resisting the torsional effects is uniformly distributed in plan.

As a matter of fact, the term $0.6/L$ is equal to the storey torque due to the "accidental eccentricity" of $0.05L$ acting on the storey seismic shear, V, divided by the moment of inertia of a uniform lateral stiffness, k_B, per unit floor area parallel to side B in plan, $k_B BL^3/12$, and further divided by the normalised storey shear, $V/(k_B BL)$. Normally there is also lateral stiffness, $k_L \approx k_B$, per unit floor area parallel to side L in plan and $k_L LB^3/12$ should be added to $k_B BL^3/12$ before it divides the storey torque $0.05LV$. The contribution of k_L is neglected and therefore the term $0.6x/L$ is safe-sided by an average factor of 2. If this additional conservatism is too high a price for the simplicity, the general approach of Sections 4.8.2 and 4.8.3 may always be used.

The general approach of Sections 4.8.2 and 4.8.3 can only be applied with a full 3D structural model. It does not apply if a separate 2D analysis is carried out for each horizontal component, as allowed by Eurocode 8 for buildings meeting the criteria in Sections 2.1.5 and 2.1.6 for regularity in plan. If such separate 2D analyses are made, the effects of the accidental eccentricity can only be estimated through the simplified approach of this section. As these analyses neglect any static eccentricity between the storey centres of mass and stiffness, the amplification factor of the simplified approach becomes in that case $(1+1.2x/L)$, to cover the effect of the neglected static eccentricity, no matter whether there is actually one.

4.8.5 Accidental Eccentricity in Nonlinear Analysis

In nonlinear dynamic analysis masses are shifted from their nominal location by the "accidental eccentricity". The shifting is in the same direction at all storeys. For analysis in 3D this gives four dynamic models to be subjected to each (in general bi-directional) input motion. If the analysis is carried out for unidirectional ground motions, masses are shifted only at right angles to the excitation and there are two models to be analysed for each ground motion. Although this sounds inconvenient and computationally demanding, it is consistent with the sophistication and complexity of nonlinear dynamic analysis.

The same approach should be followed for nonlinear static analysis, which is normally carried out separately for each horizontal component of the seismic action, giving two models to be analysed with the seismic action component applied in the positive and negative sense. The torsional effects due to each eccentrically acting horizontal component should then be calculated according to Section 4.6.1.5.

The envelope of seismic action effects from the two or four sets of analyses for unidirectional or bidirectional seismic action, respectively, is used in the design or assessment.

This approach cannot be followed unless a full 3D structural model is analysed. If a separate 2D model is used for each horizontal component of the seismic action, as allowed by Eurocode 8 for buildings meeting the criteria for regularity in plan (see Sections 2.1.5 and 2.1.6), the effects of the accidental eccentricity can only be estimated through the simplified approach described in the last paragraph of Section 4.8.4.

4.9 Modeling of Buildings for Linear Analysis

4.9.1 The Level of Discretisation

The selection of the appropriate mathematical model of the physical structure depends not only on the action(s) and the method of analysis, but also on the intended use of its results. The objective of a structural model for the purposes of seismic design or assessment is not to serve the analysis per se but the ultimate phase of member detailed design, assessment or retrofitting. The only purpose of modelling and analysis is to provide the data for that phase. Rules for practical dimensioning and detailing or assessment of members against cyclic inelastic deformations are sufficiently developed mainly – if not only – for prismatic members. Corresponding rules for 2D members are available only for special elements with a specific structural role, e.g. low-shear-ratio coupling beams in skew symmetric bending, interior or exterior beam-column joints, etc. Dimensioning or assessment of generic 2D concrete elements for strength can be done using Strut-and-Tie models, which are still developing and have not penetrated yet everyday practice. Moreover, rules for detailing for ductility elements dimensioned on the basis of the Strut-and-Tie approach are not well-developed yet. So, the structural model should employ mainly 3D beam elements.

According to codes the structural model for linear analysis should represent well the distribution of stiffness and mass. This may not be sufficient in design or assessment. The model and the discretisation of the structure should correspond closely to its layout in 3D, to provide the seismic action effects for the dimensioning and detailing or assessing members and sections. For instance, a stick model, with all members of a storey lumped into a single mathematical element connecting adjacent floors with only 3 DoFs per storey (for analysis in 3D) is insufficient. At the other extreme, a very detailed Finite Element (FE) discretisation, providing

very "accurate" predictions of elastic displacements and stresses at a point-by-point basis, may be practically useless. Reliable and almost equally accurate predictions of the "average" seismic action effects needed for member dimensioning or assessment, such as stress resultants or chord rotations at member ends, can be directly obtained from an appropriate space frame model of the structure. Moreover, certain fine effects captured by a detailed FE analysis, such as those of non-planar distribution of strains in the cross-section of deep members, or shear lag in members with composite cross-section, etc., lose their relevance during inelastic seismic response or are anyway neglected in ULS calculations and member verifications. Note also that the connectivity of:

- a 2D element or region modelled via 2D FEs, with
- 3D beam elements in the plane of the 2D FEs,

requires special treatment, as even in shell FEs the rotation DoFs about the normal to the shell surface do not possess stiffness and cannot be directly connected to 3D beam elements in the plane of the 2D FE.[9] For all these reasons, the analysis model appropriate for seismic design or assessment is a member-by-member type of model, where every beam, column or part of a wall between floors is represented as a 3D beam element, with the 3 translations and the 3 rotations at each node between such elements considered as DoFs. Masses may also be lumped at these nodes and associated in general with all six DoFs there. If the vertical component of the seismic action is considered, lumped masses should be included at intermediate points of long-span girders or at the ends of cantilevers. This requires nodes with 6 DoFs at these points, even when no other element frames into these nodes.

4.9.2 Effective Elastic Stiffness of Concrete Members

Section 3.2.3.3 has pointed out that the elastic stiffness in an analysis for seismic design should correspond to the elastic branch of a bilinear force-deformation behaviour. Accordingly, current seismic design codes, e.g. CEN (2004a), BSSC (2003) and SEAOC (1999) require that design of concrete buildings be based on an analysis in which member stiffness takes into account the effect of cracking.[10]

---

[9] One way to achieve a non-pinned connection of a region modelled with 2D FEs to a 3D beam element in the same plane, is to provide the end of the 3D beam element with an almost rigid extension into the region modelled with 2D FEs, connecting the node at the physical end of the beam element with any FE node inside the 2D FE region.

[10] As a matter of fact, in the context of US codes (BSSC 2003, SEAOC 1999) a realistic stiffness for concrete members has little practical implication for strength-based member design, as the design base shear is not allowed to be less than 80% of the value computed from the design spectrum on the basis of empirical period formulas (SEAOC 1999), or less than that given by the design spectrum at a multiple between 1.4 and 1.7 of the empirical period (BSSC 2003). The reduction in lateral force demands due to concrete cracking may account partly for the high values of the force

Eurocode 8, in particular, specifies the stiffness at incipient yielding of the reinforcement. A default stiffness value equal to 50% of that of the uncracked member neglecting the effect of the reinforcement is normally accepted by seismic design codes – including Part 1 of Eurocode 8 (CEN 2004a) in case the cracked member is not modelled more accurately. This default value is much higher than the experimental secant stiffness at incipient yielding, including the effect of bar slippage from the joints (see Section 3.2.3.3). So, it is considered as safe-sided for force- and strength-based design of new buildings, because it underestimates the period and increases the design spectral acceleration and the design forces. However, it leads to underestimation of storey drifts and P-Δ effects, which is not safe-sided.

Although torsion does develop in beams and columns of concrete buildings during the seismic response, it is almost immaterial for their earthquake resistance. Cracking reduces the torsional rigidity much more than the shear- or flexural-rigidity. So, considering that overestimation of member torsional moments may be at the expense of their bending moments and shears, which are more important for earthquake resistance, and that torsional moments due to deformation compatibility drop with the large reduction of torsional rigidity upon cracking, the effective torsional rigidity, $G_c C_{ef}$, of concrete members should be assigned a very small value (close to zero). This should not be done by reducing the concrete shear modulus, G_c, as this will also reduce the effective shear stiffness and unduly increase member shear deformations. In the special case of using the torsional rigidity of a supporting beam to model the restraining effect of the slab on the bending of another element (e.g. of a staircase supported on that beam), the effective torsional rigidity of at least part of the length of the beam should be assigned an artificially high value. Torsional rigidity may also be important in U-shaped structural walls subjected to large torques (see Section 4.9.4).

4.9.3 Modelling of Beams and Columns

Beams and columns are normally modelled as prismatic 3D beam elements. Their parameters for linear analysis are the cross-sectional area, A, the moments of inertia, I_y and I_z, with respect to the principal axes y and z of the section, the shear areas A_y and A_z along these local axes (for shear flexibility, which is important in members with low shear span ratio) and the torsional moment of inertia, C or I_x for St. Venant torsion about the centroidal axis x.

Members with cross-section comprising more than one rectangular parts (L-, T-, C-sections, etc.) are normally dimensioned or assessed for action effects (moments, shears, curvatures or chord rotations) defined with respect to axes parallel to the section sides. So, the analysis should provide action effects referring to such axes. In columns or walls without double symmetry of the section (L-, T-sections, etc.),

---

reduction factors R of US codes. The stiffness used for concrete members has implications mainly for the calculated interstorey drifts.

such axes normally are not principal ones. When the deviation is large and, in addition, the flexural rigidity differs significantly between the two actual principal directions (as, e.g., in an L-shaped section), it may be desirable to have this difference reflected in the action effects from the analysis (e.g. for consistency of the relative magnitude of the bending moment demands with that of flexural capacities in these two directions). Then, the product of inertia I_{yz} with respect to centroidal axes y and z parallel to the sides of the section, should also be specified together with the moments of inertia about these axes (alternatively, the principal moments of inertia and the orientation of the principal axes with respect to the global coordinate system should be given). Shear areas of such sections along their sides may be taken equal to the full area of the rectangle(s) having the long side parallel to the direction in question. These shear areas may then be projected onto the principal centroidal axes, to compute the shear areas in the principal directions, A_y and A_z.

Concrete beams integral with a floor slab are considered to have T- or L-, etc., section, with a constant effective flange width throughout their span. The effective width of the slab on each side of the web, taken in design for convenience the same as for gravity loads, is normally specified in design codes as the sum of a fraction of the distance between adjacent points of inflection of the beam (10% in Eurocode 2) plus another fraction (again 10% in Eurocode 2) of the clear distance to the adjacent parallel beam. More realistic estimates of the effective slab width are proposed in Section 4.10.5.1 for nonlinear analysis. In a long girder providing support (at intermediate points) to secondary joist beams or to vertically interrupted ("floating") columns, intermediate nodes are normally introduced along the span and the girder is modelled as a series of short beams, all with the same effective flange width, as determined from the overall span of the girder between supports on vertical elements. By contrast, the effective flange width of the secondary joist beams depends on their shorter spans between girders.

What has been said above for members of non-doubly symmetric section notwithstanding, beams integral with a floor slab should be assigned local y and z axes normal and parallel to the plane of the slab, respectively, even when their web is not at right angles to the slab (as, e.g., in a horizontal beam supporting a sloping roof).[11] The moment of inertia I_z is computed for the T- or L-section on the basis of the effective flange width. The shear area A_y is that of the beam web alone. If the slab is considered as a rigid diaphragm, the values of A, I_y and A_z are immaterial. If it isn't, they may have to be determined so that the flexibility of the diaphragm is included in the model, e.g., according to Section 4.9.5.

[11] The beam is dimensioned for the ULS in bending, or assessed on the basis of its ultimate deformation, for action effects about an axis parallel to the slab, using as beam depth the projection, $h\sin\beta$, of the actual depth h on the normal to the slab and as web width the value $b_w/\sin\beta$ (β is the angle of the web to the plane of the slab). Assessment of the beam and of its transverse reinforcement in shear can be based on the actual depth and width of the web, h and b_w, but with a shear force equal to the shear V_y from the analysis or capacity design in the direction of the normal to the slab, divided by $\sin\beta$.

The model should account for the effect of sizeable joints between members to the stiffness of these members and of the structure as a whole. The length of the 3D beam element falling in the physical region of its joints with another member is often considered as rigid. If this is done for every member framing into a joint, the global stiffness is overestimated, even when slippage and pull-through of longitudinal bars from the joint is indirectly taken into account as an apparent increase in the flexibility of these members, because the shear deformation of the joint panel zone is neglected. It is preferable to consider as rigid just the parts within the physical joint that belong to the less bulky and stiff among the elements framing in it (normally of the beams).

There are two options for modelling the end region(s) of a member as rigid:

1. To consider the clear length of the member as its real "elastic" length and use a (6×6) transfer matrix to express the kinematic constraint between the DoFs at the real end of the member at the face of the joint and the ones of the mathematical node, where the elements of the model are interconnected.
2. To insert a fictitious almost rigid short element between the real end of the "elastic" member and the mathematical node.

Apart from the increase in computational burden brought about by the additional elements and nodes, approach No. 2 may produce ill-conditioning, because of the large difference in stiffness between the connected elements, real and fictitious. If this approach is used owing to lack of computational tools for approach No. 1, the sensitivity of the analysis results to the stiffness of the fictitious members should be checked, e.g. by ensuring that results are almost the same when the stiffness of a fictitious element changes by an order of magnitude.

If the member end region within a joint is modelled as rigid, stress resultants or chord rotations at member ends, routinely given as output of the analysis, can be used directly for dimensioning or assessing the member at its end section at the joint face. When such rigid ends are not employed, unless the stress resultant or chord rotation at the joint face is separately calculated on the basis of the joint dimensions, a safe-sided member dimensioning or assessment may be carried out assuming that the stress resultants or chord rotations at the mathematical nodes apply at the face of the joint.

Often the centroidal axes of connected members do not intersect. Then the mathematical node is placed on the centroidal axis of one of the connected members, typically a vertical one, with the ends of the other members connected to that node at an eccentricity. This eccentricity can easily be incorporated in the modelling of the member end region within the joint as rigid: the rigid end will be at an angle to the member axis.

Distributed gravity loads on members with rigid ends are often considered by the analysis program to act only on the "elastic" element between the rigid ends. Any gravity load unaccounted for, as falling outside the "elastic" element length, should be specified separately as a concentrated nodal force.

4.9.4 Special Modelling Aspects for Walls

The part of a wall between successive floors and/or substantial openings should be modelled as a single 3D beam element. Such a modelling is often called "wide-column-analogy". Elastic displacements and stress resultants predicted by the "wide-column-analogy" in the wall itself and the rest of the system compare well with those of detailed FE analysis, provided that shear deformations in the wall are accounted for through a finite shear area.

Code rules regarding the amount and detailing of their horizontal reinforcement ensure that walls with composite section, consisting of connected or intersecting rectangular segments (L-, T-, U-, H-shaped, etc.), work as a single integral unit. So, no matter how they are modelled for the analysis, such walls are dimensioned or verified in flexure with axial force and in shear along and normal to the long sides of their constituent rectangles. For each of the two directions of bending considered, the part of the section parallel to the shear force and normal to the moment vector is taken as the web and the parts orthogonal to it are the flanges. The Eurocode 8 rules for the confinement reinforcement of such walls also presume a single integral section. So, it is most convenient for the subsequent phases of dimensioning and detailing or assessment to model walls of any section using storey-tall 3D beam elements with the cross-sectional properties of the entire section. The only question regarding this approach may concern the modelling of torsion in walls with section other than (nearly) rectangular, as detailed below.

Except possibly in walls with semi-closed channel-section addressed later in this section, compatibility torsion is not an important component of the seismic resistance of walls. So, accurate estimation of torsion-induced shear for the design or assessment of the wall itself is unimportant. The main relevant issue is whether potentially unrealistic modelling of the torsional stiffness and response of a wall with section other than (nearly) rectangular, has a significant effect on the seismic action effects calculated for other structural members. If storey-tall 3D-beam elements are used with the cross-sectional properties of the entire section, the accuracy of the prediction of seismic action effects in other members is improved if the axis of the 3D beam element modelling the wall passes through the shear centre of its cross-section, instead of its centroid. For L- or T-shaped sections this is very convenient, as the shear centre is near the intersection of the two rectangular parts of the section, through which the axis of the beams framing into the wall often pass. The offset from the centroid to the shear centre introduces some error in the calculation of the vertical displacement of the end of a beam eccentrically connected to that node of the wall. Another issue is that the torsional rigidity, $G_c C$, of the section estimated for pure St. Venant torsion – i.e. as $G_c \sum (l_w b_w{}^3/3)$, with l_w and b_w denoting the length and thickness of each rectangular part of the section - does not account for the resistance of the wall to torsion-induced warping of the section. When evaluating these questions, though, we should keep in mind the large uncertainty regarding the reduction of torsional rigidity due to concrete cracking (see last paragraph of Section 4.9.2).

An alternative to the single-element modelling of walls with a section consisting of connected or intersecting rectangular segments is to use a separate 3D beam element at the centroidal axis of each such segment of the section. To dimension and detail the entire section in bending with axial force, computed bending moments and axial forces of the individual 3D beam elements need to be composed into a single M_y, a single M_z and a single N for the entire section. If these elements are connected at floor levels to a common mathematical node (e.g. via rigid horizontal arms or equivalent kinematic constraints), the model is fully equivalent to a single 3D beam element along the centroidal axis of the full section. According to Xenidis et al. (1993) the overall torsional behaviour is better represented if the constituent elements of the section are not connected to a common mathematical node at each floor, but to individual end nodes at the centroid of each segment of the wall section. The connection between the individual elements may best be effected through arms within the plane of the section, connected to each other at the intersection of adjacent segments of the section. These arms should be rigid in bending, shear or axial extension, but should have finite torsional rigidity: $G_c C = G_c H_{st} b_w{}^3/3$ (where H_{st} is the storey height and b_w the thickness of the web of the corresponding wall segment). Then the individual 3D beam elements of the wall may bend relatively independently of each other in the vertical plane of their length dimension, developing, through their in-plane shear forces, a torque with respect to the centroid of the composite section. This multiple vertical 3D element model with connection through horizontal arms meeting at the corner(s) of the section has one drawback: the replacement of the continuous shear stress distribution along the vertical connection of the individual wall segments by a discrete vertical force at the node where the horizontal arms meet induces fictitious counterflexure moments in the individual elements (Stafford-Smith and Girgis 1986, Kwan 1993). The counterflexure decreases the shear stiffness of individual wall segments and hence the apparent torsional rigidity of the wall. More important, the fictitious moments have maximum value at the two ends of the element, i.e. at storey levels, and distort most the calculated moments at the most critical cross-sections of the wall. To remove the effect of parasitic counterflexure on these end moments, Kwan (1993) suggested introducing another set of nodes at storey mid-height and use two sets of elements per storey, in lieu of one. Then the "real" end moments at storey levels can be estimated by linear extrapolation from the moments at storey quarter-height, as these are estimated by averaging the end moments of the half-storey individual elements.

Channel-shaped walls with openings regularly spaced vertically and separated by deep spandrel beams are semi-closed sections. Their torsion is dominated by circulatory shear flow. So, they can be modelled with a single element at the centroid or shear centre of the full section, with torsional rigidity according to Bredt's formula for closed sections: $GC = 4G_c A_m{}^2/\int \mathrm{d}s/t$. In this formula A_m is the area enclosed by the centreline of the closed thin-walled section at the spandrel beam level. The integral all along the perimeter is calculated with an equivalent thickness of the spandrel beam, smeared over the storey height H_{st} (Rutenberg et al. 1986):

$$t_{\mathrm{eq}} = \frac{H_{\mathrm{st}}}{h_{\mathrm{b}}} \frac{12 E_{\mathrm{c}} I_{\mathrm{b}}}{l_{\mathrm{b}}^3 \left[G_{\mathrm{c}} + E_{\mathrm{c}} \left(\frac{h_{\mathrm{b}}}{l_{\mathrm{b}}} \right)^2 \right]} \tag{4.42}$$

In Eq. (4.42) I_{b} and h_{b} denote the moment of inertia and the depth of the spandrel beam and l_{b} its span. If the spandrel beam is very flexible, or if just the slab plays that role, the wall section is closer to an open one. In that case, if the torsional stiffness of the wall itself is an important component of the total torsional rigidity of the structure and, moreover, the overall structural layout is such that torsion is an important component of the response to the horizontal seismic action components, it may be better to use the multiple vertical 3D element model connected at the corner(s) of the section through horizontal arms which are rigid except for their finite torsional rigidity: $G_{\mathrm{c}}C = G_{\mathrm{c}}H_{\mathrm{st}}{b_{\mathrm{w}}}^3/3$, as outlined in the previous paragraph. The individual vertical elements will always suffer from torsion-induced parasitic counterflexure. In this case, however, parasitic moments at opposite sides of the wall section cancel each other, when the moments and axial forces of the individual wall elements are assembled into a resultant moment at the centroid of the full section for the dimensioning of the wall in bending with axial force.

Recall from Fig. 1.7 in Section 1.3.5 that in Eurocode 8 (CEN 2004a) design of new walls using linear analysis employs heightwise linear envelopes of wall elastic moments from the analysis (see also Section 5.7.4.1). So, bending moment values from the analysis at any level other than the base and the top of the wall are not relevant for design according to Eurocode 8.

Beams framing into a wall at floor levels, etc., should be connected to the mathematical node at the axis of the wall. An eccentricity between this node and the real end of the beam should be modelled with a rigid connection. If eccentrically framing beams are at right angles to the plane of the wall (i.e. in its weak direction), it is more accurate to give to this rigid connection a finite torsional rigidity, $G_{\mathrm{c}}C = G_{\mathrm{c}}H_{\mathrm{st}}{b_{\mathrm{w}}}^3/3$ (where H_{st} is the storey height and b_{w} the thickness of the web of the wall. Note also that less than the full length of a rectangular (part of a) wall section works effectively in out-of-plane frame action with beams connected to the wall at right angles to its plane. The fully effective width of the wall in that direction may be taken to extend up to about twice the wall thickness on each side of the beam. To take into account the anyway small contribution of the weak direction of a rectangular wall to frame action, its cross-sectional moment of inertia may be conservatively computed using a depth of b_{w} and a width of $4b_{\mathrm{w}}$.

4.9.5 Modelling of Floor Diaphragms

4.9.5.1 Rigid Diaphragms

The in-plane stiffness of floor slabs acting as diaphragms should be properly recognised and reflected by the model for the seismic analysis. Floor diaphragms are commonly assumed and modelled as rigid. The most convenient way to model a

diaphragm as rigid is by introducing at each floor level an additional node ("master" node) close to the centre of mass of the floor and preferably not coinciding with anyone of the floor nodes modelling physical connection of members. This node has only 3 DoFs: two translations in the plane of the diaphragm and a rotation about the normal to that plane. The corresponding DoFs of all floor nodes (called in this respect "slaves") are related to those of their "master" through a 3×3 transfer matrix, expressing the rigid-body kinematic constraint. If the diaphragm is horizontal, the "master" and "slave" DoFs refer to the global coordinate system and the "slave" DoFs can be condensed out of the global equations of equilibrium or motion, where only the "master" DoFs remain. If the floor is at an inclination to the horizontal, the kinematic constraints between translations in the plane of the floor and rotations about the normal to it can be introduced as linear constraints between global DoFs, after appropriate rotation transformations. The same end can be achieved in a more general way, by considering rigid 3D elements between the "master" node and the physical end of all elements with nodes on the floor in question. At the "master" node the mass of the two translational DoFs is equal to the sum of the corresponding masses of all its "slaves". The rotational mass moment of inertia about the vertical axis at the "master" is the sum of those of its "slaves" (normally neglected as small), plus the sum over all the "slave" nodes of the product of that node's mass, m_i, times the square of its distance to the "master": $m_i[(X_i–X_m)^2 + (Y_i–Y_m)^2]$.

If the analysis program has neither one of the above computational capabilities or an equivalent alternative to express kinematic constraints between the floor nodes, the floor diaphragm can be included in the model as non-rigid but with high in-plane stiffness, e.g., using the modelling approach of the next section.

4.9.5.2 Flexible Diaphragms

In-plane flexibility of floor diaphragms should be realistically modelled, if:

1. the layout in plan of the floor diaphragm and of some lateral-force-resisting elements is such that the distribution of seismic action effects in these elements may deviate significantly from the result of the rigid diaphragm assumption; or
2. if in-plane seismic action effects of the floor diaphragm, needed for its verification, cannot be accurately computed on the basis of the rigid diaphragm assumption; or
3. the floor itself and/or some of its beams are post-tensioned, and the flexible floor diaphragm model of the floor-frame system is anyway necessary for a reliable calculation of the in-plane action effects due to post-tensioning.

If diaphragm flexibility is included in the model for reason No. 1, a FE model of the diaphragm within its plane is not the best option. Combining FE with 3D beam elements in the same model is fairly expensive and tricky. One FE for each panel of the floor between beams is not sufficient. To use several FEs for a panel, each surrounding beam should be broken up in several 3D beam elements with intermediate nodes, increasing computational demands and unduly complicating the

subsequent phases of beam dimensioning/detailing or assessment. Shell FEs should preferably be used, and not 2D FEs with just in-plane translational DoFs.

Unless there is compelling need to use FEs for the diaphragm, its in-plane flexibility can be approximated through the value of the moment of inertia I_y of its beams about the normal to the plane of the diaphragm, with or without X-bracing added to the model of each slab panel. For a diaphragm with thickness h, plan dimensions l_x and l_z (with direction y reserved for the normal to the diaphragm, as in the local coordinate system of the beams), Young's Modulus E and a Poisson ratio value of 1/3, the stiffness for in-plane extension or shear is essentially reproduced if the panel is modelled as a horizontal frame with X- bracing having the following properties (Yettram and Husain 1966):

– Frame members with length l_x are assigned:
  - a flexural rigidity about the normal to the diaphragm:

$$(EI)_y = \frac{Eh}{60} l_x^2 l_z \tag{4.43a}$$

  - an axial stiffness:

$$(EA) = \frac{Ehl_z}{2}\left[1 - 0.2\left(\frac{l_x}{l_z}\right)^2\right] \tag{4.43b}$$

– X-diagonals have only axial stiffness:

$$(EA)_d = \frac{Eh}{10}\frac{(l_x^2 + l_z^2)^{3/2}}{l_x l_z} \tag{4.43c}$$

For frame members parallel to l_z subscript x replaces z and vice-versa. Since the 3D beam elements around the diaphragm panel are already in the model with out-of-plane flexural properties EI_z and GA_y, only X-bracing elements need to be added.

The above modelling approach works well if the aspect ratio l_x/l_z of each diaphragm panel is not far from 1.0. For panels with $l_x >> l_z$ Eq. (4.43b) may give negative stiffness, which does not make sense. A simpler and more reasonable, but generally less accurate, alternative is to omit the 2nd term in brackets in Eq. (4.43b) and the X-bracing, and increase instead by a factor of 4 the flexural stiffness of the frame members in Eq. (4.43a). The new expressions for the in-plane parameters of the beams of length l_x are then as follows, including the effects of diaphragm panels (possibly) on both sides of a beam (Fardis 1997):

$$(EI)_y \approx \frac{Eh}{15} l_x^2 \sum l_z \tag{4.44a}$$

$$(EA) \approx \frac{Eh}{2}\sum l_z + Eb_w(h_b - h) \tag{4.44b}$$

The 2nd term in Eq. (4.44b) is the contribution of the web of beams to their axial stiffness. For the beams which are parallel to side l_z subscript z replaces x and vice-versa.

Eurocode 8 states in a note that the diaphragm flexibility may be neglected, if it increases horizontal displacements by more than 10%. To apply this conventional definition of a rigid diaphragm, two analyses are unfortunately needed, one neglecting and the other considering the diaphragm's in-plane flexibility.

4.9.6 A Special Case in Modelling: Concrete Staircases

If the lateral-load-resisting system itself is flexible, as e.g. in low-rise frame structures, and/or if the location of the staircase in plan is such that the torsional rigidity and response of the building is significantly affected (as, e.g., in the case of Fig. 2.13(b) and (c)), the designer may want to include the staircase in the structural model. In this way the effect of the staircase on the seismic action effects in the rest of the structure can be determined, and even the staircase could be designed or assessed under its own seismic action effects.

A staircase may be modelled as a series of prismatic 3D beam elements along its axis, inclined to the horizontal. The sectional properties (including shear areas) of these elements should be those of the full-width solid part beneath the steps. A curved axis may be modelled as multilinear. For staircases supported only at the ends, having a helical axis or one consisting of a combination of straight segments and quarter- or semi-circular segments, the 12×12 stiffness matrix of the entire stair between its ends is given in Skouteropoulou et al. (1986, 1987) and Fardis et al. (1987). Inclined beams supporting the staircase and supported, in turn, by elements of the lateral-load-resisting system, should be similarly and appropriately included in the model. Only integral connections of the staircase and/or its supporting beams to the rest of the structure should be included in the model as nodes between elements. Connections without properly detailed and anchored reinforcement will, in all likelihood, break loose in an earthquake. They cannot be relied upon under seismic actions and the designer should not only omit them from the model, but also avoid them altogether in new buildings.

At floor levels a stair is typically supported on beams. Its partial fixity there in bending and torsion is provided by its continuation into a floor slab on the other side of the supporting beam. As this slab is not included in the model of the lateral-load-resisting system, the partial fixity of the stair against rotations at its support node on the beam should be modelled either:

- by connecting the node supporting the stair to the nearest floor node in a direction close to the extension of the stair axis in plan, through a fictitious horizontal member having cross-sectional properties about the same as the stair; or
- by assigning a very large torsional rigidity to the segment of the supporting beam between the support node of the stair on the beam and the nearest common node of the supporting beam with a transverse frame.

If this is not done, the stair in the model will be almost hinged for rotation about the supporting beam.

Examples of staircases included in the model are presented in Section 4.10.5.3.

4.9.7 2nd-Order (P-Δ) Effects

It has been pointed out in Section 1.2.1 that collapse of structures during an earthquake is caused not by the seismic lateral forces per se but by the seismic lateral displacements, Δ, acting with the structure's weight to generate (P-Δ) moments in vertical elements. To appreciate the importance of P-Δ effects, think of a situation in which the P-Δ moment alone, $M = N\delta$, produced at the base of a single column by its axial force, N, and the interstorey displacement, δ, reaches the column's moment resistance, M_R. As the support of gravity loads is force-controlled, the column may collapse, no matter its ductility. Normalising M_R into $\mu_R \equiv M_R/(bh^2 f_c)$ and N into $\nu \equiv N/(bhf_c)$, column collapse may occur when the interstorey drift ratio, δ/H (equal to the sum of the average column chord rotations and beam chord rotations around a frame bay plus the average shear distortion of the joint panels, see Fig. 3.30) exceeds the value of $(\mu_R/\nu)/(H/h)$, where H/h is the column slenderness (i.e., length-to-depth) ratio. Slender columns, lightly reinforced and under high axial load (i.e., with low μ_R/ν values) might then collapse at relatively moderate interstorey drift ratios. Hence the importance of computing and limiting P-Δ effects.

All seismic design codes require taking into account 2nd-order (P-Δ) effects in buildings, whenever at any storey the aggregate 2nd-order (P-Δ) effects in vertical members exceed 10% of the 1st-order ones. The criterion is the interstorey drift sensitivity coefficient, θ, defined for storey i as the ratio of the total 2nd-order moment in storey i, to the change in the 1st-order overturning moment within that storey:

$$\theta_i = \frac{N_{\text{tot},i}\,\Delta d_i}{V_{\text{tot},i}\,H_i} \tag{4.45}$$

where:

- $N_{\text{tot,i}}$ is the total gravity load concurrent with the seismic action at and above storey i.
- $V_{\text{tot,i}}$ is the total seismic shear at storey i.
- H_i is the height of storey i.
- Δd_i is the interstorey drift at storey i, i.e., the difference of the lateral displacements at the top and bottom of the storey, d_i and d_{i-1}, at the floor centre of mass, or at the floor "master" node. In Eurocode 8 (CEN 2004a) it is the inelastic drift, estimated via the equal displacement rule according to the 2nd paragraph of Section 4.11.1 (for all practical purposes by back-multiplying by the behaviour factor q the values of d_i, d_{i-1} from the linear analysis for the design spectrum). US codes (BSSC 2003, SEAOC 1999) take for this purpose d_i and d_{i-1} directly from the analysis for the design spectrum, underestimating them by a factor of R

(where R is the force reduction factor incorporated in the design spectrum); the estimated P–Δ effects are very much on the low side.

Second-order effects may be neglected, if the value of θ_i does not exceed 0.1 at any storey. They should be taken into account for the entire structure, if at any storey θ_i exceeds 0.1. If θ_i does not exceed 0.2 at any storey, seismic design codes, such as Eurocode 8 (CEN 2004a), allow taking P–Δ effects into account without a 2nd-order analysis, but in approximation: by multiplying a-posteriori all 1st-order action effects due to the horizontal component of the seismic action by $1/(1–\theta_i)$. For given lateral forces, this approximation gives seismic action effects in fairly good agreement, on average, to those of an exact 2nd-order analysis carried out as described below. The simplified approach fails to capture, though, the global effect of the lengthening of the natural periods due to the 2nd-order effects. Note that, although it is the value θ_i of the individual storeys that can be used in this amplification, it is safe-sided to use for the entire the building the maximum value of θ_i in all storeys. It also respects equilibrium in the framework of 1st-order analysis.

In the very unlikely for RC buildings case that θ_i exceeds 0.2 at any storey, an exact 2nd-order analysis is required (CEN 2004a). This analysis may be performed with the modelling described below.

If the vertical members connect floors which are considered as rigid diaphragms, the P-Δ effects can be calculated exactly as highlighted in the next paragraph. If there are no such floors, or if they may not be taken as rigid diaphragms, P-Δ effects may be considered at an individual column basis, by subtracting from the column elastic stiffness matrix its linearised geometric stiffness matrix. If the analysis is elastic using the design spectrum, the linearised geometric stiffness matrix of each column should be multiplied by the displacement amplification factor for conversion of elastic displacement estimates from the analysis into inelastic ones (as pointed out in the definition of Δd_i in connection with Eq. (4.45)). In the context of elastic analysis, axial forces in the geometric stiffness matrix of the column may be taken constant and equal to the value due to the gravity loads alone.

If diaphragms can be considered as rigid, P–Δ effects may be accounted for exactly in the analysis without subtracting the linearised geometric stiffness matrix of each individual vertical element from the corresponding elastic stiffness matrix. It has been proposed in Rutenberg (1982) to introduce instead a fictitious vertical element between adjacent floors i and i–1, with negligible axial stiffness EA and flexural rigidities EI_y, EI_z, but with negative shear areas: $GA_y = GA_z = -q(\sum N)_i$ and negative torsional rigidity: $GC = -q(\sum Nr^2)_i$, where N and r denote respectively the axial force in the individual columns of storey i and their distance from the centroid of the axial forces in all the columns. These fictitious vertical elements should be connected (through horizontal rigid elements or rigid-body kinematic constraints in the horizontal plane) to the centroids of the axial forces in all columns, $(\sum N)_i$, of storeys i and i–1. These centroids differ from the storey centres of mass, as the axial forces include contributions from all storeys above. P–Δ effects can thus be introduced in a direct and exact way in computer codes that lack the element geometric stiffness facility.

4.9.8 Modelling of Masonry Infills

Before any guidance for linear modelling of infills, a few words are in order about its scope.

Modelling for linear analysis is primarily of interest for the seismic design of new buildings. The provisions of Eurocode 8 for the design of new frame buildings having masonry infills are outlined in Sections 2.1.13 (regarding the global aspects) and 5.7.3.6 (for the potential adverse local effects on columns). Their underlying concept is to prevent any adverse effect of the infills, while not profiting explicitly from the beneficial ones to reduce the seismic action effects in structural members. In this context, analysis of a 3D structural model explicitly including the infills is required by Eurocode 8 (CEN 2004a) only for new buildings with a severely irregular layout of the infills in plan. It can be argued that this approach is neither rational nor cost-effective, as it does not explicitly account for an effect (that of the infills) which is generally important and normally beneficial. Note that, to account rationally for this influence, individual infill panels should be:

(a) explicitly included in the model for the seismic analysis of the building, and
(b) considered as structural elements and verified for the seismic action demands computed for them from the analysis for the seismic action.

In the verifications under (b) above the resistance of the infills should be expressed in terms of design values of their strength properties. This implies that, at the design stage, nominal (lower characteristic) values of these properties are specified and sampling of infill materials (masonry units, mortar, etc.) for testing takes place during execution, exactly as in masonry buildings designed according to Eurocodes 6 and 8. It also implies that modifications of infill panels or of their openings is not allowed at a later stage, without re-visiting the seismic design of the building and assessing the impact on the seismic safety of the entire system and all its elements. This would be a major change in the current practice of design, execution and maintenance of masonry-infilled buildings. Moreover, the costs incurred for the additional design effort and the quality assurance for masonry infills may outweigh any savings in the members of the structural system. So, no matter the rationality of a design approach that explicitly accounts for all individual infill panels, the one adopted by Eurocode 8 seems to provide a good balance of simplicity in design and execution, overall construction cost and seismic safety.

In the light of the above, what follows regarding linear modelling of masonry infills is meant to be used primarily for new buildings with a strongly irregular layout of the infills in plan, required by Eurocode 8 to be analysed including the infills explicitly. It also serves as a prelude to Section 4.10.2, dealing with nonlinear modelling of masonry infills primarily for the purposes of assessment and retrofitting of existing new buildings.

A solid infill panel can be conveniently modelled as a strut along its compressed diagonal (see Fig. 4.4). A widely-known strut model is based on the beam-on-elastic-foundation analogy for the estimation of the strut width (Mainstone 1971).

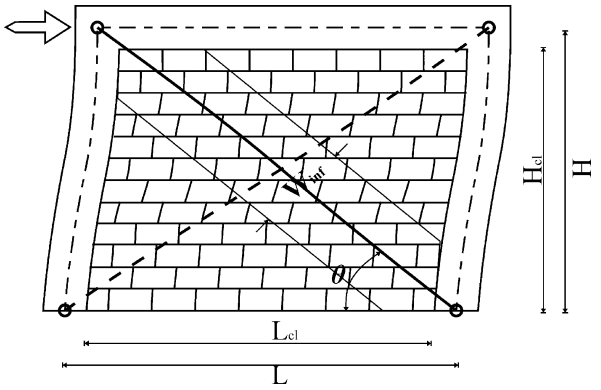

Fig. 4.4 Modelling of solid infill panel with strut along the compressed diagonal

According to that model, the strut has the same thickness as the infill wall, t_w, and width in the plane of the infill, w_{inf}:

$$w_{inf} = \frac{0.175 L_{cl}}{\cos\theta\,(\lambda H)^{0.4}} \tag{4.46a}$$

where:

$$\lambda = \left(\frac{E_w t_w \sin 2\theta}{4 E_c I_c H_{cl}}\right)^{\frac{1}{4}} \tag{4.46b}$$

- L_{cl} : clear horizontal dimension of the infill panel;
- θ : arctan(H_{cl}/L_{cl}) = inclination of the diagonal to the horizontal;
- H, H_{cl} : theoretical and clear column height, respectively;
- E_c, E_w, : Elastic modulus of the column concrete and of infill masonry (ranging according to Eurocode 6 from 500 to 1000 times the masonry compressive strength), respectively;
- t_w : infill wall thickness;
- I_c : moment of inertia of the column section about the normal to the infill panel.

As an alternative to Eq. (4.46a), Eurocode 8 (CEN 2004a) allows a strut width equal to a fraction of the clear length of the panel diagonal, $L_{cl}/\cos\theta$. A strut width around 10–15% of the length of the diagonal is a good approximation, at least for new buildings designed for Life Safety performance ("Significant Damage" in Part 3 of Eurocode 8 (CEN 2005a)) under the design seismic action. For lower level response – e.g., that normally associated with Immediate Occupancy performance ("Damage Limitation" Limit State in Part 3 of Eurocode 8) – a value around 20% of the length of the diagonal is more appropriate. Whenever the integrity of frame members is questionable or of interest (notably at the Near Collapse performance level), it is preferable to assume that the diagonal strut has disintegrated and does not contribute anymore to the global lateral strength and stiffness. Of course, infill

panels having clearly adverse effects on the seismic performance of the structural frame, locally or globally, should be retained in the model with their Life Safety performance width. This may be the case of infills with a strongly irregular heightwise distribution that may have "open-storey" and "soft-storey" effects, or of partial-height infills that produce captive columns, etc. In that latter case the strut which models the infill should run not along the diagonal of the frame panel, but along that of the infill itself, i.e., between an intermediate node introduced in the column at the level of the top of the partial-height infill (i.e., at that of the sill) and the diagonally opposite node at the bottom of the column.

In linear analysis a solid infill panel may be modelled as an elastic strut along the compressed diagonal, with cross-sectional area equal to t_w times w_{inf} and modulus equal to E_w (taken, e.g., according to Eurocode 6). This is realistic for the estimation of both the panel's local effects on the surrounding frame members, as well as of its effects on the global response. A strut only along the compressed diagonal is, however, a nonlinear modelling feature. The only difference that a strut along the tension diagonal would make on the response is in the sign of the axial forces in the columns bordering the panel. Unlike the axial forces due to the overturning moment, those associated with the action of infills are all tensile and nearly uniformly distributed in the columns of the entire plan (except in the columns of the "lee-ward" side, where no axial force is induced in columns by the infills). The resultant of all these axial forces is equal and opposite to the vertical resultant of all strut forces in the infills. In static analysis – linear with the lateral force procedure or nonlinear "pushover" – the diagonal of the panel where the strut is placed can be chosen according to the perceived sense of deformation of the panel. In frames (about) parallel to the horizontal seismic action component, it is easy to identify the diagonal where the strut should be placed. By contrast, in frames at (about) right angles to this direction the choice of panel diagonal for the strut relies on intuition, judgement or – possibly – iterations. As modal response spectrum analysis gives results without signs, it is almost immaterial whether the struts modelling the infills are placed along one diagonal or the other. However, unlike other seismic action effects from modal analysis that are taken both positive and negative, strut forces should always be taken compressive (and double its value from the modal response spectrum analysis, if struts are placed along both diagonals of a panel), while axial forces induced in columns by the infills should be tensile. It is not easy, however, to identify which part of a column's axial force is due to the infills.

The most challenging open issue for modelling infills is the influence of openings. A panel with openings may be modelled with multiple struts starting at opposite corners of the panel, passing near the corners of the openings and ending at intermediate points along the members framing the panel. A simpler way to take into account the effect of infill openings on the global response is through reduction factors on the infill stiffness. The value of these factors depends on the shape, size and location of the opening(s) within the infill panel, and – in panels with asymmetric openings – the direction of loading. They should be established through systematic parametric analyses of infilled RC frame panels with openings, using detailed FE models for the infill and its interaction with the surrounding frame. Figure 4.5 gives such reduction factors, λ, on the stiffness of the solid infill panel, as derived

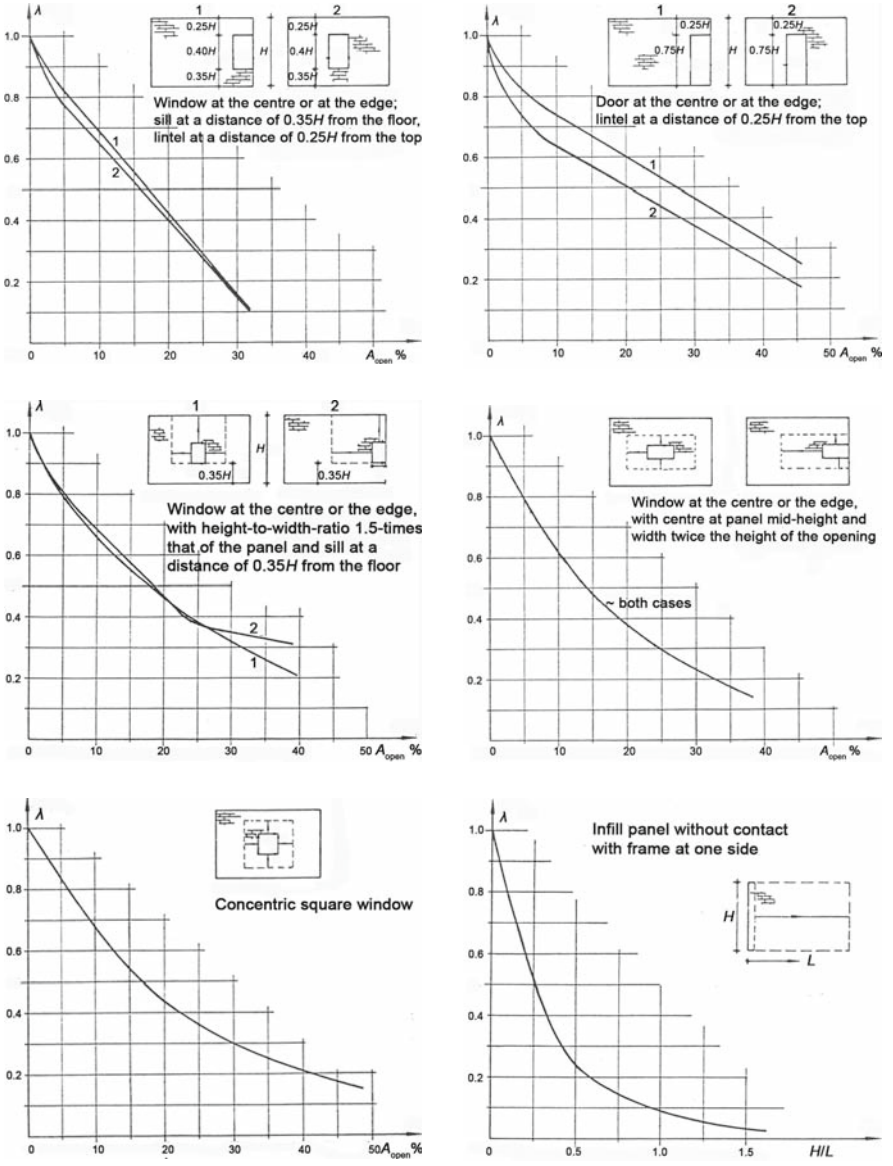

Fig. 4.5 Reduction factor on solid infill stiffness, in terms of fraction of panel area in elevation taken up by opening. *Bottom-right*: reduction factor on panel stiffness, for no contact with frame on one side, as a function of panel height-to-width-ratio (Giannakas et al. 1987)

from elastic FE analyses of single panels with openings. If there are more than one openings in the panel, the overall reduction factor is bounded by the sum of the individual λ_i's minus 1.0 and by their product (Giannakas et al. 1987). Note that Eurocode 8 (CEN 2004a) instructs the designer to neglect in the model infill panels

with two or more significant openings. Models, especially those for nonlinear analysis (see Section 4.10.2) should be validated or calibrated on the basis of the few available cyclic test results on infills with an opening, such as those given in CEB (1996a) and Kakaletsis and Karayannis (2008).

4.9.9 Modelling of Foundation Elements and of Soil Compliance

4.9.9.1 Introduction

No matter whether we are talking about seismic design or design just for other, non-seismic actions, in order to use analysis results to design or assess piles or elements of shallow foundations, such as tie- or foundation-beams or a raft (mat) foundation, we should include these elements in the model and take into account the compliance of the ground.

The superstructure, especially if founded on two-way deep foundation beams, as in the box-type systems of Section 2.3.3.3, is sometimes analysed separately from the foundation, considered fixed at the top of the foundation system. The so-computed stress resultants at the base of the vertical elements are taken as external actions for the foundation system, which is in turn analysed accounting for the compliance of the soil, in order to compute the action effects in foundation elements, necessary for their dimensioning or verification. There are many examples of the limited accuracy of this uncoupled approach: (1) if the walls of a dual system are assumed fixed at the base, their contribution to lateral strength and stiffness is overestimated, especially at the lower storeys; (2) if a column is taken fixed at the foundation, seismic moments are overestimated at its base and underestimated at the top of the storey; (3) fixity of vertical elements at the base leads to underestimation of lateral drifts and of P–Δ effects, etc. Note, though, that, if soil compliance does not change the magnitude of storey seismic shears and overturning moments, neglecting it in a linear seismic response analysis does not adversely affect the overall earthquake resistance of a ductile structure. Such a structure can redistribute internal forces from where they have been underestimated in the analysis to adjacent regions where they were overestimated.

Uncoupled modelling and analysis of the superstructure and the foundation system is also computationally inconvenient. It requires setting up two different structural models and transferring the (reaction) output from the analysis of the superstructure as input to the foundation, for several load cases and their combinations.

Today's computational capabilities allow including the superstructure, the foundation system and the soil into a single, coupled linear model for seismic response analysis. Such a model reflects much better the seismic response of the lateral-load-resisting system, as affected by the degree of fixity of the vertical elements at the base.

Codes and standards do not seem ready yet to consider full-fledged soil-structure-interaction in seismic design, especially as its effects are mostly favourable. BSSC

(2003) has taken the bold step to allow a (up to 30%) reduction of the base shear computed for rigid ground and full fixity of the structural elements to it, if the lengthening of the 1st mode period due to the horizontal and rotational (rocking) deformation of the ground and the additional material and radiation damping in the soil are explicitly and separately accounted for as specified there. Practically all codes for everyday seismic design of ordinary buildings derive the seismic action effects implicitly assuming that the structure as a whole is fixed to the ground. For instance, the global displacement ductility factor implicit in the values of the behaviour factor, q, or force reduction factor, R, specified by a code refers to a global yield displacement of the structure fully fixed to the ground, without any contributions from the compliance of the soil. So, when working in the framework of these codes, incorporation of the effects of soil compliance in the design should not violate this key point, either by increasing the effective damping, or by overly reducing lateral force demands. In other words, soil-structure-interaction phenomena to be considered should have mainly "internal" effects on the structure, notably redistributing internally seismic action effects, without reducing the overall seismic demands from the "outside".

4.9.9.2 Elastic Support Conditions

A convenient way to take into account soil compliance in linear analysis is through elastic support conditions at support nodes, normally at the bottom of foundation elements. These nodes should be connected to nodes at the physical ends of structural elements (walls, columns, tie- or foundation beams) either via rigid connecting elements, or (preferably) through kinematic constraints expressing rigid-body connection.

Not all 6 DoFs of a support node need to be elastically supported. In a sound conceptual design of a building for earthquake resistance the base of all foundation elements is at the same level and all foundation elements are tied together in both horizontal directions, so that the foundation system moves almost as a rigid body (see Section 2.3.2). Then both horizontal translations and the rotation about the vertical axis can be fully constrained at all foundation nodes. The main effect of elastic supports in these directions would had been a horizontal rigid-body-component dominant in the lowest three modes and a significant lengthening of their periods (in all likelihood reducing the corresponding base shears), without a significant and physically meaningful effect on the distribution of seismic forces and deformations in the structure. Moreover, there is significant uncertainty about the elastic constants for soil compliance in the horizontal direction(s), mainly due to the effect of embedment.

The displacements of the foundation in a horizontal plane can be fixed only if all foundation nodes are at the same horizontal level. As pointed out in Section 2.3.2, if foundation nodes are elastically supported in the vertical direction and against rotation about the two horizontal axes and, in addition, support nodes placed at different horizontal levels are horizontally constrained, the full overturning moment will be taken by horizontal reactions at these latter fixed supports, rather than by

nonuniform vertical reactions. In other words, rocking of the structure will be prevented by an artificial horizontal support condition that distorts the distribution of seismic action effects in the elements of the foundation and those it supports. Note that, if there are support nodes at different horizontal levels but only those at the lowest level are horizontally constrained, no horizontal reactions develop at the other support nodes and the vertical elements supported there will have zero seismic shears. So, modelling considerations lead to the same end as a sound conceptual design: a strong horizontal connection of all foundation elements that maybe at different horizontal levels, through stiff tie-beams or foundation walls, so that the entire foundation is almost rigid in both horizontal directions. Then, only support nodes at the lowest level may be constrained in both horizontal directions and about the vertical, without fictitious effects on the seismic shears and axial forces of vertical structural elements.

When it is meaningful to include elastic support conditions in the horizontal direction, as e.g., in structures supported on piles (see Section 4.9.9.5), horizontal elastic supports may be placed at different horizontal levels, as needed.

Note that, if soil compliance in the vertical or horizontal direction is taken into account, this should be done at all support nodes; translational constraint of just a few of them may change drastically the pattern of action effects in the foundation. Constraint of rotations about the horizontal will totally distort the effect of vertically elastic supports, but not vice-versa.

For foundation on spread footings with tie-beams or on piles, the distribution of seismic internal forces in the superstructure and in the foundation system is mainly influenced by the rotational elastic supports and relatively little by the translational ones. In raft (mat) foundations and foundation beams, the effect of vertical elastic supports on the distribution of seismic internal forces is at least as much as that of the rotational ones.

Elastic support "constants" are in general function of the frequency of vibration. In view of the uncertainty of soil parameters on which these "constants" depend, the effect of frequency is normally neglected and the (larger) static stiffness is used. This is safe-sided for internal forces, but not always for deformations.

If there are no elastic supports in the library of the analysis software, the designer can introduce fictitious elements between the support node and a fictitious one below at an arbitrary vertical distance h and with all its six DoFs fully restrained. The axial stiffness of the fictitious element, EA/h, is set equal to the target vertical impedance at the support node, K_z. With the support node restrained in both horizontal directions, the fictitious element's flexural rigidities, EI_x, EI_y, are chosen so that $4EI_x/h$ and $4EI_y/h$ match the target rotational impedances, $K_{\varphi x}$ and $K_{\varphi y}$, respectively.

4.9.9.3 Foundation Beams and Raft Foundations

Soil compliance under foundation beams or raft (mat) foundations is almost always modelled using the subgrade reaction modulus (or Winkler spring) approach, which assumes that a soil pressure p applied at a point of the soil-structure interface causes an absolute displacement of that point, y_s, which is proportional to p:

$$p = k_s y_s \tag{4.47}$$

The constant k_s is the subgrade modulus (or Winkler constant). Note that Eq. (4.47) entails lack of coupling between different points at the soil-structure interface, as if the soil were a system of independent vertical springs, each with spring constant (vertical impedance):

$$K_z = k_s A_f \tag{4.48}$$

where A_f is the tributary area of the spring.

Foundation beams should be modelled by special-purpose beam-on-elastic-foundation elements connecting two adjacent physical joints of the beam with other structural elements (walls, columns, foundation beams). The stiffness matrix of this type of element is a function not only of the properties of the beam, but of k_s as well. Shear deformations should always be accounted for, if the depth of the foundation beam is large.

If the library of the analysis software used does not include the special-purpose beam-on-elastic-foundation element, recourse to a "poor-man's" alternative may be necessary, that is less accurate, but computationally more demanding and inconvenient to apply. In this option the length of the foundation beam between two adjacent physical joints with other structural elements is broken up, via intermediate nodes, into a string of conventional 3D beam elements. The intermediate nodes, as well as those corresponding to physical joints of the beam with other structural elements, are elastically supported in the vertical direction. The vertical impedance at these supports may be taken from Eq. (4.48), with A_f being the tributary area of the node at the soil-foundation beam interface. An average soil pressure may be estimated at each support node, as the vertical reaction there divided by the tributary area, A_f. The shear force diagram along the foundation beam is discontinuous at the support nodes (as only self-weight acts between them), each discontinuity being equal to the vertical reaction there. The bending moment diagram is multilinear. Note the inconvenience for dimensioning and detailing of a so-modelled foundation beam, as the bending moment and shear force diagrams of the subelements along its length should be assembled into a single moment- or shear-diagram for the whole beam.

Rotational DoFs about the horizontal axes can be taken as completely free at all support nodes along the foundation beam, unless its bottom flange is asymmetric with respect to the web and the so-induced torsion needs to be taken into account, along with the restraining of the twisting by the subgrade. In that case, an impedance K_φ against rotation about the longitudinal axis x of the foundation beam should be assigned to each support node:

$$K_\varphi = k_s \frac{A_f b_f^2}{5.75} \tag{4.49}$$

where b_f is the width of the bottom flange.[12] The x axis of the foundation beam should pass then through the shear centre of the flanged beam section at the intersection of the web and the flange, instead of its centroid. This reflects the horizontal eccentricity between the web, which takes the torsion, and mid-flange, where the support nodes are placed.

Raft (mat) foundations, integral with beams connecting the bases of adjacent vertical elements, are sometimes modelled as a two-way system of foundation beams, each with a flange between panel mid-spans on either side of the beam. This computationally convenient approximation is fairly good for the calculation of the global response, but gives insufficient information for the design of the raft slab itself. If the raft is an inverted flat plate with no beams except at the perimeter, its approximation as a grid of strip-like "foundation beams" between adjacent vertical elements is not good enough. A finer two-way grid of intersecting "beams" is certainly an improvement. However, the best and only accurate model of such a raft is by plate FEs,[13] with each panel of the slab between adjacent vertical elements discretised into a (fair) number of FEs. All nodes of these elements should be elastically supported vertically, with elastic constant from Eq. (4.48), using as A_f the tributary area of the node. Such a model can depict well the distribution and magnitude of soil pressures and is sufficiently accurate for the internal forces in the slab (including around column bases) to be used in its dimensioning. Beams along the perimeter, as well as any beams connecting the base of adjacent vertical elements, should be modelled as a string of conventional 3D beam elements following the discretisation of the slab. The elastically supported nodes for the plate FEs render the use of special beam-on-elastic-foundation elements for these beams not only meaningless, but also wrong. Note that 4-node plate elements for the slab, having as nodal DoFs the displacement normal to the mid-plane and the two rotations about axes within that plane, fit well with the DoFs of the 3D beam elements used for the beams. Note also that, a rigid-body connection between a raft slab modelled with "shell" FEs (i.e., with plate elements possessing active DoFs and stiffness in-plane, in addition to out-of-plane) and the eccentric centroidal axis of a beam's web induces coupling of the beam bending with the in-plane deformations of the slab. This is an effective flange effect in the beam. However, it is questionable if the results would reflect realistically the composite action of the beam in bending with the slab. Note also that, unless judiciously placed so that they don't obstruct any deformation of the raft's slab within its plane, constraints of the horizontal DoFs of the slab's "shell" elements will obstruct or even suppress any bending of those beams that have rigid-body connection of their eccentric centroidal axis to the slab's nodes. It is therefore preferable and computationally simpler to specify an effective flange width for the beam and employ for the slab plate FEs (not "shell"), without active in-plane DoFs and stiffness. Alternatively, the centroidal axis of the beam elements could be shifted

[12] Equation (4.49) approximates the rotational impedance of a strip footing about its longitudinal axis from Eq. (4.53b), using Eq (4.54) for k_s.

[13] If the slab is thick, thick-plate FEs, e.g. of the Midlin type, should preferably be used.

to the mid-plane of the slab. But this may not be meaningful for very deep beams, e.g., perimeter walls.

4.9.9.4 Footings

According to a common rule-of-thumb, a footing may be considered as rigid, if it does not protrude in plan from the vertical element it supports by more than twice the footing depth.

When the footing is considered rigid, the impedance of the underling soil may be lumped at the centroid of the footing in plan, in 3 uncoupled springs: one vertical (z) and two rotational about the centroidal horizontal axes x and y of the footing. Expressions for these impedances have been developed on the basis of analytical or FE studies of footings embedded in elastic soil and in full contact with it. For instance, Kausel and Roesset (1975) and Elsabee et al. (1977) developed Eqs. (4.50) and (4.51) for footings with effective embedment depth d[14] in an elastic stratum having depth D_s above rigid bedrock. The impedance in the vertical direction is:

$$K_z = \frac{4Gr_a}{1-\nu}\left(1 + 0.4\frac{d}{r_a}\right) \tag{4.50}$$

and for rotation about the x or y axis:

$$\begin{aligned} K_{\varphi x} &\approx \frac{8Gr_{mx}^3}{3(1-\nu)}\left(1+\frac{2d}{r_{mx}}\right)\left(1+\frac{0.7d}{D_s}\right)\left(1+\frac{r_{mx}}{6D_s}\right), \\ K_{\varphi y} &\approx \frac{8Gr_{my}^3}{3(1-\nu)}\left(1+\frac{2d}{r_{my}}\right)\left(1+\frac{0.7d}{D_s}\right)\left(1+\frac{r_{my}}{6D_s}\right) \end{aligned} \tag{4.51}$$

In these expressions $r_a = \sqrt{(A_f/\pi)}$, $r_{mx} = (4I_x/\pi)^{1/4}$ and $r_{my} = (4I_y/\pi)^{1/4}$ are the radii of a circular footing with the same area or moment of inertia, respectively. G is the secant shear modulus of the soil at the expected shear strain level at a depth of $2r_a$ for K_z, or of $0.75r_{mx}$ or $0.75r_{my}$ for $K_{\varphi x}$, $K_{\varphi y}$, respectively. Part 5 of Eurocode 8 (CEN 2004c) gives indicative values of G equal to 80, 50 or 36% of its value at small strains ($<10^{-5}$), if the peak ground acceleration, a_gS, is 0.1, 0.2 or 0.3 g, respectively. The soil's Poisson ratio, ν, may be taken equal to 0.4 for stiff clays, 0.45 for soft clays or 0.33 for clean sands and gravels.

The fitting of Eqs. (4.50) and (4.51) to FE results applies if r_a, r_{mx}, r_{my} are all less than 50% of the stratum depth, D_s, but greater than the effective embedment depth, d.

More general and recent FE-based alternatives to Eqs. (4.50) and (4.51) are given in (ASCE 2007):

[14] Full lateral contact should develop over the effective embedment depth, capable of both sidewall friction and passive earth pressure. So, d cannot be more than the thickness of the footing and normally is less.

$$K_z = \frac{G_s\, b_x}{1-\nu}\left[1.55\left(\frac{b_y}{b_x}\right)^{\frac{3}{4}} + 0.8\right]\left[1 + \frac{2}{21}\frac{t}{b_x}\left(1 + 1.3\frac{b_x}{b_y}\right)\right]\left[1 + 0.32\left(\frac{d\,(b_y + b_y)}{b_x\, b_y}\right)^{\frac{2}{3}}\right] \tag{4.52}$$

$$K_{\varphi x} = \frac{G_s\, b_x^3}{1-\nu}\left[0.47\left(\frac{b_y}{b_x}\right)^{2.4} + 0.034\right]\left[1 + 1.4\left(\frac{d}{b_y}\right)^{0.6}\left(1.5 + 3.7\frac{\left(\frac{d}{b_y}\right)^{1.9}}{\left(\frac{d}{t}\right)^{0.6}}\right)\right] \tag{4.53a}$$

$$K_{\varphi y} = \frac{G_s\, b_x^3}{1-\nu}\left[0.4\frac{b_y}{b_x} + 0.1\right]\left[1 + 2.5\frac{d}{b_x}\left(1 + \frac{\frac{2d}{\sqrt{b_x\, b_y}}}{\left(\frac{d}{t}\right)^{0.2}}\right)\right] \tag{4.53b}$$

In these expressions b_x always denotes the smaller of the two plan dimensions of the footing and b_y the larger one ($b_x < b_y$); the x-axis is normal to b_x and the y-axis normal to b_y; d is again the effective embedment depth defined for Eqs. (4.50) and (4.51) and t the soil depth from the surface to the underside of the footing. The results of Eqs. (4.52) and (4.53) are consistent with those of Eqs. (4.50) and (4.51).

Sometimes, the elastic constants for the compliance of the soil under the footing are expressed in terms of k_s, for consistency with the subgrade reaction modulus approach followed for foundation beams and rafts. In that case, if Eq. (4.48) is retained for the soil's impedance in the vertical direction with $A_f = b_x b_y$, the following value of k_s should be used for consistent results with Eqs. (4.49) and (4.51) in approximately square footings:

$$k_s \approx \frac{2.3G}{b_x(1-\nu)} \tag{4.54}$$

where b_x is the smaller of the two plan dimensions of the footing. Note that Eq. (4.54) gives values about 75% higher than the expression normally used for k_s (Horvath 1983):

$$k_s \approx \frac{1.3G}{b_x(1-\nu)} \tag{4.54a}$$

The rotational impedances should then be computed from Eqs. (4.51) or (4.53), using in them a value of G obtained by inverting Eq. (4.54) for G in terms of k_s.

If the footing cannot be considered as rigid, the underlying soil should be modelled via Winkler springs spread out over the underside of the footing, having only vertical impedance. To better reflect the rotational impedance, the springs should be concentrated close to the edges of the footing in plan. The simplest layout would employ just four springs, each one close to a corner of the footing. The constant

of the springs should be chosen to reproduce the total vertical impedance of a rigid footing from Eqs. (4.50) or (4.52). With the so-determined spring constant, their distance in x and y should be chosen so that the rotational impedances from Eqs. (4.51) or (4.53) is reproduced. All this is arduous enough to dissuade the designer from choosing flexible footings. As pointed out at the beginning of this section, a thickness not less half the largest outhang of the footing from the vertical element it supports is commonly considered sufficient for a footing to be considered rigid.

4.9.9.5 Pile Foundations

When piles are used for the foundation of a building elastic supports in the horizontal directions are worth including, provided that this is done at all foundation elements, regardless of whether they are at the same horizontal level or not.

Groups of piles can be replaced by elastic supports at the group's centroid at the underside of the pile-cap. The group vertical or horizontal impedance is the sum of those of the individual piles, k_{zi}, k_{xi}, k_{yi}. Its rotational impedances about the horizontal axes are:

$$K_{\varphi x} = \sum_i (y_i^2 k_{zi} + k_{\varphi xi}), \quad K_{\varphi y} = \sum_i (x_i^2 k_{zi} + k_{\varphi yi}) \tag{4.55}$$

where x_i and y_i are measured from the centroid of the pile group. Point bearing is usually taken for a pile and the pile-head vertical stiffness, k_{zi}, is taken equal to the pile full axial stiffness, $E_c A/L$. The impedance of an individual pile in the horizontal directions, $k_x = k_y$, the rotational impedance, $k_{\varphi x} = k_{\varphi y}$, and the coupling stiffness, $k_{\varphi x,y} = k_{\varphi y,x}$, between the force along one axis and the rotation about the other, or the moment about one axis and the translation along the other, may be taken from the expressions given in Part 5 of Eurocode 8 (CEN 2004c) in terms of the pile diameter and Modulus of Elasticity, D and E_c:

– If the Modulus of Elasticity of the soil, E_s, is taken constant with depth:

$$\begin{aligned} k_x = k_y &= 1.08 D E_s \left(\frac{E_c}{E_s}\right)^{0.21} \quad k_{\varphi x} = k_{\varphi y} = 0.16 D^3 E_s \left(\frac{E_c}{E_s}\right)^{0.75} \\ k_{\varphi x-y} &= k_{\varphi y-x} = -0.22 D^2 E_s \left(\frac{E_c}{E_s}\right)^{0.5} \end{aligned} \tag{4.56a}$$

– If the soil Modulus is proportional to depth, with value E_s at a depth equal to the pile diameter:

$$\begin{aligned} k_x = k_y &= 0.6 D E_s \left(\frac{E_c}{E_s}\right)^{0.35} \quad k_{\varphi x} = k_{\varphi y} = 0.14 D^3 E_s \left(\frac{E_c}{E_s}\right)^{0.8} \\ k_{\varphi x-y} &= k_{\varphi y-x} = -0.17 D^2 E_s \left(\frac{E_c}{E_s}\right)^{0.6} \end{aligned} \tag{4.56b}$$

For soil Modulus proportional to the square root of depth, the coefficients and exponents in the applicable expressions assume average values between those in Eqs. (4.56a) and (4.56b).

4.9.9.6 Separating the Rigid-Body Motion from Seismic Analysis Results with Soil Compliance

It has been pointed out in Section 4.9.9.1 that, unless a rigid, box-type foundation system is provided for the entire structure, a representative picture of the distribution of seismic demands in the lateral load resisting system cannot be obtained, unless the model includes the compliance of the ground. This is also essential for the calculation of the action effects, seismic or not, which are necessary for the design or assessment of any tie-beams, foundation beams or a raft foundation.

If the soil compliance is recognised in the model by providing throughout the foundation elastic supports in the vertical direction and for rotation about the two horizontal axes, the inertial soil-structure-interaction effect of rocking is fully reflected in the 1st translational mode in each horizontal direction. Although, at least for elastic response, the ensuing reduction in the base shear and internal forces corresponds to physical reality, it might in some cases be beyond what is allowed by the code, or felt by the designer to be safe-sided. In such cases, most of (if not all) the favourable effects of soil-structure interaction on the period(s) and base shear(s) could be removed, without adversely affecting the accuracy of the distribution of internal forces in the structure. Measures to this end are outlined below.

Rigid body rocking of the structure is made possible, and affected, mainly by the vertical elastic supports, and less by the rotational ones about the two horizontal axes. The effect of rocking is normally confined in the 1st predominantly translational mode in each horizontal direction. Dunkerley's rule allows removing it from the value of the 1st period in direction X, T_{1X}, computed including soil compliance in the model:

$$T_{1X}^{*} = \sqrt{T_{1X}^{2} - T_{\varphi X}^{2}} \tag{4.57}$$

where T^{*}_{1X} is the estimate of the 1st mode period of the structure fixed to the ground and $T_{\varphi X}$ is the period of its rigid-body rocking in the vertical plane through direction X:

$$T_{\varphi X} = 2\pi \sqrt{\frac{\sum_{i} m_i (x_i^2 + z_i^2)}{\sum_{j} (K_{zj} x_j^2 + K_{\varphi yj})}} \tag{4.58}$$

In Eq. (4.58) i indexes the masses of the entire structure and j the support nodes at the foundation. Heights z are measured from the level of the foundation, while x is horizontal distance from the centroid in plan of the vertical impedence:

$$\sum_j K_{zi} x_j = 0 \tag{4.59}$$

The (modal) spectral acceleration can then be read from the response spectrum using the value of the period from Eq. (4.57). Similarly for direction Y.

Rigid-body rocking induces no internal forces. If desired, the influence of rocking on the 1st mode response in each horizontal direction can be essentially removed, not only from the internal forces, but also from the modal participation factor, the modal mass and the displacements that determine interstorey drifts and are of interest for the control of damage in nonstructural elements. Rigid-body rotation in the 1st mode within vertical plane XZ (positive when it is in the +Y direction) can be estimated from the ratio of the 1st mode overturning moment at the level of the foundation to the corresponding rotational stiffness:

$$\Phi_X \approx \frac{\sum_j (R_{zj} x_j - M_{yj})}{\sum_j (K_{zj} x_j^2 + K_{\varphi yj})} \tag{4.60a}$$

where j indexes again the support nodes, R_{zj} is the modal vertical reaction force (positive when it acts upwards on the structure) and M_{yj} is the modal reaction moment about axis Y (positive when its vector on the structure is in the +Y direction). To remove the effect of rocking from this mode, its eigenvector is modified by:

- subtracting Φ_X from all nodal rotations about the positive Y-axis;
- subtracting $\Phi_X z_i$ from all nodal displacements in direction X; and
- adding $\Phi_X x_i$ to all nodal vertical displacements (taken positive upwards).

where i indexes nodes on the structure. Modal internal forces obtained from the revised mode shape do not incorporate the effect of rocking (i.e., they refer to a structure fixed to the ground) and will be the same as from a model that includes soil compliance. The modal participation factor, the modal mass and the modal displacements will be different, though.

The rigid-body rotation in vertical plane YZ, Φ_Y, (positive when it is in the +X direction) is estimated as:

$$\Phi_Y \approx -\frac{\sum_j (R_{zj} y_j + M_{xj})}{\sum_j (K_{zj} y_j^2 + K_{\varphi xj})} \tag{4.60b}$$

where M_{xj} is modal reaction moment about axis X (positive when its vector on the structure is in the +X direction).The eigenvector of this mode is modified by:

- subtracting Φ_Y from all nodal rotations about the positive X-axis,
- subtracting $\Phi_Y z_i$ from all nodal displacements in direction Y, and
- adding $\Phi_Y y_i$ to the nodal displacements in direction Z.

Note that P–Δ effects include the contribution of rigid-body rocking on lateral drifts and should be computed before removing it.

If design for the vertical component of the seismic action uses the results of an elastic analysis of the full structure including vertical compliance of the soil, the effect of the latter should be removed from the calculated dynamic characteristics of the structure. Dunkerley's rule can be applied to the computed period, T_{1Z}, of the mode with the largest modal mass in direction Z:

$$T_{1Z}^{*} = \sqrt{T_{1Z}^{2} - T_{Z}^{2}} \tag{4.57a}$$

with the period of rigid-body vertical vibration of the structure on flexible soil computed as:

$$T_z = 2\pi \sqrt{\frac{\sum\limits_i M_i}{\sum\limits_j K_{zj}}} \tag{4.61}$$

To remove the contribution of rigid-body vertical vibration from the shape of this mode, a vertical displacement:

$$\delta_z = \sum_j R_{zj} / \sum_j K_{zj} \tag{4.62}$$

should be added to the modal vertical displacements (taken positive if upwards) of all nodes *i*. This changes the modal participation factor and the modal mass, but not the modal internal forces.

4.10 Modelling of Buildings for Nonlinear Analysis

4.10.1 Nonlinear Models for Concrete Members

4.10.1.1 The Level of Discretisation

Concrete structures are often discretised for nonlinear static analysis under monotonically increasing non-seismic loads at a point-by-point basis and modelled at the material level. A large number of FEs in 2D or 3D is used, with different Elements for the concrete and for the reinforcing steel and possibly for their interaction through bond. Such (micro-)modelling allows us, in principle, reproduce even minor details in the geometry of the members and follow the history of stresses and strains at every point. There has been immense progress in constitutive modelling of plain or reinforced concrete under generalised multiaxial loading (including reversals), in

mesh-independent FE representation of crack initiation and propagation and of the behaviour of crack interfaces, etc. (CEB 1996b, *fib* 2008). These advances notwithstanding, computational and memory requirements confine point-by-point nonlinear modelling to the analysis of the seismic response of individual members (especially shear walls) or subassemblies of members (e.g. beam-column joints, along with the beams and columns framing into them) and hamper its application to entire structures in 3D.

Practical nonlinear seismic response analysis, static or dynamic, of full RC structures is normally carried out using less sophisticated member-by-member modelling, with one-to-one correspondence between elements of the model and members of the structure. A single element is used for a beam, a column, the part of a wall between two floors, a panel of a floor-diaphragm between adjacent frames, etc. Although this does not account for every minute detail in the geometry and the reinforcement of a member, it allows a sufficiently close representation of the key features of its behaviour. Furthermore, it is capable of describing the distribution of inelasticity and damage among and within members with reasonable computational requirements even for large 3D structures. So, macro- or member-by-member modelling has been established as the main workhorse for practical nonlinear seismic response analysis of concrete structures and will remain so in the foreseeable future. Accordingly, only this modelling approach is covered here.

The starting point of the overview of member models is Fibre modelling. Fibre models fall in-between micro- and macro-modelling. They resemble macro-models in using member models as their building block. To develop the member model, though, the detailed σ-ε response at a large number of points over several cross-sections of the member is traced during the entire multi-step response analysis. Therefore, Fibre models may be considered as an application of the FE method to the one-dimensional continuum of a prismatic member, using the Bernoulli assumption of plane sections as a kinematic constraint to express the DoFs of the various points of a cross-section in terms of the three deformation measures of the section. They are the most fundamental, physically-based approach, capable of treating the general case of biaxial flexure and varying axial load, a special case of which is uniaxial bending with constant axial force. Fibre models are also closer to point-by-point FE modelling in what concerns their requirements in computer time and memory. Simpler member models are also derived in Sections 4.10.1.3 and 4.10.1.4 as simplifications of the fundamental Fibre approach.

If no member yields during the seismic response, nonlinear analysis degenerates into a linear one. Therefore, the models used in nonlinear analysis and their parameters should be such that linear-elastic behaviour can be described as a special case, without major discrepancies from the results of an ordinary linear analysis. This does not mean that the level of discretisation should be identical in the two types of analysis. Nonlinear analysis models may well be more refined, using at the member level, e.g., Fibre models, provided that they give about the same elastic stiffness as the simple member models used in linear analysis.

Before entering the description of the various modelling approaches and models, it is worth recalling that at each (time-)step *i* of a nonlinear seismic response analysis:

- the element tangent stiffness matrix, $\mathbf{K}_m{}^t$, is computed, to be assembled in the global stiffness matrix $\mathbf{K}_i$ in Eqs. (4.23),
- the vector of element internal nodal forces, $\boldsymbol{F}_m$, should be derived from the current deformation state of the element, to be assembled in the global internal force vector; and
- the difference between $\boldsymbol{F}_i$ in Eqs. (4.23) and the global internal force vector is equilibrated by iterations within the current step of the analysis, before proceeding to the next one.

4.10.1.2 Fibre Models

The most general, fundamental and powerful model for one-dimensional members is the Fibre model. It is also best suited for inhomogeneous materials, like RC (CEB 1996a). In a Fibre model the member is discretised both longitudinally, into segments represented by discrete cross-sections or slices, and at the cross-sectional level, into finite regions. If bending takes place within a single plane (uniaxial), the discretisation is into strips or "fibres" normal to this plane (e.g. Aziz 1976, Mark 1976). If bending is biaxial, the cross-section is divided into a number of rectangular finite regions, with sides parallel to the cross-sectional axes, y and z, see Fig. 4.6 (e.g. Menegotto and Pinto 1973, Aktan et al. 1974, Zeris and Mahin 1984). The generic fibre comprises concrete and/or reinforcing steel, lumped at the fibre centroid. The nonlinear uniaxial σ-ε laws of these two materials are

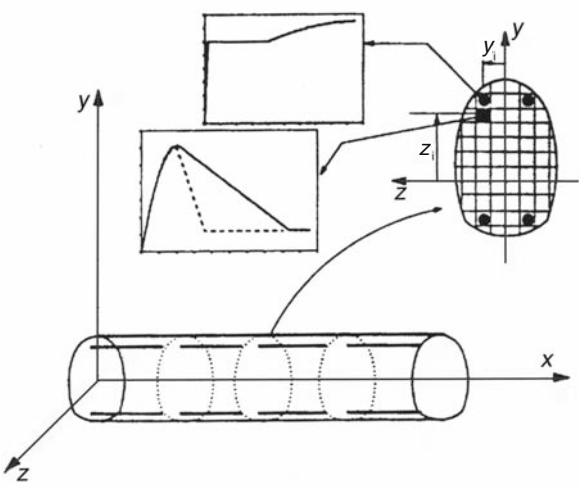

Fig. 4.6 Monitored sections and section subdivision in a Fibre model, adapted from CEB (1996a)

employed at that level. They take into account, in principle, stress reversals, concrete cracking, tension-stiffening and confinement, buckling of discrete reinforcing bars, etc.

In a Fibre model the normal strain at a point (y, z) of the member section at x along its axis is related to the section deformation vector[15]:

$$\boldsymbol{\varepsilon}_{\mathrm{s}}(x) = [\varphi_{\mathrm{y}}(x), \varphi_{\mathrm{z}}(x), \varepsilon_{\mathrm{o}}(x)]^{\mathrm{T}} \tag{4.63}$$

on the basis of the plane-sections assumption:

$$\varepsilon(x, y, z) = \boldsymbol{B}_{\mathrm{s}}(y, z)\boldsymbol{\varepsilon}_{\mathrm{s}}(x) \tag{4.64}$$

where:

$$\boldsymbol{B}_{\mathrm{s}}(y, z) \equiv [z, -y, 1] \tag{4.65}$$

The section force vector:

$$\boldsymbol{S}_{\mathrm{s}}(x) \equiv [M_{\mathrm{y}}(x), M_{\mathrm{z}}(x), N(x)]^{\mathrm{T}} \tag{4.66}$$

is derived from the normal stresses, $\sigma(y, z)$, over the section A as:

$$\boldsymbol{S}_{\mathrm{s}}(x) = \int_{\mathrm{A}} \boldsymbol{B}_{\mathrm{s}}{}^{\mathrm{T}}\sigma(x, y, z)\mathrm{d}A \tag{4.67}$$

It is incrementally related to $\boldsymbol{\varepsilon}_{\mathrm{s}}$ as:

$$\mathrm{d}\boldsymbol{S}_{\mathrm{s}}(x) = \mathbf{K}_{\mathrm{s}}{}^{\mathrm{t}}(x)\mathrm{d}\boldsymbol{\varepsilon}_{\mathrm{s}}(x) \tag{4.68}$$

where the section tangent stiffness matrix is:

$$\mathbf{K}_{\mathrm{s}}{}^{\mathrm{t}}(x) = \int_{\mathrm{A}} E^{\mathrm{t}}(x, y, z)\boldsymbol{B}_{\mathrm{s}}{}^{\mathrm{T}}\boldsymbol{B}_{\mathrm{s}}\mathrm{d}A \tag{4.69}$$

The tangent modulus $E^{\mathrm{t}}(x, y, z)$ is the ratio of $\mathrm{d}\sigma$ to $\mathrm{d}\varepsilon$ at point (y, z) of section x. It depends on the type of material at that point (i.e., whether it is steel or concrete), as well as on its previous σ- and ε-history, through the material cyclic σ-ε law.

The element nodal force vector at member end nodes A and B:

$$\boldsymbol{S}_{\mathrm{m}} \equiv [M_{\mathrm{y}}{}^{\mathrm{A}}, M_{\mathrm{z}}{}^{\mathrm{A}}, M_{\mathrm{y}}{}^{\mathrm{B}}, M_{\mathrm{z}}{}^{\mathrm{B}}, N, T]^{\mathrm{T}} \tag{4.70}$$

---

[15] In Eq. (4.63) φ_{y} denotes the curvature from the analysis and index y signifies the cross-sectional axis about which φ_{y} is defined. In this case index y has nothing to do with yielding.

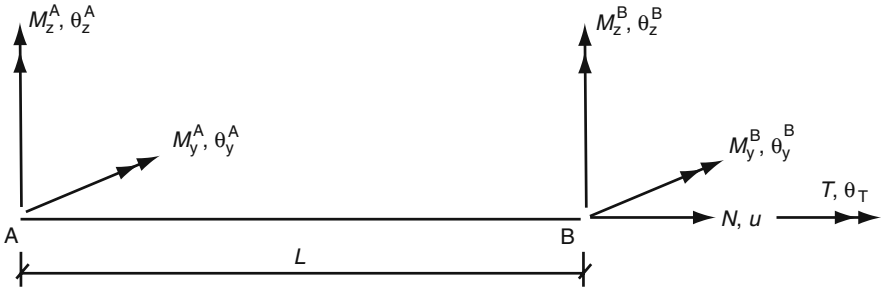

Fig. 4.7 Internal forces and element deformations at member ends

is incrementally related to the corresponding element deformation vector:

$$\boldsymbol{v}_{\mathrm{m}} \equiv [\theta_{\mathrm{y}}{}^{\mathrm{A}}, \theta_{\mathrm{z}}{}^{\mathrm{A}}, \theta_{\mathrm{y}}{}^{\mathrm{B}}, \theta_{\mathrm{z}}{}^{\mathrm{B}}, N, T]^{\mathrm{T}} \tag{4.71}$$

where θ_{y}, θ_{z} are the chord rotations at nodes A and B[16] and u, θ_{T} the relative displacement and the twist of these two nodes along and about the member axis x (see Fig. 4.7):

$$\mathrm{d}\boldsymbol{S}_{\mathrm{m}} = \mathbf{K}_{\mathrm{m}}{}^{\mathrm{t}}\mathrm{d}\boldsymbol{v}_{\mathrm{m}} \tag{4.72}$$

$\mathbf{K}_{\mathrm{m}}{}^{\mathrm{t}}$ in Eq. (4.72) is the element tangent stiffness matrix.

Following the classical elastic FE formulation, early Fibre models adopted for the construction of the element stiffness matrix a "stiffness-based" approach (Aktan et al. 1974). They postulate an invariant interpolation function matrix $\mathbf{B}_{\mathrm{m}}(x)$ for element deformations such that[17]:

$$\mathrm{d}\boldsymbol{\varepsilon}_{\mathrm{s}}(\mathrm{x}) = \mathbf{B}_{\mathrm{m}}(x)^{\mathrm{T}}\mathrm{d}\boldsymbol{v}_{\mathrm{m}} \tag{4.73}$$

Then, the principle of virtual displacements is invoked, to compute $\mathbf{K}_{\mathrm{m}}{}^{\mathrm{t}}$ as:

$$\mathbf{K}_{\mathrm{m}}{}^{\mathrm{t}} = \int_{\mathrm{L}} \mathbf{B}_{\mathrm{m}}(x)^{\mathrm{T}}\mathbf{K}_{\mathrm{s}}{}^{\mathrm{t}}(x)\mathbf{B}_{\mathrm{m}}(x)\mathrm{d}x \tag{4.74}$$

[16]In this section M^{A} and θ^{A} denote the moment and the chord rotation from the analysis at member end node A. Index y signifies the cross-sectional axis about which $M_{\mathrm{y}}{}^{\mathrm{A}}$ and $\theta_{\mathrm{y}}{}^{\mathrm{A}}$ are defined and has nothing to do with yielding.

[17]Note that the distribution of inelasticity along the member changes during the response. After plastic hinging, further flexural deformations take place mainly in the vicinity of the yielding end(s), spreading thereafter over the rest of the length with further loading. So, an interpolation function matrix $\mathbf{B}_{\mathrm{m}}(x)$ which is invariant during the response is against this physical reality.

as well as the increment of the internal nodal force vector:

$$\mathrm{d}\boldsymbol{F}_{\mathrm{m}} = \int_{\mathrm{L}} \mathbf{B}_{\mathrm{m}}(x)^{\mathrm{T}} \mathrm{d}\boldsymbol{S}_{\mathrm{s}}(x)\mathrm{d}x \tag{4.75}$$

with $\mathrm{d}\boldsymbol{S}_{\mathrm{s}}(\mathrm{x})$ from Eq. (4.68), etc.

For the integrations over its area, A, the cross-section at x is discretised into "fibres" or "filaments" of surface area $\mathrm{d}A$. For the calculation of $\mathrm{d}\sigma$ at point (x, y, z) and of $E^{\mathrm{t}}(x, y, z) = \mathrm{d}\sigma/\mathrm{d}\varepsilon$, the value of $\mathrm{d}\varepsilon$ calculated at the current step from Eqs. (4.64) and (4.73) and the cyclic σ-ε law of the material are not sufficient. Any other past-history information required by this law should be kept in memory at the section fibre level.

Integration over x along the member length L is in principle performed numerically. Integration stations may be equidistant, if the trapezoidal rule is used, or at irregular intervals more closely spaced near the ends, if a more elaborate but efficient scheme is adopted, such as Gauss or Gauss-Lobatto (with integration stations at each end and at three to seven sections in-between). Serious problems sometimes arise from the numerical integration. Once inelasticity develops at member ends, the variation of $\boldsymbol{\varepsilon}_{\mathrm{s}}(\mathrm{x})$ with x deviates significantly from that imposed by the use in Eq. (4.73) of an invariant $\mathbf{B}_{\mathrm{m}}(x)$ matrix (typically based on cubic Hermitian polynomials as in elastic FEs). This may cause, e.g., a spurious variation with x of the internal axial force $N(\mathrm{x}) = \int_{\mathrm{A}} \sigma(x, y, z)\mathrm{d}A$, which cannot be corrected through equilibrium iterations (CEB 1996a). A more serious problem can arise when the analysis proceeds beyond the ultimate strength at an end section. Then, if the end section continues loading on the post-ultimate strength softening branch, intermediate sections will unload elastically (CEB 1996a, Zeris and Mahin 1984). If post-ultimate strength softening is included in the model, this behaviour cannot be reflected by an invariant $\mathbf{B}_{\mathrm{m}}(x)$ matrix and causes numerical problems.

Nonlinear analysis programs with "stiffness-based" Fibre models sometimes attempt to by-pass the problems above by providing intermediate nodes between member ends, at a number sufficient to capture the distribution of inelasticity along the member even when using an invariant $\mathbf{B}_{\mathrm{m}}(x)$ matrix between the intermediate nodes (Izzuddin and Elnashai 1989, Millard 1993). Some programs even have the capability of automatically generating such internal nodes when member inelasticity develops and subsequently refine the mesh with the progression of inelasticity (Izzuddin and Elnashai 1989). To reduce computations for the solution of Eq. (4.22), all DoFs of these intermediate nodes may be condensed out statically, provided that there are no lumped masses there. Even without condensation, intermediate nodes do not overly increase the computational demands, as these are determined mainly from the need to keep track of fibre stresses and strains at the monitored sections and to perform the integration over the section.

"Flexibility-based" fibre models (Zeris and Mahin 1984, Kaba and Mahin 1984) tackle the problems above, but not fully. In them the section tangent flexibility matrix, $\mathbf{F}_{\mathrm{s}}{}^{\mathrm{t}}(x)$, obtained by inverting $\mathbf{K}_{\mathrm{s}}{}^{\mathrm{t}}(x)$, is integrated to give the element tangent flexibility matrix, $\mathbf{F}_{\mathrm{m}}{}^{\mathrm{t}}$:

$$\mathbf{F}_{\mathrm{m}}{}^{\mathrm{t}} = \int_{\mathrm{L}} \mathbf{e}(x)^{\mathrm{T}} \mathbf{F}_{\mathrm{s}}{}^{\mathrm{t}}(x) \mathbf{e}(x) \mathrm{d}x \tag{4.76}$$

The element equilibrium matrix, $\mathbf{e}$(x), relating $\boldsymbol{S}_{\mathrm{s}}(x)$ to $\boldsymbol{S}_{\mathrm{m}}$ as:

$$\boldsymbol{S}_{\mathrm{s}}(x) = \mathbf{e}(x) \boldsymbol{S}_{\mathrm{m}} \tag{4.77}$$

is exact irrespective of the distribution of inelasticity along the member, if no loads are applied between its two ends. As $\mathrm{d}\boldsymbol{\varepsilon}_{\mathrm{s}}(x) = \mathbf{F}_{\mathrm{s}}{}^{\mathrm{t}}(x)\mathrm{d}\boldsymbol{S}_{\mathrm{s}}(x) = \mathbf{F}_{\mathrm{s}}{}^{\mathrm{t}}(x)\mathbf{e}(x)\mathrm{d}\boldsymbol{S}_{\mathrm{m}} = \mathbf{F}_{\mathrm{s}}{}^{\mathrm{t}}(x)\mathbf{e}(x)\mathbf{K}_{\mathrm{m}}{}^{\mathrm{t}}\mathrm{d}\boldsymbol{v}_{\mathrm{m}}$, incremental internal nodal forces, $\mathrm{d}\boldsymbol{F}_{\mathrm{m}} = \int_{\mathrm{L}} \mathbf{B}_{\mathrm{m}}(x)^{\mathrm{T}} \mathrm{d}\boldsymbol{S}_{\mathrm{s}}(x)\mathrm{d}x$, can be calculated using a non-invariant flexibility-dependent matrix $\mathbf{B}_{\mathrm{m}}(x)$, continuously updated during the analysis as: $\mathbf{B}_{\mathrm{m}}(x) = \mathbf{F}_{\mathrm{s}}{}^{\mathrm{t}}(x)\mathbf{e}(x)\mathbf{K}_{\mathrm{m}}{}^{\mathrm{t}}$ while the internal nonlinearities vary (Mahasuverachai and Powell 1982). An inconsistency persists regardless, this time between the section forces $\boldsymbol{S}_{\mathrm{s}}(x)$ computed at the section level from Eq. (4.67) and those derived from nodal forces through Eq. (4.77). So do most numerical and physical problems associated with the "stiffness-based" approach. To solve them without introducing intermediate nodes, more complex mixed two-field models (with assumed force and deformation distributions) have been proposed (Taucer et al. 1991).

Although Fibre models are based on the plane-sections assumption, they can account for nonlinear shear deformations of the member. A shear strain, γ, that depends on the element shear force $V = (M^{\mathrm{A}} + M^{\mathrm{B}})/L$ through the nodal moments M^{A}, M^{B}, may be considered as a fictitious chord rotation and added to the flexural ones at member ends (CEB 1996a). However, the possibility of shear failure cannot be detected and accounted for in this way.

Fixed-end rotation at the end section of the member due to slippage of longitudinal bars from the joint region beyond that end may be taken into account by introducing a nonlinear rotational spring at that end, similar to those of the one-component point-hinge model in Sections 4.10.1.4 and Fig. 4.9. The tangent flexibility of such a rotational spring at end A or B within one of the two orthogonal planes of bending, xy or xz, is denoted here by f_{A} or f_{B}, respectively. These terms are added to the diagonal ones, f_{AA} and f_{BB}, relating the increments of inelastic chord rotations, $\mathrm{d}\theta_{\mathrm{A}}$, $\mathrm{d}\theta_{\mathrm{B}}$, with respect to chord AB to those of the end moments, $\mathrm{d}M_{\mathrm{A}}$, $\mathrm{d}M_{\mathrm{B}}$, in the Fibre model's element tangent flexibility matrix, $\mathbf{F}_{\mathrm{m}}{}^{\mathrm{t}}$ (obtained from Eq. (4.76) in the "flexibility-based" approach, or by inverting the element tangent flexibility matrix $\mathbf{K}_{\mathrm{m}}{}^{\mathrm{t}}$ of Eq. (4.74) in the "stiffness-based" one):

$$F_{\mathrm{m,total}}{}^{t} = \begin{bmatrix} f_{\mathrm{AA}} + f_{\mathrm{A}} & f_{\mathrm{AB}} \\ f_{\mathrm{AB}} & f_{\mathrm{BB}} + f_{\mathrm{B}} \end{bmatrix} \tag{4.78}$$

The total element tangent flexibility matrix, $\mathbf{F}_{\mathrm{m,total}}{}^{\mathrm{t}}$, obtained by adding diagonal flexibility terms, f_{A}, f_{B}, within each one of the two orthogonal planes of bending, xy or xz, is then inverted to give the tangent stiffness matrix of the element. At each end, let's say A, and within the corresponding plane of bending, this

term may be approximated as $f_A = \theta_{y,slip}/M_y$ before flexural yielding and as $f_A = \Delta\theta_{u,slip}/(M_u\text{-}M_y)$ afterwards; $\theta_{y,slip}$ and $\Delta\theta_{u,slip}$ may be estimated from Eqs. (3.42) in Section 3.2.2.3 and (3.63) in Section 3.2.2.9, respectively, while M_y, M_u can be obtained as $\int_A \sigma y_{cg} dA$ from the fibre discretisation of the end section, or according to Sections 3.2.2.2 and 3.2.2.5, respectively (with the effects of any lap-splicing, FRP-wrapping or prestressing taken into account on the basis of Sections 3.2.3.9, 3.2.3.10 or 3.2.3.11, respectively). As shown in Fig. 3.45(d), the hysteresis loops of the fixed-end rotation due to bond-slip are narrow, with inverted-S shape. This type of behaviour may be captured by the hysteresis rules of models with pinching (Roufaiel and Meyer 1987, Costa and Costa 1987, Park et al. 1987, Reinhorn et al. 1988, Coelho and Carvalho 1990) in Section 4.10.1.6 and Table 4.4, if the pinching parameters are judiciously chosen.

Fibre models account for the details of the geometry of the cross-section and of the distribution of the reinforcement, can follow the spreading of inelasticity along the member and reproduce realistically pinching of moment-curvature hysteresis loops. As they use directly realistic σ-ε laws of the individual materials (possibly including confinement of concrete, strength and stiffness degradation due to low-cycle fatigue, buckling of bars, etc.) Fibre models are "fundamental" models. In principle, they can take into account the effects of biaxial bending (see Sections 3.2.3.7 and 3.2.3.8), the coupling between bending and the axial direction (Section 3.2.3.6), as well as the effects of a varying axial load (see Section 3.2.2.8). The simplified member-type models described in the following, by contrast, try to capture the complex overall behaviour of the member through phenomenological rules and semi-empirical hysteresis relations between moment and curvature or moment and plastic hinge rotation (see Sections 4.10.1.5 and 4.10.1.6). Notwithstanding their power and rationality, Fibre models require at each step of the analysis lengthy computations to construct the member tangent stiffness matrix and calculate stresses and strains at the fibre level at each slice, as well as tracing all the σ- and ε-history information of each fibre which is necessary for the calculation of the tangent modulus and the stress at the current strain. So, Fibre models are far more demanding in computer time and storage than the simplified member-type models described in Sections 4.10.1.3, 4.10.1.4, 4.10.15 and 4.10.1.6. Note that the larger the number of nonlinear operations required by a computational scheme, the higher is the likelihood of a local numerical instability spreading throughout the structure. Last, but not least, the input properties and parameters of Fibre models should be carefully tuned, to reproduce the experimental behaviour of the member, including its connections. Such tuning requires specialised knowledge and experience, beyond current capabilities of design professionals. All things considered, it is not at all certain that the power and rationality of Fibre models warrant their generalised practical use.

To avoid the large computational requirements of Fibre models while retaining their main strength, namely their ability to capture biaxial effects and axial-flexural coupling, it has been proposed to replace discretisation of the section and monitoring of the σ-ε history at the fibre level with incremental relations between the section force and deformation vectors, $\boldsymbol{\varepsilon}_s(x)$ and $\boldsymbol{S}_s(x)$, or between the nodal force and deformation vectors, $\boldsymbol{S}_m$ and $\boldsymbol{v}_m$. Such models are overviewed in Fardis

(1991) and CEB (1996a). Some of them use forms of Plasticity Theory in 3D (e.g. Sfakianakis and Fardis 1991a, b, Bousias and Fardis 1994, Bousias et al. 2002). They may suffer though from similar or even worse numerical problems than Fibre models. Besides they do not enjoy their generality. So, they do not seem to be viable alternatives.

The unique advantage of Fibre models is their ability to take into account the effects of biaxial bending and the coupling between bending and the axial direction. When bending is essentially in a single plane and axial-flexural coupling is of no interest (e.g. in beams) there may be little point in using a Fibre model instead of the simpler alternatives described in Sections 4.10.1.3, 4.10.1.4, 4.10.15 and 4.10.1.6. When using a Fibre model in such cases, tinkering with its axial DoFs or with those associated with out-of-plane bending should be avoided. For example, if the cross-section is asymmetric with respect to what is considered as a single plane of bending, restraining its out-of-plane rotation will have a parasitic (normally stiffening) effect on the computed in-plane flexure. By the same token, constraining the nodal displacements at the two ends of the element to be the same introduces a fictitious axial force in the element and changes its inelastic flexural behaviour. If we want to restrain or constrain such DoFs for reasons of computational efficiency, we would better use a simple model for uniaxial bending without axial-flexural coupling, of the type described in Sections 4.10.1.3 or 4.10.1.4.

4.10.1.3 Spread Inelasticity Models with Phenomenological M-φ Relations for Uniaxial Bending Without Axial-Flexural Coupling

In beams bending is uniaxial while axial-flexural coupling is commonly considered as irrelevant.[18] For walls, only inelastic flexure in their strong direction of bending is of interest, while axial-flexural coupling, although important (see Section 2.2.2.4), is often ignored. In columns, as we will see in Section 4.10.1.4, the inelastic flexural response is often treated independently in the two directions of bending for simplicity, while only few aspects of axial-flexural coupling are considered in each direction. Therefore, uniaxial bending with axial-flexural coupling ignored or treated in a simplified way, is of prime practical importance.

For uniaxial bending the tangent flexibility matrix of section x, $\mathbf{F}_s{}^t(x)$, degenerates into a scalar section flexibility, $f_s{}^t(x) = \mathrm{d}\varphi\,/\mathrm{d}M$ and its tangent stiffness matrix into the section rigidity, $k_s{}^t(x) = \mathrm{d}M/\mathrm{d}\varphi$. The element tangent stiffness matrix, $\mathbf{K}_m{}^t$, is of dimension 2×2 and relates the nodal moment increments vector, $[\mathrm{d}M^A, \mathrm{d}M^B]^T$, to the chord rotations increments vector, $[\theta^A, \theta^B]^T$. The spreading of flexural inelasticity along the member renders meaningless the constant elastic interpolation vector, $\boldsymbol{b}_m(x) = (2/L)[(3x/L–2), (3x/L–1)]$, into which the elastic interpolation function matrix $\mathbf{B}_m(x)$ of Eq. (4.73) degenerates (see footnote to Eq. (4.73)). So, it makes more sense physically to adopt the flexibility approach and compute the 2×2 member tangent flexibility matrix $\mathbf{F}_m{}^t$ of Eq. (4.76), using $f_s{}^t(x) = \mathrm{d}\varphi\,/\mathrm{d}M$ for $\mathbf{F}_s{}^t(x)$ and $\mathbf{e}(x) = [(x/L\text{-}1), x/L]$ as the equilibrium matrix.

[18] It is also very uncertain and difficult to model, as it very much depends on the width of the slab which is effective as a flange of the beam.

In the present case the prime strength of Fibre modelling at the section level, namely their ability to capture biaxial effects and axial-flexural coupling, is irrelevant. So, to determine the tangent rigidity of the section it is not necessary to discretise the generic cross-section into fibres, monitor the σ-ε response there and perform the integration in Eq. (4.69). Instead, a hysteretic relation between moment and (smeared) curvature may be adopted, describing phenomenologically the experimental behaviour or the one analytically derived, e.g., from a fibre model used once to fit the phenomenological one. The *M*-φ relation may be chosen among the models presented in Section 4.10.1.6. This is the first simplification advanced here.

The second step for the reduction of the large computational demands of the fundamental fibre approach and bypassing some of its problems, is to construct the member tangent flexibility matrix without calculating the tangent flexibility at various intermediate control sections of the member and numerically integrating Eq. (4.76). Instead, Eq. (4.76) is integrated analytically, using control sections only at the ends, but still accounting for the actual distribution of inelasticity along the member ("spread inelasticity" models). In this way the inconsistency between the section forces $\boldsymbol{S}_s(x)$ from Eq. (4.67) and those from Eq. (4.77) is bypassed.

If the instantaneous bending moment diagram due to the combination of the seismic and the gravity actions is approximately linear near each member end, plastification extends up to a distance (normalised to the member length, *L*) from end A or B, respectively, equal to:

$$\lambda_A = (M_A - M_y^A)/(V_A L) \geq 0, \qquad \lambda_B = (M_B - M_y^B)/(V_B L) \geq 0 \tag{4.79}$$

with the yield moment, $M_y{}^A$ or $M_y{}^B$, taken constant throughout each plastic zone. If the phenomenological *M*-φ relation adopted is multi-linear, having elastic rigidity *EI* before yielding and tangent rigidities in primary loading, unloading or reloading expressed through their piece-wise constant ratios to *EI*, φ will also vary linearly along each dimensionless length λ_A and λ_B. Then, the element tangent flexibility matrix $\mathbf{F}_m{}^t$ of Eq. (4.76) may be analytically computed, using $f_s{}^t(x) = d\varphi/dM$ for $\mathbf{F}_s{}^t(x)$ and $\mathbf{e}(x) = [(x/L–1), x/L]$ for the equilibrium matrix (Filippou and Issa 1988):

$$\mathbf{F}_m{}^t = \begin{bmatrix} f_{AA} & f_{AB} \\ f_{AB} & f_{BB} \end{bmatrix} \tag{4.80}$$

where:

$$f_{AA} = \frac{1 + \dfrac{1-(1-\lambda_A)^3}{p_A} + \dfrac{\lambda_B^3}{p_B}}{3EI/L}, \; f_{AB} = -\frac{1 + \dfrac{\lambda_A^2\left(3-2\lambda_A\right)}{p_A} + \dfrac{\lambda_B^2\left(3-2\lambda_B\right)}{p_B}}{6EI/L},$$
$$f_{BB} = \frac{1 + \dfrac{1-(1-\lambda_B)^3}{p_B} + \dfrac{\lambda_A^3}{p_A}}{3EI/L} \tag{4.81}$$

In Eq. (4.81) p_A and p_B denote the ratios of the effective tangent rigidity within the plastic zone near end A or B, respectively, to the difference of that rigidity from *EI*. It is assumed that when the end section unloads, reloads or is in primary loading, the full length of the corresponding plastic zone does the same. If the plastic zone near end A is in primary loading, all its sections have the same tangent rigidity, *pEI*, where *p* is the hardening ratio in primary loading. Then $p_A = p/(1–p)$. If it unloads or reloads, the tangent section rigidity is not constant anymore along its length. It has its minimum value, EI_A, at the end section, which unloads or reloads from the maximum curvature in the zone, while it is equal to *EI* at a distance $\lambda_A L$ from A, where the section is elastic. If the effective tangent rigidity of the plastic zone corresponds to the average tangent flexibility along $\lambda_A L$, i.e., to $(1/EI+1/EI_A)/2$, then $p_A = 2EI_A/(EI–EI_A)$ (which gives $1/p_A = 0$ in Eq. (4.81) for unloading parallel to the elastic branch). Similarly for the plastic zone near end B and p_B (Filippou and Issa 1988).

The values of λ_A, λ_B in Eq. (4.81) are non-decreasing, giving the maximum ever length of plastification at the corresponding end. The flexibility matrix evolves owing to changes in the state of the two plastic zones from loading (or reloading) to unloading, or vice-versa, or to an increase in their length.

The elastic rigidity, *EI*, to be used in Eq. (4.81) and as the basis for p_A and p_B may be taken equal to M_y/φ_y, with M_y and φ_y computed according to Section 3.2.2.2. For *primary loading* p_A or p_B may be taken equal to:

$$p_A(or\ p_B) = \frac{\left(M_u - M_y\right) / \left(\varphi_u - \varphi_y\right)}{M_y/\varphi_y - \left(M_u - M_y\right) / \left(\varphi_u - \varphi_y\right)} \tag{4.82}$$

with M_u and φ_u determined according to Sections 3.2.2.5 and 3.2.2.4, respectively. The effects of any lap-splicing, FRP-wrapping or prestressing on M_u, M_y, φ_u, φ_y, may be taken into account on the basis of Sections 3.2.3.9, 3.2.3.10 or 3.2.3.11, respectively, as relevant. Different values of unloading or reloading rigidity $EI_A = dM/d\varphi$ applies at A for each unloading or reloading branch and a different value of p_A is derived from it as $p_A = 2EI_A/(EI–EI_A)$ (similarly for end B and p_B). The phenomenological hysteretic M-φ model determines how the unloading rigidity depends, in general, on the point of (M and φ) reversal where unloading starts and how the reloading rigidity depends on the value of φ where reloading starts and on the M-φ point where it is heading at, etc. (see Section 4.10.1.6).

Strictly speaking the value of $EI = M_y/\varphi_y$ in Eq. (4.81) for loading that induces tension at one side of the section at A and at the opposite side at B (i.e., hogging moment at A and sagging at B) is different from the *EI*-value applying for loading that induces compression at these two sides (sagging moment at A, hogging at B). This is very inconvenient, as the *EI* values of members determine the global dynamic characteristics of the elastic structure (natural periods and mode shapes), which are considered as independent of the direction of loading. So, we should use in Eq. (4.81) the average *EI* value of the two ends (also average value for positive and negative bending, if the section is asymmetrically reinforced). Different values

of p_A and p_B can be used at A and B (and for positive or negative bending for asymmetrically reinforced sections).

Spread inelasticity models with phenomenological M-φ relations account only for flexural deformations within the clear length of the member. Fixed-end rotations at the end sections due to slippage of longitudinal bars from the joint region beyond the end may be taken into account as in Fibre models, i.e., via nonlinear rotational springs at the ends as described in Section 4.10.1.2 in conjunction with Eq. (4.78).

Spread inelasticity models cannot, in principle, account for coupling of the two directions of bending, and between them and the axial forces and deformations. If used for columns, they are commonly in the form of two uncoupled uniaxial models, one for each of the two orthogonal directions of bending. Although the two twin elements representing the column share its axial force and each has 50% of its full axial stiffness, the full value of the axial force should be used for the calculation of the properties of each one of the two twin elements. The value of the elastic stiffness, EI, should be fixed during the response and calculated from the values of M_y, φ_y due to the axial force for gravity loads alone. It is fairly simple, though, and normally does not create numerical problems, to update the yield moment, M_y, and (with it) the maximum-ever values of λ_A and λ_B from Eq. (4.79), and the hardening ratios p_A, p_B from Eq. (4.82) using the current axial force value. This will make a difference in exterior columns of medium- or high-rise buildings and in piers of coupled walls, where the axial force varies a lot during the response. The value of M_y, and the post-elastic primary loading branch derived from it through Eq. (4.82), may be considered constant during further primary loading. After reversal, by contrast, and while reloading in the reverse direction, the value of M_y in that direction should be updated according to the evolution of the axial force. By the same token, the value of the uniaxial yield moment signalling plastification of the end section may be taken to decrease with increasing current moment component in the orthogonal direction (see Sections 3.2.3.7 and 3.2.3.8). This is computationally more cumbersome, though, than tracing the axial load and accounting for it, not only owing to the complications associated with biaxial moment interaction diagrammes, but also because each one of the two uncoupled uniaxial elements used for the column normally is unaware of the current state of bending in its companion. All in all, the returns in accuracy from attempts to emulate Fibre models may not warrant the sacrifice in simplicity they entail.

4.10.1.4 "Point-Hinge" or "Lumped Inelasticity" Models

Under lateral actions flexural inelastic deformations are concentrated at and near member ends, since it is there that bending moments have maximum values. So in the early inelastic beam models inelasticity was taken to be concentrated ("lumped") at the ends of the member in zero-length "point hinges".

In the earliest inelastic model, the *two-component element* (Clough et al. 1965), the member is considered as a system of two components *in parallel* (Fig. 4.8):

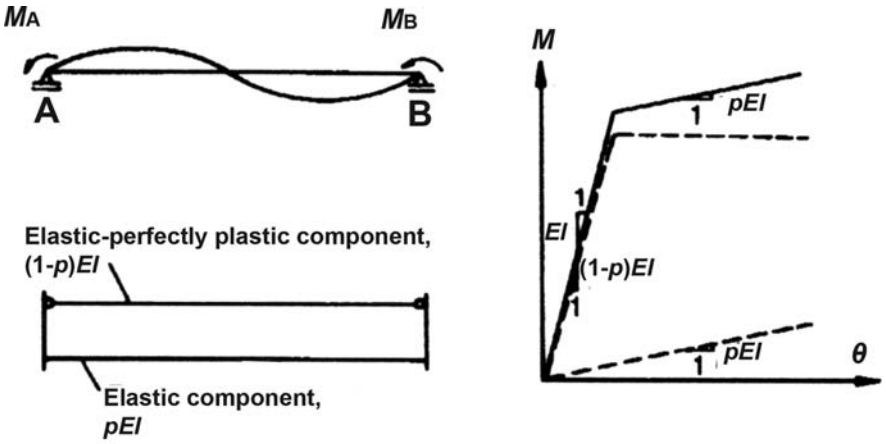

Fig. 4.8 Two-component element model

- The first component is an elastic-perfectly plastic beam and represents yielding. Before yielding at the beam's ends, it is an elastic beam element. After the moment reaches the yield value at an end, the tangent stiffness matrix becomes that of an elastic member with a moment release there. If the yield moment is reached at the other end as well, the tangent stiffness matrix is that of a member with moment releases at both ends.
- The second component is an elastic beam and represents post-yield hardening. Its section rigidity is a small fraction, p, of the elastic rigidity, EI, of the member.

The tangent stiffness matrices of the two components are added and the composite member exhibits a bilinear (elastic-linearly strain hardening) moment-rotation behaviour with a hardening rigidity of pEI. In order for the sum of the elastic section rigidities of the two components to give that of the member, EI, the elastic rigidity of the elastic-perfectly plastic component is equal to $(1–p)EI$.

The hysteretic behaviour of the two-component model is bilinear, with unloading and reloading branches parallel to those in primary (virgin) loading. Such a cyclic behaviour may fit well steel members with stable hysteresis loops exhibiting a moderate Bauschinger effect. It does not represent well the degradation of unloading and reloading stiffness and the narrow hysteresis loops of concrete members. So, it is appropriate only when there is essentially a single inelastic excursion of the member and we are interested only in the magnitude of the peak inelastic deformation. The two-component model significantly overestimates energy dissipation when the member goes through several inelastic cycles. It has been included regardless in the libraries of widely used general purpose nonlinear dynamic analysis software, because in some cases it has certain advantages over the equally simple alternatives represented by the one-component model described next.

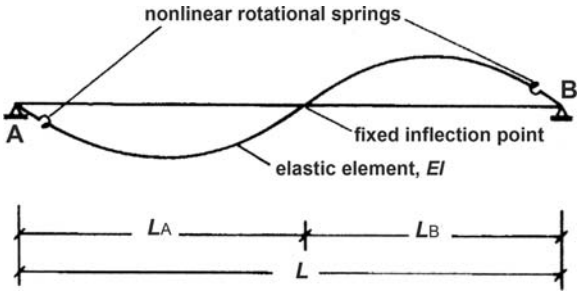

Fig. 4.9 One-component element model

To avoid the bilinear hysteresis inherent in the two-component model, a *one-component element* has been proposed in Giberson (1967). It is a *series model* of an elastic element and nonlinear rotational springs at its ends (Fig. 4.9). All inelastic deformations are lumped at the two end springs. The two nonlinear end springs are taken to contribute to the tangent flexibility matrix of the member with diagonal terms f_A, f_B alone, as in Eq. (4.78). For uniaxial bending $\mathbf{F}_m{}^t$ is:

$$\mathbf{F}_m{}^t = \frac{L}{6EI}\begin{bmatrix} 2 + a_A / p_A & -1 \\ -1 & 2 + a_B / p_B \end{bmatrix} \tag{4.83}$$

where:

- a_A and a_B are zero-one variables for plastic hinging at the end sections:
  - $a_A = 0$ before plastic hinging at end A, i.e., so long as $M^A < M_y{}^A$;
  - $a_A = 1$ after plastic hinging there, i.e., for $M^A \geq M_y{}^A$;

  and similarly for a_B at end B;
- $p_A = (L/(6EI))/f_A$, $p_B = (L/(6EI))/f_B$ are the current tangent stiffnesses of the rotational springs, as a fraction of the elastic stiffness of the member in skew-symmetric bending, $6EI/L$.[19] During the course of cyclic loading or response, piece-wise constant values of f_A, f_B are derived from the multilinear rules in Section 4.10.1.5 for primary loading and Section 4.10.1.6 for unloading-reloading.

$\mathbf{F}_m{}^t$ is inverted to give the member's tangent stiffness matrix, $\mathbf{K}_m{}^t$. For uniaxial bending $\mathbf{K}_m{}^t$ is:

$$\mathbf{K}_m{}^t = \frac{6EI/L}{3 + 2\,(a_A/p_A + a_B/p_B) + (a_A/p_A)\,(a_B/p_B)}\begin{bmatrix} 2 + a_B/p_B & 1 \\ 1 & 2 + a_A/p_A \end{bmatrix} \tag{4.84}$$

[19] Unlike the two-component element, which turns into a fully elastic model if $p = 1$, the one-component element can reproduce elastic overall behaviour only through very large values of the yield moments, $M_y{}^A$, $M_y{}^B$, at which the point hinges at the ends A and B are activated. As the rotational springs are in series with the elastic element in-between, setting $p_A = p_B = 1$ for them just increases the overall flexibility of the element (doubles it for skew-symmetric bending).

In the two- or the one-component element the rigidity of the member section, EI, may be taken equal to the secant-to-yield-point stiffness, EI_{eff}, from Section 3.2.3.3, Eq. (3.68). Fixed-end rotations due to slippage of longitudinal bars from the joint region beyond the member ends can then be reflected in EI_{eff}, through the term involving a_{sl} in Eq. (3.66). If the longitudinal reinforcement is different at the two end sections of the member, Eq. (3.68) gives two different values of EI_{eff} there. Moreover, if the end sections are asymmetrically reinforced (as in beams with different reinforcement at top and bottom), the value of EI_{eff} is different for each sense of bending (positive or negative). According to the reasoning at the 2nd paragraph from the end of Section 4.10.1.3, the average value of EI_{eff} over the two ends and the two senses of bending is used then as rigidity of the member section, EI, in the two- or the one-component model.

The calculated nonlinear seismic response does not depend heavily on the exact value of the single hardening ratio in primary loading, p, of the two-component model, or of the two hardening ratios, p_{A}, p_{B}, of the one-component one in the individual members. So, default constant values, such as 0.05, 0.1, or even sometimes zero, are often used for *primary loading*. More representative values may be estimated from the member properties:

$$p = \frac{\left(M_u - M_y\right) / \left(\theta_u - \theta_y\right)}{M_y/\theta_y - \left(M_u - M_y\right) / \left(\theta_u - \theta_y\right)} \tag{4.85}$$

For the purposes of Eq. (4.85) M_{u}, M_{y} may be computed according to Sections 3.2.2.5 and 3.2.2.2, respectively. Sections 3.2.3.5 (or 3.2.3.4) and 3.2.3.2, may be used for the calculation of the chord rotations θ_{u} and θ_{y}, respectively. The effects of any lap-splicing or FRP-wrapping may be taken into account on the basis of Sections 3.2.3.9 and 3.2.3.10, respectively. Note that hardening ratios for primary loading have higher values in terms of chord rotations (i.e. from Eq. (4.85)) than curvatures (from Eq. (4.82)), often by a factor of 2 to 3. A single hardening ratio, p, is used in the two-component model, namely the average over the two ends and for positive and negative bending. The one-component model can use different values of p_{A} and p_{B} at A and B (and for positive or negative bending for asymmetrically reinforced sections, although an average value is also acceptable).

Implicit in the use of the secant stiffness to the yield-point from Section 3.2.3.3, Eq. (3.68), as EI_{eff} in the one- or two-component model is the assumption of constant values of the member axial load and of the shear span, L_{s}, at each end. The same for the estimation of the hardening ratio in primary loading from Eq. (4.85). For all practical purposes the axial load may be taken equal to the value due to gravity loads alone. The choice of a constant value for the shear span (i.e, the distance of an end section where plastic hinging may take place under lateral loading to the inflection point) is less clear cut. For a frame member, especially a beam, the natural choice is to assume that plastic hinges will develop in skew symmetric bending at both sections where the member frames into transverse ones within the plane of bending. Then, the shear span is half the clear length from one beam-column joint to the next

within the plane of bending: $L_s = L_{cl}/2$.[20] Plastic hinging in walls takes place only at the storey's bottom section and indeed with an imaginary point of inflection well above that storey. As pointed out in Section 2.2.2.2, the shear span of the entire part of a wall between floors, defined as the moment-to-shear ratio at the storey's bottom section, is about 50% of the height from that section to the top of the wall, $L_s = H_{tot}/2$.

An inflection point that stays steady after the first excursion of the member into the inelastic range is also a necessary condition for the inelastic part of the one-component model's tangent flexibility matrix to be diagonal, i.e., with diagonal terms f_A, f_B alone, without coupling between the two ends. Establishing the values of the hardening ratios, p_A, p_B, of this model on the basis of a fixed shear span value at the corresponding end implies that a steady inflection point has indeed been assumed.

A point-hinge or lumped inelasticity member model is intentionally very simple. So, it does not, and cannot, aspire to account for coupling of the two directions of bending, and between them and the axial forces and deformations. It can be used for columns as two separate and uncoupled uniaxial models, one for each of the two orthogonal directions of bending, sharing the axial force and the column's full axial stiffness. As pointed out in the last paragraph of Section 4.10.1.3, any plastic hinge property in each one of the two twin elements should be calculated on the basis of the full axial force of the column. The value of EI_{eff} should be considered fixed during the response, as calculated from the values of M_y, θ_y due to the axial force for gravity loads alone. It is fairly simple, though, and normally does not give rise to numerical problems, to activate a hinge when the end moment reaches the current yield moment, M_y, as determined from the current value of the axial force. The value of M_y and the post-elastic primary loading branch derived from it may be considered constant during further primary loading. After reversal and during reloading in the opposite direction, the value of M_y in that direction should be updated according to the evolution of the axial force. The plastic hinge will be activated in the reverse direction when this updated value of M_y, or the post-elastic primary loading branch derived from it, are reached. Finally, as pointed out in the last paragraph of Section 4.10.1.3, in principle a non-zero concurrent moment component in the orthogonal direction may be taken into account to reduce the value of the uniaxial yield moment for activation/re-activation of a plastic hinge (see Section 3.2.3.8). However, with the same reasoning as at the end of Section 4.10.1.3, any gains in accuracy are not worth sacrificing the inherent simplicity of the one-component point-hinge model.

---

[20] In a beam indirectly supported on another beam at one end, plastic hinging can take place only at the other end and the beam's shear span may be taken equal to the beam full clear span. In girders connected at intermediate points with cross-beams or girders, plastic hinging will develop only at the girder's connection with vertical members. Then the shear span is determined on the basis of the girder clear span between columns into which the girder frames. Although the parts of a girder between joints with cross-beams may be modelled as individual beam elements, their effective elastic stiffness and hardening ratios should be taken the same, as established from the clear span of the overall girder.

Notwithstanding its lack of generality and inherent limitations, the lumped inelasticity one-component model has become the workhorse for practical nonlinear – especially dynamic – seismic response analysis. Obvious incentives for the user are its flexibility, intuitive appeal, simple computational implementation and use, minimal computational requirements and superior numerical robustness. There are good technical reasons as well for its practical application:

- The most common form of the one-component point-hinge model works directly with chord rotations, which encompass shear deformations of the member and fixed-end rotations due to bond-slip of longitudinal bars from their anchorage zones. So, compared with Fibre or spread inelasticity models based on curvatures, it lends itself better to fitting or calibrating model parameters using directly the wealth of member test results, typically given as force-deflection (i.e., -chord rotation) hysteretic loops, without differentiating between flexural and shear deformations or bond-slip effects of longitudinal bars from the anchorage. As a matter of fact, most (if not all) empirical hysteresis rules of Section 4.10.1.6 have been empirically developed from such test data and suit better models that use chord rotations. For the same reason, the portfolio of tools offered in Chapter 3 for the derivation of model parameters in terms of chord rotations are wider in scope and more robust (i.e., associated with smaller scatter or bias) than those for curvatures.
- The material σ-ε behaviour traced in Fibre models, including yielding, rupture or even buckling of bars and local crushing of concrete, cannot be directly translated into loss of member lateral- or axial-load resistance. By contrast, member ultimate conditions, conventionally identified with permanent loss of peak lateral load resistance, are most conveniently described by response variables at the member level, notably by chord rotations or shear forces for ultimate condition due to flexure or shear, respectively.

All things considered, the one-component point-hinge model seems to provide at present the best option for practical nonlinear seismic response analysis, static or dynamic, of concrete buildings with realistic size and complexity in 3D, either for evaluation of the performance of a new design or for assessment and retrofitting of an existing building. The rationality, power and generality of Fibre models can best be used in the realm of research.

4.10.1.5 The Uniaxial M-φ or M-θ Curve for Monotonic or Primary Loading

To be consistent with the linear analysis into which it degenerates if no member yields during the seismic response, nonlinear analysis should use about the same pre-yield stiffness as a usual linear analysis. As emphasised in Sections 3.2.3.3 and 4.9.2, the elastic stiffness of the monotonic force-deformation relation of members should be the secant stiffness to the yield-point, so that the global elastic stiffness corresponds to the elastic branch of a bilinear monotonic global force-deformation relation. It has also been pointed out there that, if a default elastic

stiffness of one-half the uncracked gross section stiffness is used, e.g., for consistency with linear analysis, deformation demands are seriously underestimated. This may ruin the very end of nonlinear analysis, namely the estimation of seismic deformation demands to be compared to the corresponding capacities, be it for assessment (and/or retrofitting) of existing buildings or for performance evaluation of new designs. Normally, realistic values are used for the capacities, as, e.g., given in Chapter 3 and in Annex A of CEN (2005a). Therefore, the estimates of the demands should also be realistic. This can indeed be achieved if the effective elastic stiffness of members is taken equal to their secant stiffness to the yield-point from Eq. (3.68), as Annex A of CEN (2005a) recommends doing in assessment and retrofitting of concrete buildings on the basis of nonlinear or linear analysis.

A realistic value of the elastic stiffness up to the yield point of all members is more vital for nonlinear dynamic than for static analysis, because important contributions of higher modes to inelastic response often entail post-yield excursions in members which may stay in the elastic range under the fundamental mode alone. In pushover analysis it is primarily (if not only) the "target displacement" that is affected by the global stiffness of an effective elasto-plastic system normally fitted to the capacity curve on the basis of equal deformation energy (equal areas, see Fig. 4.2). This stiffness is in turn not seriously affected by a fictitiously high early stiffness of certain members.

The corner point of a bilinear force-deformation relation in primary loading is the yield point of the member, as governed by the member's most critical (i.e. weakest) mechanism of force transfer, in flexure, brittle shear or bond of longitudinal bars. Brittle shear failure before plastic hinging is catastrophic and once it occurs lateral load resistance is considered to be lost. The M-φ or M-θ relation in monotonic or primary loading stops then at a value of the end moment $M = V_R L_s < M_y$ where V_R is the resistance in brittle shear and L_s and M_y are the shear span and the yield moment at the end in question. By contrast, ductile shear failure occurs in a flexural plastic hinge, after the hinge forms. The yield point is still at the yield moment.

In addition to the elastic stiffness and the yield strength, a main parameter of a bilinear monotonic force-deformation relation is the post-elastic stiffness. A meaningfully long post-elastic branch is due to flexural inelastic deformations and normally exhibits strain hardening. A constant hardening ratio (: post- to pre-yield stiffness) is given by Eq. (4.82) or (4.85) in M-φ or M-θ terms, respectively. Recall, however, that the monotonic (also called primary) M-φ or M-θ curve serves as skeleton to the hysteresis loops in cyclic loading, which may entail significant strength decay when ultimate deformation is approached.[21] So, to make room for post-elastic strength degradation, positive strain hardening in flexure may be neglected for simplicity and zero post-yield stiffness may be used, as Eurocode 8 allows doing.

The end point of the primary loading curve is the ultimate deformation. If governed by flexure, it is the ultimate curvature, φ_u, or chord rotation, θ_u, in M-φ or M-θ terms, respectively. Sections 3.2.2.4 and 3.2.3.5 (or 3.2.3.4) may be used to compute φ_u and θ_u, respectively, with the effect of any lap-splicing, FRP-wrapping or

[21] Recall, in this connection, that the ultimate deformation is conventionally identified with a drop in peak force resistance after ultimate strength equal to 20% of the ultimate strength value.

prestressing taken into account on the basis of Sections 3.2.3.9, 3.2.3.10 or 3.2.3.11, respectively, as relevant. For cyclic loading the primary loading curve may end at the point where the acting shear force in the plastic hinge is found to exceed the cyclic resistance against ductile shear failure according to Sections 3.2.4.3, 3.2.4.5 or 3.2.5.4, at a value of the chord rotation less than θ_u.

A residual post-ultimate moment resistance may be retained in the model afterwards. However, there is no solid technical support for the selection of its level. Note, though, that the question of residual resistance is academic. For the performance of a structure to be verified as acceptable in practical applications, every single member (new, retrofitted, or existing and non-retrofitted) should be verified in the end to have ultimate deformation well above the seismic demand (see Section 6.5.6 and Table 6.1). So, there is no real need to introduce an abrupt drop in resistance after the ultimate deformation.

Unlike the elastic stiffness, which should be the same, all other parameters of the primary loading curve may be different for positive and negative loading, depending on how symmetric the geometry and the reinforcement of the section is.

Eurocode 8 requires as a minimum a bilinear primary loading curve in nonlinear member models. It allows, though, using instead a trilinear curve, as, e.g., in Takeda et al. (1970), Park et al. (1987), Reinhorn et al. (1988) and Costa and Costa (1987) to take into account the difference between pre- and post-cracking stiffness. If used as skeleton curve for cyclic loading, such a trilinear curve produces certain hysteretic damping before yielding, which increases from zero at cracking to a maximum value at yielding. Moreover, from cracking to yielding the secant stiffness of the trilinear model does not have a unique value. This ambiguity does not allow direct comparisons with the elastic response spectrum predictions, let alone conformity with linear analysis in the pre-yielding stage. So, it is strongly recommended to use in nonlinear dynamic analysis member models with bilinear force-deformation relationship in primary loading.[22] After all, by the time of a strong earthquake concrete members most likely will be cracked owing to gravity loads, thermal strains and drying shrinkage, or even previous shocks. In nonlinear static analysis a trilinear monotonic force-deformation relationship for members affects only the initial part of the "capacity curve", without the problems and ambiguities it causes in nonlinear dynamic analysis.

4.10.1.6 Phenomenological Models for the Cyclic Uniaxial M-φ or M-θ Behaviour

The M-φ or M-θ curve in primary loading suffices for nonlinear static analysis and serves as skeleton curve in nonlinear response-history analysis. It is supplemented there with hysteresis rules for post-elastic unloading-reloading cycles.

The main objective of nonlinear response-history analysis in practical applications is the estimation of member peak seismic deformation demands, to be compared to the corresponding capacities. Estimates of member peak deformation demands depend on the hysteretic energy dissipation inherent in

[22] By the same token, the tensile strength of concrete should be neglected in Fibre models.

unloading-reloading rules, but are little affected by their precise shape and other details.[23] For this reason, the only requirement posed by Eurocode 8 on hysteretic models is to realistically reflect energy dissipation within the range of displacement amplitudes induced in members by the seismic action used for the analysis. Moreover, as the predictions of nonlinear dynamic analysis for peak response are not highly sensitive to the hysteresis rules, a more essential feature of the hysteretic model for applications is its numerical robustness under any potential response history. This is of utmost importance, as any numerical weakness of the model will certainly show up during at least one of the ground motions for which a system with hundreds of members is analysed in thousands of time-steps, possibly with a few iterations in each step. Numerical problems at the member level might spread and develop into global ones, preventing convergence. Even when the stabilising effect of inertia forces and damping salvages global stability, local numerical problems may lead to errors in member demands, which an inexperienced eye cannot detect. Simple and clear hysteretic models, using few rules to describe the response under any (small or large, full or partial) cycle of unloading and reloading, are less prone to numerical problems than elaborate and presumptuous ones, especially when complexity obscures certain unlikely possibilities with dangerous outcomes.

Multilinear unloading and reloading from and to the skeleton curve or to a reloading branch (Fig. 4.10) is simple and computationally efficient. Using δ as the generic symbol for deformation (φ or θ), unloading from a maximum ever value of $\delta = \mu\delta_y$ on the primary loading branch is typically taken linear down to a residual deformation on the δ-axis, $\delta_{res} = \varepsilon\delta_y$, which is different in different hysteretic models according to Table 4.3. Note that the models in Park et al. (1987), Reinhorn et al. (1988) and Costa and Costa (1987) have trilinear monotonic or primary loading curve, using its pre-cracking branch to define the unloading slope. This definition may be retained even when a bilinear model is used, with the first two branches

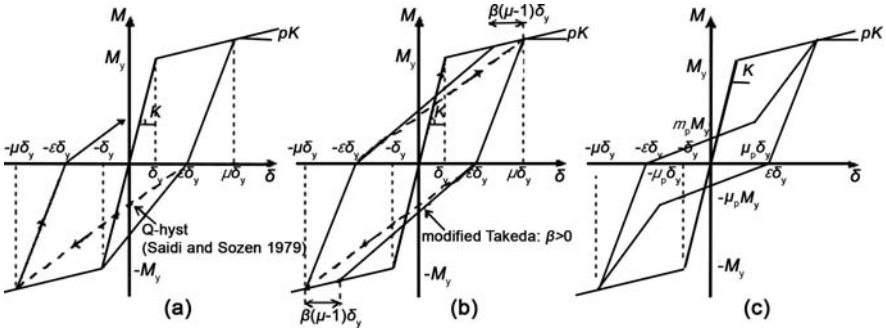

Fig. 4.10 Multilinear hysteretic models: (**a**) straight reloading to past peak point; (**b**) straight reloading to point before past peak (Otani 1974, Litton 1975); (**c**) with pinching

[23]Residual deformations are very much affected by the details of the hysteresis rules. However, their estimation is even more influenced by the details of the ground motion. So, if estimation of residual deformations is indeed of interest, current rules about the minimum number of input motions and their conformity to 5%-damped elastic response spectrum should be revisited.

Table 4.3 Residual deformation after unloading from deformation $\delta = \mu\delta_y$ on primary loading curve ($\mu > 1$, p: hardening ratio of post-yield primary loading branch)

Hysteresis model	Unloading rule	Residual deformation $\delta_{res}=\varepsilon\delta_y$
Takeda et al. (1970), and Clough and Johnston (1966)	Unloading stiffness = elastic stiffness	$\varepsilon = (1-p)(\mu-1)$
Saiidi and Sozen (1979), Coelho and Carvalho (1990), Anagnostopoulos (1972), and Costa and Costa (1987)	Unloading stiffness = μ^{-a} times the elastic stiffness ($a \approx 0.5$ or from Eq. (4.90))	$\varepsilon = \mu - (1 + p(\mu-1))\mu^{a}$
Otani (1974), and Litton (1975)	Unloading to residual deformation (1–α) times that in elastic unloading ($\alpha \approx 0.3$ or from Eq. (4.91))	$\varepsilon = (1-\alpha)(1-p)(\mu-1)$
Park et al. (1987), and Reinhorn et al. (1988)	Extension of unloading passes through point on opposite direction's pre-cracking elastic branch where $M = aM_y$ ($a \approx 2$)	$\varepsilon = \dfrac{a(1-p)(\mu-1)}{a+1+p(\mu-1)}$
Roufaiel and Meyer (1987)		$\varepsilon = \dfrac{(1-p)(\mu-1)}{1+2p(\mu-1)}$

replaced by a single one to yielding, as suggested here. The models in Otani (1974), Litton (1975), Clough and Johnston (1966), Saiidi and Sozen (1979), Roufaiel and Meyer (1987), Park et al. (1987), Reinhorn et al. (1988), Coelho and Carvalho (1990) and Costa and Costa (1987) include degradation of unloading stiffness (see point 2 in Section 3.2.2.6).

If unloading to the δ-axis continues into first-time loading in the reverse direction, it heads linearly towards the yield point of the primary loading curve in that direction and follows its post-elastic branch thereafter. If the reverse direction has been revisited before, we have reloading. It is in reloading that the model accounts or not for pinching of the hysteresis loops. If it doesn't, then the extreme point ever reached on the primary loading curve in that direction normally becomes an effective yield point to which reloading linearly heads[24] (Fig. 4.10). In (Otani 1974, Litton 1975) this straight reloading branch is directed towards a point on the primary loading curve before the previous peak, at a deformation of $[\mu-\beta(\mu-1)]\delta_y$ instead of $\mu\delta_y$ ($0 < \beta < 1$). Models without pinching (Takeda et al. 1970, Otani 1974, Litton 1975, Clough and Johnston 1966, Saiidi and Sozen 1979) are more suitable for the M-φ behaviour.

[24]Except in Saiidi and Sozen (1979), where this branch always heads towards the point on the primary loading at the maximum deformation ever reached in any of the two directions, even when this is first-time loading or real reloading.

Table 4.4 Moment and deformation at corner of bilinear reloading for models with pinching

Model	Reloading branch from (–) to (+) starting at residual deformation $-\varepsilon_{-}\delta_y^{-}$	m_p for $M_p = m_p M_y$, and μ_p for $\delta_p = \mu_p \delta_y$
Park et al. (1987)	Reloading heads first toward point where $M = \gamma M_y$ ($\gamma \approx 0.5$) on extreme branch of past unloading in (+) direction from peak past deformation $\delta^+ = \mu_+ \delta_y{}^+$ on primary loading branch to residual deformation $\delta_{res}{}^+ = \varepsilon_+ \delta_y$. It stiffens towards δ^+ on primary loading branch when $\delta_{res}{}^+$ is reached	$m_p^+ = \dfrac{(\varepsilon_+ + \varepsilon_-)\,\gamma\left[1 + p_+(\mu_+ - 1)\right]}{(\varepsilon_+ + \varepsilon_-)\left[1 + p_+(\mu_+ - 1)\right] + \gamma(\mu_+ - \varepsilon_+)}$ $\mu_p^+ = \varepsilon_+$ For reloading from (+) to (–) $m_p^- = \dfrac{(\varepsilon_+ + \varepsilon_-)\,\gamma\left[1 + p_-(\mu_- - 1)\right]}{(\varepsilon_+ + \varepsilon_-)\left[1 + p_-(\mu_- - 1)\right] + \gamma(\mu_- - \varepsilon_-)}$ $\mu_p^- = \varepsilon_-$
Reinhorn et al. (1988)	Reloading heads first toward point where $M = \gamma M_y$ ($\gamma \approx 0.5$) on pre-cracking elastic branch in (+) direction. It stiffens towards past peak point on primary loading branch when peak residual deformation $\delta_{res}{}^+ = \varepsilon_+ \delta_y$ is reached	$m_p^+ = \dfrac{(\varepsilon_+ + \varepsilon_-)\,\gamma}{\gamma + \varepsilon_-}$, $\mu_p^+ = \varepsilon_+$ For reloading from (+) to (–): $m_p^- = \dfrac{(\varepsilon_+ + \varepsilon_-)\,\gamma}{\gamma + \varepsilon_+}$, $\mu_p^- = \varepsilon_-$
Roufaiel and Meyer (1987)	Reloading to point on elastic branch where $M = mM_y$ ($m = \min[1; (0.4L_s/h – 0.6)] \geq 0$). It stiffens then towards peak past deformation on primary loading branch	$m_p = m$, $\mu_p = m$
Coelho and Carvalho (1990)	Reloading has stiffness m-times that of reloading to the peak past deformation $\delta^+ = \mu_+ \delta_y{}^+$ on primary loading branch. It stiffens towards peak past point on primary loading branch when M-axis is reached ($m < 1$).	$m_p^+ = \dfrac{m\varepsilon_-\left[1 + p_+(\mu_+ - 1)\right]}{\mu_+ + \varepsilon_-}$, $\mu_p = 0$ For reloading from (+) to (–): $m_p^- = \dfrac{m\varepsilon_+\left[1 + p_-(\mu_- - 1)\right]}{\mu_- + \varepsilon_+}$, $\mu_p = 0$
Costa and Costa (1987)	Reloading first has stiffness $\mu_+{}^{-\beta}$-times that of reloading to the peak past deformation $\delta^+ = \mu_+ \delta_y{}^+$ on primary loading branch ($\beta > 0$). It stiffens towards peak past point on primary loading branch when secant from origin to that point is reached.	$\mu_p^+ = \dfrac{\varepsilon_-\left[1 + p_+(\mu_+ - 1)\right]}{\mu_+\left(\varepsilon_-\mu_+^{\beta-1} + \mu_+^{\beta} - 1\right)}$ $m_p^+ = \dfrac{\varepsilon_-}{\varepsilon_-\mu_+^{\beta-1} + \mu_+^{\beta} - 1}$ For reloading from (+) to (–): $\mu_p^- = \dfrac{\varepsilon_+\left[1 + p_-(\mu_- - 1)\right]}{\mu_-(\varepsilon_+\mu_-^{\beta-1} - 1 + \mu_-^{\beta})}$ $m_p^- = \dfrac{\varepsilon_+}{\varepsilon_+\mu_-^{\beta-1} + \mu_-^{\beta} - 1}$

To include pinching, reloading heads first towards a corner point where the moment is denoted by $M_p = m_p M_y$ ($m_p < 1$) and the deformation by $\delta_p = \mu_p \delta_y$. It turns then towards the extreme point ever reached on the primary loading curve in the current direction of reloading (Fig. 4.10). Table 4.4 gives the values of m_p and μ_p for different hysteretic models that include pinching (Roufaiel and Meyer 1987, Park et al. 1987, Reinhorn et al. 1988, Coelho and Carvalho 1990, Costa and Costa 1987). Such models are more suitable for the overall M-θ behaviour that includes the effects of shear deformations and fixed-end rotation.[25] With appropriately chosen pinching parameters they may also describe the flexibility of nonlinear rotational springs added at ends A and B of a Fibre model, to account separately for the fixed-end rotations due to slippage of longitudinal bars from the joint region beyond that end (terms f_A, f_B in Eq. (4.78)).

Reloading after partial unloading (i.e., before the horizontal axis is reached) follows the unloading path toward the point of last reversal. If unloading resumes before that point is reached, it continues along the same unloading branch towards the δ-axis. If reloading turns into unloading before reaching its destination, i.e., the extreme past point on the primary loading curve in the current reloading direction, the unloading stiffness is the one corresponding to the original destination of reloading.

In some models (Park et al. 1987, Reinhorn et al. 1988, Coelho and Carvalho 1990, Costa and Costa 1987) reloading is directed to a point below (i.e. with lower peak resistance) than the extreme past point on the primary loading curve of that direction. In new buildings with detailing of members for ductility, degradation of strength with cycling is negligible. Besides, in general cyclic strength decay has small effect on the computed response. For given primary loading curve, the response is more sensitive to the amount of hysteretic energy dissipation, an issue addressed in the next section.

4.10.1.7 Hysteretic Damping Ratio in Cyclic Uniaxial Models

The hysteretic energy dissipation in post-yield cycles of given amplitude may be conveniently expressed as an equivalent hysteretic damping ratio, ζ, of a linearly-damped oscillator with the same natural period, that dissipates the same amount of energy per cycle as the nonlinear one:

$$\zeta = \frac{E_h}{4\pi E_{el}} \tag{4.86}$$

where E_h is the energy dissipated in a full cycle of loading-unloading-reloading and E_{el} is the elastic strain energy, $F_{max}\delta_{max}/2$, at the peak force and displacement of the cycle.

With ε according to Table 4.3, the *first full cycle* of loading-unloading-reloading to peak ductility ratio $\pm\mu$ gives the following hysteretic damping ratio (Fardis and Panagiotakos 1996):

[25] The pinching parameters of the model in Roufaiel and Meyer (1987) depend indeed on the shear span ratio, to reflect the more pronounced pinching of squat members.

$$\zeta_{n=1} = \frac{2(\mu-1)(1-p+\varepsilon p)+3\varepsilon}{4\pi\mu(1+p(\mu-1))} \tag{4.87}$$

except for the Q-hyst model in Saiidi and Sozen (1979), which gives:

$$\zeta_{n=1,Q} = \frac{(\mu-1)(1-p+3\varepsilon p)+3\varepsilon}{4\pi\mu(1+p(\mu-1))} \tag{4.87a}$$

Models without pinching (Takeda et al. 1970, Clough and Johnston 1966, Saiidi and Sozen 1979) or strength decay (Fig. 4.10a) produce the following hysteretic damping ratio in a *full subsequent cycle* of unloading-reloading to peak ductility ratio $\pm\mu$ (Fardis and Panagiotakos 1996):

$$\zeta_{n>1,no-pinching} = \frac{\varepsilon}{\pi\mu} \tag{4.88}$$

except in Otani (1974) and Litton (1975), where reloading towards a point on the primary loading curve at deformation $[\mu\text{-}\beta(\mu\text{-}1)]\delta_y$ instead of $\mu\delta_y$ (Fig. 4.10b) gives a hysteretic damping ratio in a full subsequent cycle (Fardis and Panagiotakos 1996):

$$\zeta_{n>1,\boldsymbol{Otani}} = \frac{\varepsilon}{\pi\mu}\left(1+\frac{\beta(1-p-p\varepsilon)}{2(1-\alpha)(1+p(\mu-1))}\right) \tag{4.88a}$$

If strength decay is neglected, models with pinching (Roufaiel and Meyer 1987, Park et al. 1987, Reinhorn et al. 1988, Coelho and Carvalho 1990, Costa and Costa 1987) according to Fig. 4.10c and with m_p and μ_p from Table 4.4 produce the following hysteretic damping ratio in a subsequent full cycle of unloading-reloading to peak ductility ratio $\pm\mu$ (Fardis and Panagiotakos 1996):

$$\zeta_{n>1,pinching} = \frac{1}{2\pi\mu}\left(\varepsilon-\mu_p+\frac{m_p(\varepsilon+\mu)}{1+p(\mu-1)}\right) \tag{4.89}$$

Note that the equivalent damping given by Eqs. (4.87), (4.88), (4.88a) and (4.89) as a function of ductility ratio $\pm\mu$ refers to the energy dissipation in a single cycle to that ductility ratio, at the same period of oscillation as the linear system. If applied using the peak ductility ratio, μ, that takes place in a seismic response history having cycles of varying amplitude, Eqs. (4.87), (4.88), (4.88a) and (4.89) significantly overestimate the average damping ratio of a linear system with the same period of oscillation. They can only be used to evaluate a model's ability to reflect the hysteretic energy dissipation in members, as derived through Eq. (4.86) from the experimental response. On this basis, Fardis and Panagiotakos (1996) used about 190 cyclic uniaxial tests with several cycles of pre- and post-yield loading to derive through Eq. (4.86) experimental pairs of μ and ζ for RC members. The large scatter of individual data, even within a family of specimens with the same geometric and mechanical properties or even in a single test, obscures the difference between

the first post-yield cycle and subsequent ones reflected by Eqs. (4.87) and (4.88). For given value of $\mu > 1$, ζ on average increases with increasing shear span ratio, L_s/h, decreasing axial load ratio, ν, increasing ratio of confining steel and decreasing ratio of longitudinal reinforcement. However, only the dependence on L_s/h is statistically strong. Statistical fitting with a presumed hardening ratio p=0.02 has given the following expressions for certain model parameters (Fardis and Panagiotakos 1996):

– exponent a for unloading in (Saiidi and Sozen 1979, Coelho and Carvalho 1990, Anagnostopoulos 1972, Costa and Costa 1987):

$$a = 0.84 - 0.09\frac{L_s}{h} \tag{4.90}$$

– coefficient α for unloading in (Otani 1974, Litton 1975):

$$\alpha = 0.75 - 0.095\frac{L_s}{h} \tag{4.91}$$

– pinching parameter m in (Roufaiel and Meyer 1987):

$$m = 0.465 \tag{4.92}$$

The data suggest significant energy dissipation in post-cracking, pre-yield load cycles, equivalent to a damping ratio of about 8%, almost independently of the amplitude of loading and of specimen characteristics. This may mean that, if a bilinear model is used, it may be physically more appropriate to use a damping value higher than 5% in the damping matrix **C** characterising elastic response. However, this will bring about inconsistencies with the default, conventional value of 5% associated with elastic response spectra in codes.[26]

4.10.1.8 Concluding Remarks on Concrete Member Models for 3D Analyses

It is natural to expect that a nonlinear seismic response analysis is at least as good as a linear one in tackling general design situations in their full complexity. However, the nonlinear static analysis method has been developed for analysis of the seismic response in 2D (no matter whether the structural model is in 3D) and its applicability for truly 3D response is still questionable. The nonlinear dynamic method can, in principle, be applied for seismic response analysis in 3D, although it has been developed primarily for 2D analysis. Application of nonlinear seismic response analysis

[26] As a matter of fact, the universal value of 5% damping associated in codes with elastic response spectra is just a compromise between the lower values acknowledged for prestressed concrete and structural steel with bolted or welded connections on one hand and the higher ones for cracked concrete members.

in 3D presumes that appropriate member models under 3D loading are available. As emphasised is Section 4.10.1.2, Fibre models serve well this end. However, their large requirements in computer time and memory, the exponential increase of the risk of numerical problems with the amount of calculations and the specialised knowledge and experience needed to tune Fibre models to the experimental behaviour, limit currently their applicability in practical design and assessment. Point hinge models cannot represent well the post-elastic behaviour of members in two orthogonal directions without sacrificing the simplicity, flexibility and reliability/numerical stability that make them the model of choice for practical nonlinear analysis in 2D. The currently common use of one independent and uncoupled point hinge model in each horizontal direction is acceptable, when the nonlinear response is primarily in one of the two directions of bending, as is often the case in fairly symmetric buildings under a single horizontal seismic action component. However, it may be insufficient – and as a matter of fact unconservative – for two concurrent horizontal components and/or for strongly torsional response due to irregularity in plan. All in all, the lack of reliable, yet simple and inexpensive models for the inelastic cyclic behaviour of vertical members in two transverse directions is still the single most serious challenge for full-fledged nonlinear seismic response analysis in 3D, static or dynamic.

4.10.2 Nonlinear Modelling of Masonry Infills

4.10.2.1 Modelling of the Cyclic Behaviour

As the main features of the cyclic behaviour of infills have not been presented elsewhere in the book, they are highlighted here, together with their modelling.

The macroscopic behaviour of an infill panel may be described in terms of either:

1. the total infill shear force, V, and the relative horizontal displacement between top and bottom of the panel, δ; the ratio of δ to the clear infill panel height, H_{cl}, gives the smeared shear strain of the panel, $\gamma = \delta/H_{\mathrm{cl}}$, which is essentially the interstorey drift ratio of the surrounding frame; or
2. the axial force in the compressed diagonal (the equivalent strut), F, and the corresponding shortening of the diagonal, or, equivalently, the compressive strain along the diagonal, ε.

The panel shear strain, γ, and the diagonal compressive strain, ε, are related as: $\gamma = 2\varepsilon/\sin 2\theta$. The infill shear force, V, is the horizontal projection of the diagonal strut's axial force, F: $V = F\cos\theta$, where θ is the angle between the horizontal and the panel diagonal: $\theta = \arctan(H_{\mathrm{cl}}/L_{\mathrm{cl}})$. So the pairs V-γ and F-ε are interchangeable. With this in mind, the infill panel behaviour is described and modelled in what follows in generic force-deformation terms, F-δ.

The response of an infill panel to monotonic or primary loading may be approximated as a multilinear curve (dashed line $\mathrm{OA_oU_oR_o}$ in Fig. 4.11). A minor change in stiffness at the first separation of the infill from the frame may be neglected and

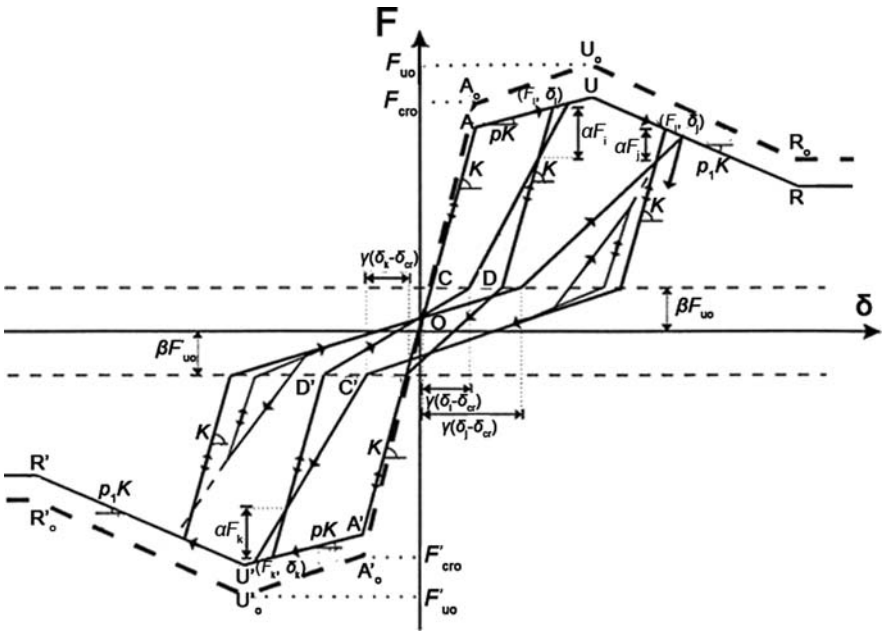

Fig. 4.11 Cyclic force-deformation model of infill panel in Panagiotakos and Fardis (1994) and Fardis and Panagiotakos (1997a)

the first change in slope at point A_o may be taken to correspond to the first visible cracking of the panel. The peak point, U_o, is at ultimate strength. The post-ultimate-strength branch may also be taken linear, leading to the horizontal residual strength branch. If there are asymmetric openings, the virgin loading curve in the opposite direction, $OA_o'U_o'R_o'$, may not be a mirror image of $OA_oU_oR_o$ with respect to O.

Under cyclic loading the primary loading curve is the skeleton and envelope for reloading. In the model described here (Panagiotakos and Fardis 1994, Fardis and Panagiotakos 1997a), which is a refinement and extension of Tassios (1984), the primary loading curve, OAUR in Fig. 4.11 gradually degrades with cyclic deformations. Specifically, if in a post-cracking half-cycle i, a maximum ever peak deformation is reached, δ_i, for positive, δ_i', for negative, then the ordinates of the corner points of the primary curve decrease as:

$$F_j = F_{jo}\, e^{-a\frac{\sum_i \delta_i}{\delta_{cr}} - a'\frac{\sum_i \delta'_i}{\delta'_{cr}}} \tag{4.93}$$

where j denotes points A (or cr), U (or u) and R, j' points A′, U′, and R′ in the reverse direction, $\delta_{cr} = F_{cro}/K_o$ is the cracking displacement, (with δ_{cr}' defined similarly in the reverse direction) and a, a' are parameters.

Before the infill cracks, unloading and reloading takes place along the non-degraded first branch of the virgin loading curve with the initial elastic stiffness

K_o (respectively K'_o). After cracking, unloading from the skeleton curve, e.g., from (F_i, δ_i), takes place initially with a slope equal to the degraded (by cycling) elastic stiffness, $K = F_{cr}/\delta_{cr}$, until the force is reduced to a fraction α of the non-degraded value of the ultimate force, F_{uo}. Unloading below that force level and continuation into first loading or reloading in the opposite direction after the δ-axis is reached are softer, as cracks open in the direction of reloading and contact with the frame is lost. This takes place before full closure of the cracks and re-instatement of contact in the past (opposite) direction of loading. The softer unloading-reloading branch heads towards point D′, where cracks and interfaces in the previous loading direction do close and cracking and loss of contact in the new loading direction stabilises. Point D is at a force $-\beta F_{uo}'$ and at a horizontal distance $\gamma(\delta_k - \delta_{cr}')$ from point C′, which is also at a force $-\beta F_{uo}'$ but on the elastic branch. $\delta_k - \delta_{cr}'$ is the maximum past post-cracking excursion in the current direction of reloading and $\gamma < 1.0$ is a parameter. If cracking has not taken place in a previous cycle in the direction of reloading, point D′ coincides with C′. Then, after reaching C′ reloading turns into primary loading in that direction. If, instead, there has been in the past a post-cracking excursion to a peak point (F_k, δ_k) on the degraded skeleton curve beyond A′, reloading from D′ heads straight to a point on the unloading branch from (F_k, δ_k) at a force level $(1-\alpha)F_k$. Reloading past that point continues to the degraded skeleton curve OA′U′R′, beyond which it follows the skeleton curve as in primary loading.

Reversal during the initial, stiffer part of an unloading branch, e.g., the one starting at (F_i, δ_i) on the degraded skeleton curve takes place along that same branch until its starting point (F_i, δ_i). From there on it follows the primary loading branch from where the unloading had started. A reversal from the subsequent, softer unloading-reloading branch starts renewed loading towards a point on the unloading branch from the most extreme deformation in this direction, δ_i, but at a lower force level, $(1-\alpha)F_i$. Reversal during the subsequent, stiffer reloading branch produces unloading with the degraded elastic stiffness, $K = F_{cr}/\delta_{cr}$, until the nearest force level at $\pm\beta F_{uo}$ is reached and the softer branch of unloading-reloading begins.

For a full cycle to a peak deformation $\mu\delta_{cr}$ in each direction, the above hysteretic model gives the following equivalent viscous damping ratio:

– in the *first full cycle* in each direction:

  - if the deformation $\mu\delta_{cr}$ is less than that at ultimate strength, $\mu\delta_{cr}$, i.e., if $\mu < \mu_u = \delta_u/\delta_{cr}$:

$$\zeta_{n=1,\,\mathrm{pre-ult}} = \frac{1-\mathrm{p}}{2\pi}\left(\frac{\mu-1}{\mu}\right)\frac{2+\mathrm{p}(\mu-1)+0.5\beta}{1+\mathrm{p}(\mu-1)} \tag{4.94a}$$

  - if the deformation $\mu\delta_{cr}$ exceeds that at ultimate strength, $\mu > \mu_u = \delta_u/\delta_{cr}$:

$$\zeta_{n=1,\,\mathrm{post-ult}} = \frac{(\mu-1)(1+\mathrm{p}(\mu_u-1))+\mu_u(\mathrm{p}_1(\mu-\mu_u)-\mathrm{p}(\mu_u-1))+(\mu-1-\mathrm{p}(\mu_u-1)+\mathrm{p}_1(\mu-\mu_u))(1+\mathrm{p}(\mu_u-1)-\mathrm{p}_1(\mu-\mu_u)+0.5\beta)}{2\pi\,\mu(1+\mathrm{p}(\mu_u-1)-\mathrm{p}_1(\mu-\mu_u))} \tag{4.94b}$$

– in a *full unloading-reloading cycle after the first*:

- if the ultimate strength is not exceeded, i.e., if $\mu < \mu_u$:

$$\zeta_{n>1,\,\text{pre-ult}} = \frac{(1-\text{p})(\mu-1)}{2\pi\mu}\,\frac{2\beta+(1-\alpha)(1-\gamma)\,(1+\text{p}(\mu-1))}{1+\text{p}(\mu-1)} \quad (4.95a)$$

- if the ultimate strength is exceeded, $\mu > \mu_u$:

$$\zeta_{n>1,\,\text{post-ult}} = \frac{\mu-1-\text{p}(\mu_u-1)+\text{p}_1(\mu-\mu_u)}{2\pi\mu}\,\frac{2\beta+(1-\alpha)(1-\gamma)\,(1+\text{p}(\mu_u-1)-\text{p}_1(\mu-\mu_u))}{1+\text{p}(\mu_u-1)-\text{p}_1(\mu-\mu_u)} \quad (4.95b)$$

In Eqs. (4.94) and (4.95) p is the hardening ratio of the post-cracking primary branch and $p_1{=}K_2/K_o$ the post-ultimate softening ratio.

For nonlinear static (pushover) analysis, the force-deformation response of solid infill panels may be simplified to the multilinear curve of Fig. 4.12.

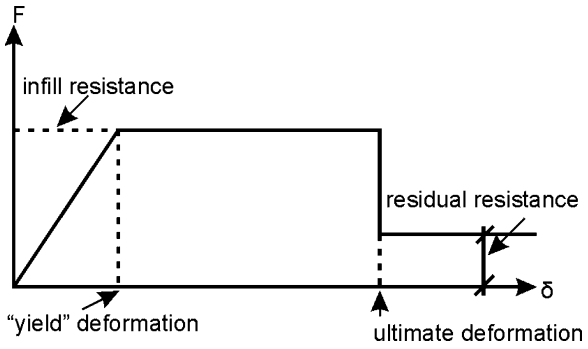

Fig. 4.12 Simplified force-deformation curve of infill panel for nonlinear static analysis

4.10.2.2 Model Parameters

Any multilinear infill model for monotonic loading with corner points at infill (visible) cracking, ultimate strength and post-ultimate residual strength is parametrised through the force and deformation values at these points. One of these values may be replaced by the slope to that point, secant from the origin or tangent to an adjacent corner of the curve. The values of these parameters should be determined on the basis of the geometry of the infill panel and of the material properties of the masonry, especially in the direction of the diagonal of the infill panel.[27] Rules for the calculation of these parameters should be developed or calibrated on the basis

[27] As there is coupling between the infill and the frame, these parameters cannot be given as if the infill panel were a stand-alone component, but depend in principle on the properties and sizes of the surrounding frame members.

of (cyclic) test results. This is, however, hampered by insufficient information on the material properties of the masonry of the tested infilled frames in the diagonal direction. Rare cases where such information has been reported are Stylianidis (1985) and Pires (1990). So, they have been used in Panagiotakos and Fardis (1994) to develop such rules, as highlighted below for the case when the force F is taken as the total infill shear force, V, and the displacement, δ, as the relative horizontal displacement between top and bottom of the panel (case 1 in Section 4.10.2.1).

1. The corner point at infill (visible) cracking (A_o in Fig. 4.11) can be specified through the shear force at cracking in monotonic loading, F_{cro}, and the initial stiffness to panel cracking, $K_o = F_{cro}/\delta_{cr}$. Among various (simple) alternatives examined in Panagiotakos and Fardis (1994), the best agreement with the test results in Stylianidis (1985) and Pires (1990) is given by:
   - an infill initial cracking strength equal to:

$$F_{cro} = \tau_{cr} A \tag{4.96}$$

   - an initial stiffness to panel cracking of:

$$K_o = G_w A / H_{cl} \tag{4.97}$$

where:

- $A = L_{cl} t_w$ and H_{cl} denote the horizontal cross-sectional area of the infill and its clear height, respectively, and
- τ_{cr} and G_w are the diagonal cracking strength and the shear modulus, respectively, of the masonry as determined from wallette diagonal compression tests (e.g., according to ASTM E519-81).

2. The ultimate strength point of the infill (U_o in Fig. 4.11) can be specified through the ultimate shear force in monotonic loading, F_{uo}, and the secant stiffness to that point from the origin. Among various (simple) alternatives examined in Panagiotakos and Fardis (1994), the best agreement with the test results in Stylianidis (1985) and Pires (1990) is given by:
   - a secant stiffness to ultimate strength, $K_u = F_{uo}/\delta_u$, obtained from that of the elastic diagonal strut given in Section 4.9.8 for linear analysis:

$$K_u = E_w (w_{inf} t_w) \cos^3 \theta / L_{cl} \tag{4.98}$$

where:

- the strut width, w_{inf}, is given from Eqs. (4.46) in Sect. 4.9.8 and
- the elastic modulus, E_w, is in the panel diagonal direction, or as close to it as possible, if the value along the diagonal is not available (e.g., in the horizontal direction if $L_{cl} > H_{cl}$, or in the vertical if $L_{cl} < H_{cl}$);

– an ultimate strength 1.3 times the cracking strength:

$$F_{uo} = 1.3\, F_{uo} \tag{4.99}$$

Alternatively F_{uo} may be taken equal to either:

- the horizontal cross-sectional area of the infill $A = L_{cl} t_w$, times the shear strength of bed joints, or
- the resistance of the diagonal strut in compression (i.e, its cross-sectional area, $w_{inf} t_w$, times the diagonal compressive strength of the masonry) projected on the horizontal direction.

3. The onset of the residual strength branch (R_o in Fig. 4.11) can be obtained from the ultimate strength point (U_o in Fig. 4.11), the residual strength and the tangent stiffness of the post-ultimate-strength softening branch in monotonic loading, K_2, expressed as the post-ultimate softening ratio, $-p_1$, times the initial stiffness to cracking, K_o. These parameters are hard to quantify from test results, but are for practical purposes less important than those in 1 and 2 above. For solid panels well confined by the surrounding frame a value of 0.05 for p_1 and of 50% of the ultimate strength, F_{uo}, for the residual strength seem to be supported by test results.

All the above refer to virgin, monotonic loading. Parameters a and a' determine according to Eq. (4.93) the cyclic decay of the monotonic curve when it serves as envelope to the hysteresis loops. If the degradation of the envelope in one direction is independent of previous infill damage in the opposite direction, then $a' = 0$. If cyclic deformations in either direction affect the same the response degradation in both directions, parameters a and a' may be about equal. The test results in Zarnic and Tomazevic (1985) and Stylianidis (1985) suggest $a + a' \approx 0.05$.

The value of the damping ratio under cyclic loading is affected by those of parameters:

– α : percentage-drop in peak force in repeated full unloading-reloading half-cycles to or beyond the peak past displacement in the same direction of loading,
– β: force at the transition from the initial stiffer unloading to the softer stage of unloading-reloading, or from this latter stage back to a subsequent stiffer reloading, as a fraction of the initial ultimate strength, F_{uo} and
– γ, which determines the displacement at the transition between the initial softer stage of reloading and the subsequent stiffer one, as a fraction of the maximum previous post-cracking excursion in the current reloading direction.

The outcome of Eqs. (4.94) for the damping ratio in the first full cycle is independent of α and γ and rather insensitive to the value of β. It is around 15% in the 1st cycle to $\mu = 2$, in good agreement with the test results in Stylianidis (1985) and Zarnic and Tomazevic (1985); if the 1st cycle takes place at larger values of μ, the damping ratio from Eqs. (4.94) increases to about 30%, but there are no 1st cycle

data at so large μ values for confirmation. For subsequent cycles the damping ratio from Eqs. (4.95) is nearly proportional to (1-α) and fairly sensitive to the values of β and γ, increasing slightly with increasing β and with decreasing γ. Values $\alpha \approx 0.15$, $\beta \approx 0.1$ and $\gamma \approx 0.8$ give fairly good overall agreement with the test results in Stylianidis (1985) and Zarnic and Tomazevic (1985).

4.10.3 Modelling of Foundation Uplift

Nonlinearities in ground compliance during the seismic response normally derive more from the no-tension feature of the soil and its interface with foundation elements, than from the behaviour of the soil itself in shear or compression. This shows up mostly as uplift of the foundation element from the ground. Uplift of rafts or long foundation beams is not so extensive and normally can be ignored. To take it into account, one should model ground compliance with springs of the no-tension type. The same modelling should be used under flexible footings.

Normally footings may be considered as rigid. The three conventional springs of Section 4.9.9.4 (the vertical one and one rotational spring per horizontal direction) at the node at the centre of the underside of a rigid footing have constant stiffness based on full contact at the footing-ground interface. So, they are sufficient for linear analysis and before any significant uplift takes place. After the onset of uplift the linear springs do not reflect:

- the significant reduction of rotational compliance (softening), due to loss of contact area;
- the (usually upward) displacement at the centre of the footing due to rotation about an axis which does not pass through the centre of the footing in plan;
- the different magnitude (normally larger) of the absolute vertical displacements of the ends of tie-beams connecting to the uplifting part of the footing perimeter, relative to those connected to the down-going part.

Such effects may be captured by using a pair of nonlinear vertical springs at opposite ends of the footing that account for uplifting. The spring at the uplifting end has lower stiffness than that at the down-going end. Such springs may be derived from the dependence of the rotation, θ, and vertical displacement at the centre of the footing, δ_o, on the applied moment M fitted in Crémer (2001) to results of nonlinear 2D FE analyses of uplifting strip footings on elastic or inelastic soil. According to Crémer (2001), if B is the width of a footing in the plane of M, the relations giving θ and δ_o in terms of a monotonically increasing M are:

$$\theta \approx \frac{\theta_o}{2 - \frac{M}{M_o}} \tag{4.100}$$

$$\delta_o \approx \frac{B\theta_o}{2}\left[\frac{\frac{M}{M_o} - 1}{2 - \frac{M}{M_o}} + \ln\left(2 - \frac{M}{M_o}\right)\right] \tag{4.101}$$

In Eqs. (4.100) and (4.101) M_o denotes the moment at the onset of uplift and $\theta_o = M_o/K_{\theta o}$ the associated (elastic) rotation derived from the elastic rotational impedance $K_{\theta o}$ of a footing in full contact with elastic soil. According to Crémer (2001), if the vertical load N at the base of the wall is very much lower than the bearing capacity of the (concentric) footing, N_u, the value of M_o on elastic soil may be taken approximately equal to:

$$M_o \approx 0.25BN \tag{4.102}$$

Note that the outcome of Eq. (4.102), fitted to the results of 2D FE analyses of elastic soil, exceeds by 50% the value of $BN/6$ predicted for a rigid footing by the subgrade reaction modulus approach. For higher values of N a more accurate approximation is (Crémer 2001):

$$M_o \approx 0.25BN \exp\left(-2.5\frac{N}{N_u}\right) \tag{4.102a}$$

The secant relation between the force $F = M/B$ at two nonlinear vertical springs introduced at the ends of the footing to model uplift and the associated vertical displacements are:

– at the uplifting edge ($\delta_1 > 0$):

$$\delta_1 = \frac{B\theta_o}{2}\left(\frac{\frac{FB}{M_o}}{2-\frac{FB}{M_o}} + \ln\left(2-\frac{FB}{M_o}\right)\right) \tag{4.103a}$$

– at the down-going opposite edge ($\delta_2 > 0$):

$$\delta_2 = \frac{B\theta_o}{2}\left(1-\ln\left(2-\frac{FB}{M_o}\right)\right) \tag{4.103b}$$

giving tangent stiffnesses:

$$\frac{dF}{d\delta_1} = \frac{2K_{\theta o}}{B^2}\frac{\left(2-\frac{FB}{M_o}\right)^2}{\frac{FB}{M_o}} \tag{4.104a}$$

$$\frac{dF}{d\delta_2} = \frac{2K_{\theta o}}{B^2}\left(2-\frac{FB}{M_o}\right) \tag{4.104b}$$

If the axial load N is low compared to N_u, there is very little hysteresis in cyclic loading, i.e. the cyclic M-θ and F-θ relations are nonlinear-elastic, recentring to approximately zero displacement for zero moment or force and dissipating very little energy. Then Eqs. (4.104) may be applied also for nonlinear response-history analysis, considering the springs as nonlinear elastic.

Column footings may uplift and rock in both orthogonal horizontal directions. Then, a different pair of nonlinear springs based on Eqs. (4.104) should be used in each horizontal direction, in a cross-like arrangement around the centre of the footing.

This procedure is exemplified in Section 6.9.2.2 for the pushover analysis of a plane frame with a shear wall at its central bay.

4.10.4 Special Provisions of Eurocode 8 for Nonlinear Analysis

Gravity loads concurrent with the seismic action should be applied on the relevant elements of the model in the course of the nonlinear analysis, as separate analyses and superposition cannot be used. Eurocode 8 (CEN 2004a) implicitly allows neglecting the effect of the variation of axial force of vertical elements during the seismic response and determining (the parameters of) their force-deformation relations on the basis of the axial force due to gravity loads alone. As we have seen in Sections 4.10.1.2, 4.10.1.3 and 4.10.1.4, however, most element models can take into account – be it approximately – the effect of this variation on the force-deformation relations of vertical elements .

For simplicity, Eurocode 8 (CEN 2004a) allows neglecting in nonlinear analysis bending moments in vertical members due to gravity loads, unless they are significant with respect to the yield moment. Note, however, that including such moments and starting the nonlinear seismic response analysis from a non-zero initial force state presents no special difficulty.

The parameters of force-deformation models for nonlinear analysis should use the best-estimate (mean) values of material strengths, which are higher than the nominal or design values.[28] For existing buildings the best-estimate of the strength of a material is the one inferred from in-situ measurements, lab tests of samples or any other relevant source of information (e.g., in the absence of hard data, from literature and judgment). Regarding the mean strength of materials to be incorporated in future, the mean strength of concrete is normally taken as 8 MPa greater than the characteristic strength, f_{ck} (CEN 2004b). For the reinforcing steel, the locally applicable data should be used, if known (e.g., from test reports of the same type of steel produced in about the same period). Statistics drawn from the widest available survey of ductile steels of the type used in the seismic regions of Europe in the early 1990s are summarised in Table 3.2. Notwithstanding the fairly large inter-country variation of the ratio of the mean yield strength, f_{ym}, to the nominal, f_{yk}, the average f_{ym}/f_{yk} ratio of the five columns of Table 3.2 is exactly equal to the commonly used default value of 1.15.

[28] Recall that, even in linear analysis, the Elastic Modulus of concrete is derived from the best-estimate (mean) value of concrete strength, f_{cm}, and not from the nominal one, f_{ck} (CEN 2004b).

4.10.5 Example Applications of Nonlinear Analysis in 3D and Comparison with Measured Dynamic Response

4.10.5.1 Computational Modelling for Seismic Response Analysis, Assessment and Retrofitting

A computational capability has been developed at the Structures Laboratory of the University of Patras for modelling and seismic response analysis of concrete buildings, as well as for their seismic assessment and retrofit design according to the relevant provisions of Eurocode 8, Part 1 (CEN 2004a) and Part 3 (CEN 2005a). It has been incorporated in computer program ANSRuop, a significantly improved and expanded version of the ANSR-I program (Mondkar and Powel 1975). All types of seismic response analysis in Eurocode 8 are covered, always in 3D. The modelling approach may be considered as the simplest one allowed in Eurocode 8, Parts 1 and 3. Yet, it represents fairly well the inelastic behaviour of members and the structure as a whole.

The key points of the nonlinear modelling approach adopted and illustrated in the present applications are the following:

1. Prismatic beam elements in 3D are used for all members (see Section 4.10.1.1). A point hinge model is adopted for them (see Section 4.10.1.4) with bilinear M-θ curve for primary loading (see Section 4.10.1.5). Nonlinear dynamic analysis uses modified-Takeda-type hysteresis rules (Otani 1974, Litton 1975) (see Section 4.10.1.6 and Table 4.3), with unloading parameter $\alpha = 0.3$ (see Table 4.3) and reloading parameter $\beta = 0$ (cf. definition of β in Section 4.10.1.7 in relation to Eq. (4.88a)).
2. The element elastic stiffness is the secant stiffness to yield-point, $(EI)_{\text{eff}}$, from Eq. (3.68) and Section 3.2.3.3. Its calculation is based on the member axial force due to gravity loads alone and on the values of the shear span at the yielding end(s) of the member suggested in Section 4.10.1.4: for beams or columns, half the clear length from one beam-column joint to the next within the plane of bending; for walls, 50% of the height from the bottom section in a storey to the top of the wall. The average secant-to-yield-point stiffness at the two end sections, in positive or negative bending is used (see Section 4.10.1.4). For beams that end at an indirect support on another beam (e.g., for beams B3, B7 and B9 in Fig. 4.14(a)) the shear span is taken equal to the beam full clear span. For girders connected at intermediate points with cross-beams or girders, the shear span is determined on the basis of the girder clear span between adjacent columns into which the girder frames (see Fig. 4.18-right for several such girders, two of which are indirectly supported at one end by another girder). Although the parts of the length of a girder between joints with cross-beams are modelled as individual beam elements, their elastic stiffness is taken the same all along the girder and equal to the value established from the secant-to-yield-point stiffness at the (two) end section(s) and the clear span of the overall girder. The effective flange width, in tension or compression, of T- or L-beams

on either side of their web is taken as 50% of the beam shear span or of the distance to the adjacent parallel beam (whichever is shorter). Slab bars parallel to such a beam and falling within this width are considered fully effective as longitudinal reinforcement of the beam's end section.

3. The strength, stiffness and behaviour of vertical members are considered independent in the two orthogonal planes of bending. The yield moment of each element is determined from the current value of its axial force, but considered constant during further primary loading. After reversal and during reloading in the reverse direction, the value of M_y is updated according to the evolution of the axial force (see last paragraph of Section 4.10.1.3 and further discussion in Section 4.10.1.4). Walls with non-rectangular section (e.g., the U-shaped wall around the elevator shaft in Fig. 2.21 and the two large walls with L-section at the corners of the right-hand side of the building in Fig. 4.18) are modelled with a single prismatic element per storey at the shear centre of the section.
4. Joints are considered as rigid, but slippage of longitudinal bars through or from a joint is accounted for, by including the effect of the resulting fixed-end rotation of member end sections on the secant-to-yield-point stiffness of Eq. (3.68) and the ultimate chord rotation (i.e., by setting $a_{sl} = 1$ in Eqs. (3.42) and (3.78), etc.).
5. Eccentricities in the connections between members are modelled through rigid elements.
6. The in-plane flexibility of floor diaphragms is included at the level of individual panels in plan, by considering the beams at the boundary of a panel (including the balconies) as prismatic elements in 3D with moment of inertia about an axis normal to the floor plane and cross-sectional area according to Eqs. (4.44) in Section 4.9.5.2.
7. Staircases are included in the model. Landings between floors, along with their supporting beams, are modelled in-plane according to point 6 above. Flights are modelled according to points 1–5 as oblique column elements (i.e. with strength and stiffness in both transverse directions) between the two nodes belonging to vertical elements closest to the axis of the flight at the two horizontal levels it connects.
8. P-Δ effects are included.
9. Masses are lumped at the nearest node of the model.
10. Rayleigh damping is used, with 5% damping ratio at the average period of the two modes with the highest modal base shears in two orthogonal horizontal directions and at half that value.
11. Damage is evaluated at member ends, using as index the ratio of the demand from the analysis to the corresponding capacity. Flexural damage is evaluated in terms of chord rotations, using as capacity the empirical ultimate chord rotation from Eqs. (3.78) in Section 3.2.3.5, with modifications due to lack of detailing for earthquake resistance, lap-splicing of vertical bars in plastic hinge zones, jacketing with FRP, etc., according to Sections 3.2.3.9 and 3.2.3.10. Shear damage is evaluated in terms of forces, using capacities for failure due to diagonal tension after yielding from Eqs. (3.114) in Section 3.2.4.3 and for shear

failure by diagonal compression before or after yielding from Eq. (3.115) in Section 3.2.4.5 or Eq. (3.127) in Section 3.2.5.4, as relevant. Demand-capacity-ratios of vertical members in the two orthogonal planes of bending are combined via the SRSS rule (see Eq. (3.84) in Section 3.2.3.8). In the calculation of the damage ratio (demand-to-capacity) both demand and capacity are updated during the response-history. The most adverse (i.e., the maximum) value of the damage index during the entire response is reported in the end. Values of this index near 1.0 signify likely or incipient failure.

The seismic response analysis and assessment capability has been applied to three concrete buildings, all designed with codes and practices applying in Greece from the 1950s to the 1970s, having various types and degrees of irregularity in plan that induce torsional response. The results of three Pseudo-Dynamic (PsD) tests of the first of these buildings provide, indeed, the basis for validation of the computational capability for seismic response analysis and member assessment, as well as of the modelling adopted here.

4.10.5.2 Verification of Modelling, Analysis and Assessment on the Basis of Pseudo-Dynamic (PsD) Test Results

The 3-storey full-scale building of Figs. 4.13 and 4.14 has been subjected to PsD testing under bi-directional excitation at the ELSA facility of the JRC in the framework of the SPEAR project. It has been designed in (Kosmopoulos et al. 2003) simulating practices of the 1950s in Greece (Fig. 4.14(a)). It was PsD-tested at ELSA (Molina et al. 2005) in three different versions (Mola and Negro 2005):

- As unretrofitted (Figs. 4.13(a) and 4.14(a));
- Retrofitted with FRPs as follows: All 0.25 m-columns were wrapped with unidirectional Glass FRP (GFRP) over a length of 0.6 m from each end section,

(a) (b)

Fig. 4.13 SPEAR test structure (**a**) unretrofitted: (**b**) retrofitted with FRP jackets

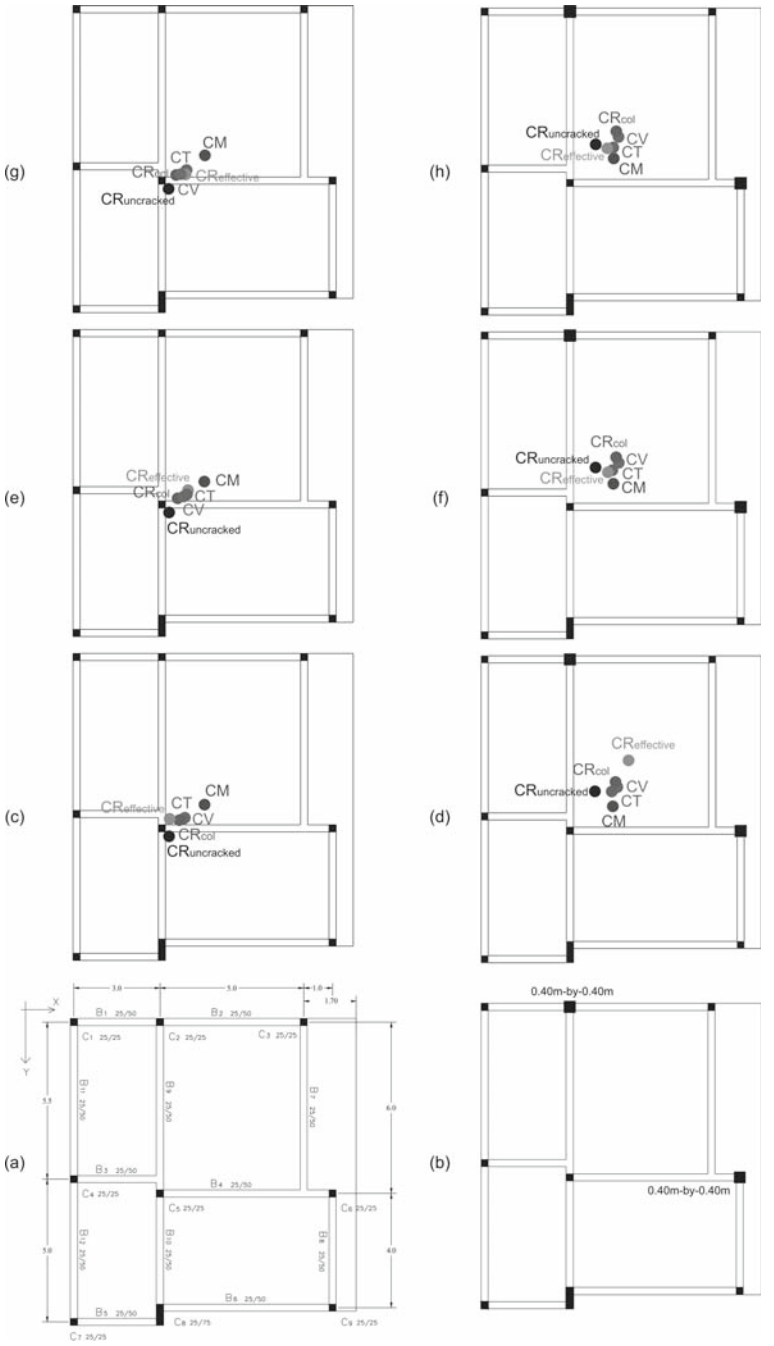

Fig. 4.14 SPEAR test structure: (**a**) framing plan of unretrofitted building: (**b**) framing plan with RC jackets at columns C2, C6; (**c**)–(**h**) centres of mass (CM), rigidity (CR), strength CV) and twist (CT) of 1st, 2nd and 3rd storey (from *bottom up*) – (*left*) unretrofitted structure; (*right*) with jacketed-columns (Kosmopoulos and Fardis 2008)

for confinement and clamping of short lap-splices (Fig. 4.13(b)). For the same purpose, but also for shear strengthening, column C8 in Fig. 4.14(a) (with 0.25 m-by-0.75 m section) was wrapped with bidirectional GFRP over its full height. Finally, the exterior faces of corner joints were strengthened in shear with bidirectional GFRP, not continued into the columns (Fig. 4.13(b)).

- In the 2nd phase the FRPs were removed and the central columns of the two "flexible" sides (C2 and C6 in Fig. 4.14(a)) were concrete-jacketed from 0.25 to 0.4 m square (Fig. 4.14(b)), to mitigate the torsional imbalance.

Further details about the retrofitting are given in Section 6.10.1.

In both its retrofitted or unretrofitted versions the building is torsionally flexible. The radius of gyration of overlying masses exceeds at every floor the torsional radius of the frame with respect to the centre of overlying masses in horizontal direction Y, violating therefore Eq. (2.4) in Section 2.1.6. To quantify further the irregularity in plan of the building, this centre, CM, is shown in Fig. 4.14(c) and (d) along with the following points:

(a) CR-uncracked: centroid of the gross section rigidity, $(EI)_c$, of storey vertical members, from Eqs. (2.2) in Section 2.1.5;
(b) CR-col: centroid of the secant stiffness of the storey vertical members at yielding, $(EI)_{eff}$, from Eq. (3.68) and according to the modelling in point 2 of Section 4.10.5.1;
(c) CR-effective: the storey centre of rigidity defined and determined as in Cheung and Tso (1986) and Tso (1990) (see Section 2.1.5);
(d) CV: centroid of resistances of storey vertical members, as controlled by shear or flexure – whichever is most critical.
(e) CT: pivoting point of the floor under storey torques with an inverted triangular heightwise pattern (see Section 2.1.5), as obtained from elastic analysis with member stiffness equal to their secant-to-yield-point stiffness from Eq. (3.68).

The nonlinear dynamic analysis follows the general modelling approach highlighted in Section 4.10.5.1, points 1–11. An additional assumption is introduced, to emulate the very tight fixing of the building's stiff and strong foundation to the laboratory's strong floor:

12. Vertical members are considered fixed at their connection with the foundation.

The bidirectional input motion applied at the PsD test and in the nonlinear analyses consists of the two Herzeg Novi records in the Montenegro 1979 earthquake, modified to simulate EC8-spectra-compatible ground motions for ground type C. Pre-test nonlinear response-history simulations have been carried out for the following PsD tests at ELSA (Kosmopoulos and Fardis 2004, Fardis et al. 2005):

- The unretrofitted structure under bidirectional motion scaled to a peak ground acceleration (PGA) of 0.15 g (Fig. 4.15, top);
- The same bidirectional motions, but scaled to a PGA of 0.2 g, applied to the test structure after its retrofitting with FRPs (Fig. 4.15, middle);

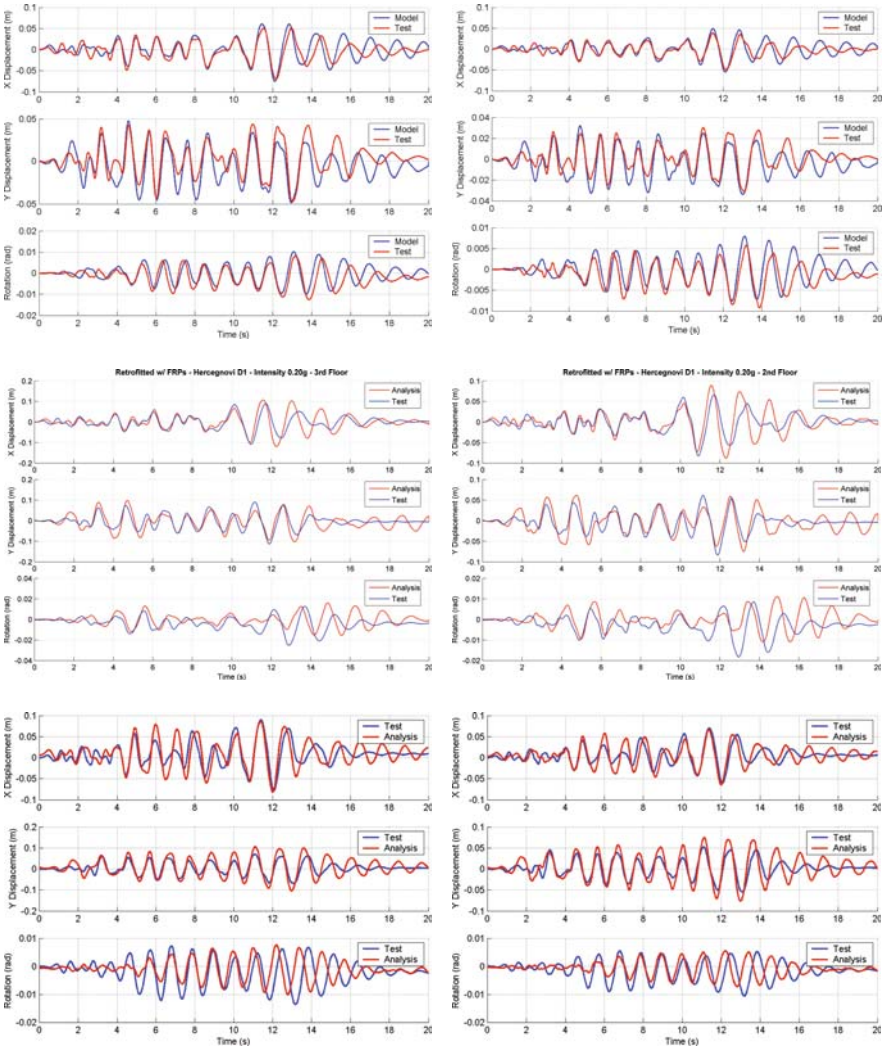

Fig. 4.15 Translation and twist histories, 3rd (*left*) and 2nd (*right*) floor in PsD test or analysis: (*top*) unretrofitted SPEAR building; (*middle*) with FRP-wraps; (*bottom*) with RC jackets (Kosmopoulos and Fardis 2004) (See also Colour Plate 11 on page 725)

- The same motions scaled to a 0.2 g PGA, applied to the test structure without FRPs but with columns C2 and C6 concrete-jacketed (Fig. 4.15, bottom).

Figure 4.15 compares the predictions of floor translation and twist time-histories for the bidirectional input ground motions applied in the PsD tests to the measured ones (Kosmopoulos and Fardis 2004, Fardis et al. 2005). Overall agreement is good, confirming the modelling assumptions above, including the use of the secant

stiffness to yield-point, Eq. (3.68). Witness, though, the initial overestimation of the dominant period of the response and of the displacements in the test of the unretrofitted building (top part of Fig. 4.15), until the time (at ~3 s) when cracking took place. From that point on the effective stiffness used in the analysis (from Eq. (3.68)) was indeed consistent with the actual member stiffness. As the peak member deformations induced by this test at ~13 s inflicted significant damage (see predicted flexural damage index at the top part of Fig. 4.16), members seem to have entered the strength degradation range of their moment-rotation relationship, not reflected in the bilinear model used in the analyses. So, the model fails to capture the ensuing lengthening of the dominant period of the measured response and the associated increase in displacement amplitudes. The pre-cracking and post-ultimate strength mismatch between predictions and test does not appear in the retrofitted versions, which were cracked from the outset and did not come as close to generalised member failure as the unretrofiited building. Witness also that analysis undershoots the twisting measured in all three tests, owing to the lack of inelastic coupling between the two directions of bending in the model used for columns. The softening and strength reduction induced by this coupling seem to have a measurable effect.

Figure 4.16 shows the maximum values of the computed damage index by the end of the dynamic response, separately for flexure and shear. Values near 1.0 signify likely or incipient failure. Failure is considered almost certain if the damage index exceeds 1 (numerals in bold in Fig. 4.16). Section 6.10.1 comments on how the predicted damage patterns for the two retrofitted versions of the SPEAR structure in Fig. 4.16 compare with the observed one.

4.10.5.3 Seismic Assessment of Two Real Buildings on the Basis of Nonlinear Dynamic Analysis

Section 2.4.2 and Figs. 2.21, 2.22 and 2.23 have presented the L-shaped building (with 5-storeys plus basement and penthouse), whose wing (to the right of the elevator shaft and of the column across the floor in Fig. 2.21) collapsed during the Athens 1999 earthquake. To identify the mechanism that led to collapse, a series of nonlinear response-history analyses have been carried out (Kosmopoulos and Fardis 2006), for six ground motions that had been derived as "most likely" at the site on the basis of several ground motion records in the Athens area and of the detailed subsoil conditions at the recording stations and at the building site.

The seismic response analyses were in accordance with the relevant rules and guidance of Eurocode 8 and followed the modelling approach highlighted in Section 4.10.5.1 under points 1–11, as well as assumption no. 12 in Section 4.10.5.2 for the SPEAR building, namely that vertical members, in this case all of them at the perimeter of the building, are fixed at their connection with the stiff, storey-high perimeter wall of the basement, which provides the foundation. An analysis has been carried out with each one of the six ground motions applied in one horizontal direction and any other one applied at right angles, giving in total 30 bidirectional motions. The displacement time-histories for each individual bidirectional motion and the natural periods and modes of the elastic structure show that the response

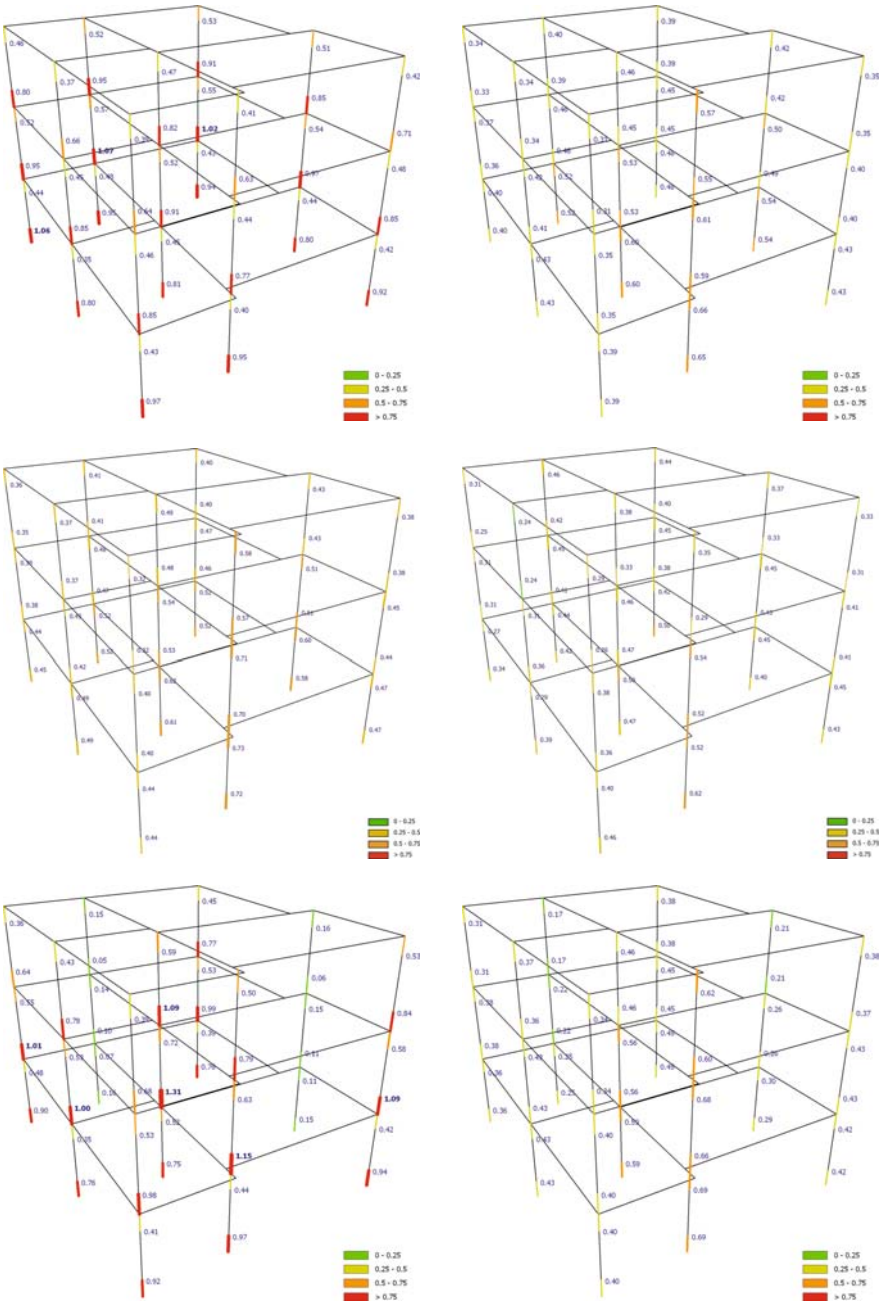

Fig. 4.16 Column damage index in flexure (*left*) or shear (*right*): (*top*) unretrofitted SPEAR building, 0.15 g PGA; (*middle*) 0.2 g PGA with FRP-wraps; (*bottom*) ibid, with RC jackets (See also Colour Plate 12 on page 726)

was controlled by higher modes. Moreover, due to the non-rigid connection of the floors to the stiff elevator shaft and to the staircase next to it, higher mode response generally entails out-of-phase twisting of the shaft/staircase and of the rest of the floor. The demand-to-capacity ratios (damage indices) in Fig. 4.17 show how close to its cyclic flexure-controlled ultimate deformation or to its cyclic shear resistance each member came. These results suggest that most critical in the building were the penthouse above the 5th floor and several columns in the upper storeys of the right-hand wing. Figure 4.17 shows also that the penthouse columns are near-critical in biaxial bending and certainly in shear. Critical in shear are also at least five of the other columns in the upper storeys, as well as the base of the elevator shaft wall. This supports the scenario advanced in Section 2.4.2 as most likely for the collapse: that it started with shear failures of columns at the penthouse and in the upper storeys of the part of the building to the right of the elevator shaft. Floor diaphragms, being almost unreinforced in their secondary direction, were unable to transfer forces from the deficient right-hand-side wing to the more resistant wing on the left of the elevator shaft. So, they teared off along a line next to the shaft, extending to the opposite side in plan.

The last case addressed here is a building constructed on the highly seismic island of Kephalonia (GR) in the early 1970s to house a theatre. As shown in Figs. 4.18 and 4.19, it consists of two structurally independent units, separated by an expansion joint that runs through the foundation. Both units are torsionally stiff, in the sense that Eq. (2.4) in Section 2.1.6 is met at all floors. Extensive vertical cracking had been observed at perimeter vertical members, owing to severe reinforcement corrosion.

The structure, designed according to codes of the 1950s for a base shear coefficient of 0.17 without detailing for ductility (corresponding to a peak ground acceleration – PGA – of about 0.1 g), is grossly inadequate against the 475 year return period earthquake with a PGA of 0.36 g specified for ordinary buildings at the site in the post-1995 seismic design code.

On the occasion of the rehabilitation of those members that suffer from reinforcement corrosion, it was decided to upgrade the entire structure to survive the design earthquake of the present-day seismic code. The seismic assessment and the retrofit design were the first application of Eurocode 8 Part 3 (CEN 2005a) to a real building.

The two parts of the as-built structure have been subjected to nonlinear dynamic analysis under semi-artificial bidirectional (two component) ground motions. Each motion emulates the two components of seven historic earthquakes, with each component modified to fit the 5%-damped Type 1 elastic spectrum recommended in Eurocode 8 for soil type C.[29] The two components of each bidirectional motion are normalised to a PGA of 0.1 g and interchanged between horizontal directions X and Y. Owing to certain asymmetry of the framing plan, each component of the

[29]One of these bidirectional motions was used in all PsD tests of the SPEAR building and in the analyses of Sect. 4.10.5.2, but scaled to a different PGA.

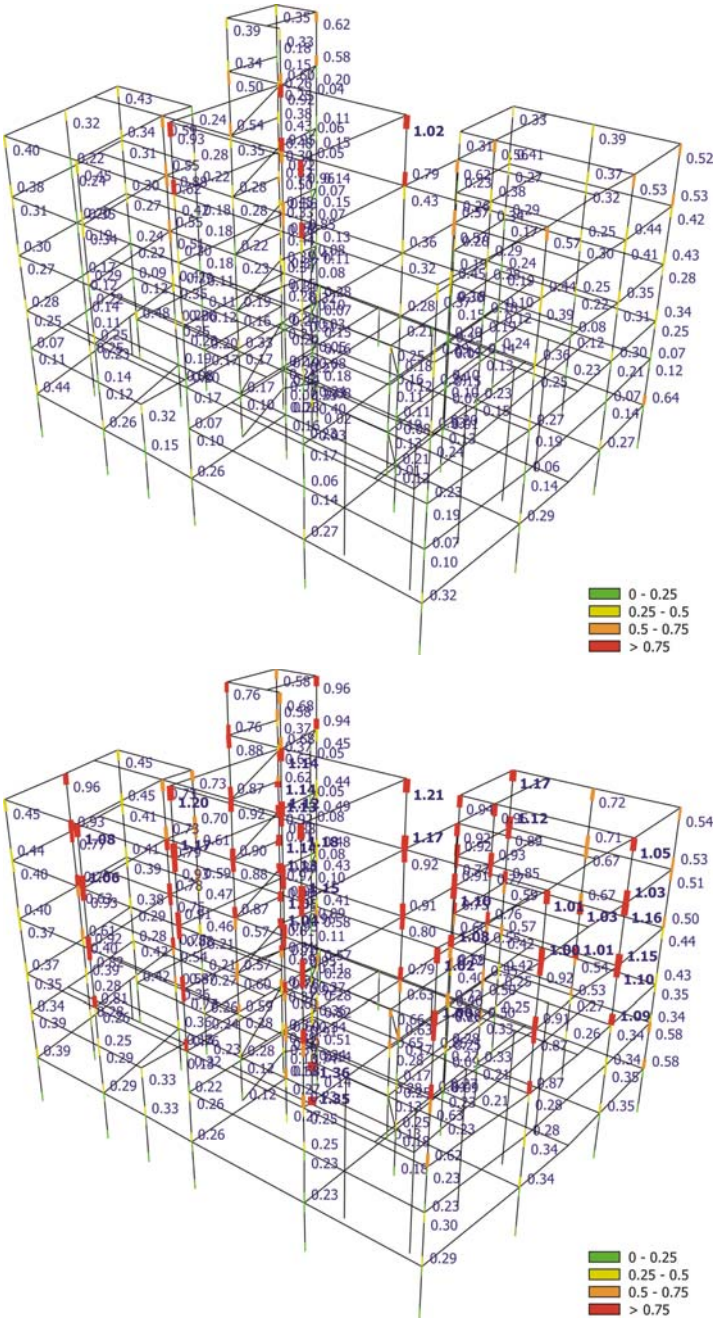

Fig. 4.17 Column damage index (demand-capacity ratio) in flexure (*top*) or shear (*bottom*); mean values from seismic response analyses of the 6-storey building subjected to the 30 "most likely" bidirectional ground motions at the site in the Athens 1999 earthquake (Kosmopoulos and Fardis 2006) (See also Colour Plate 13 on page 727)

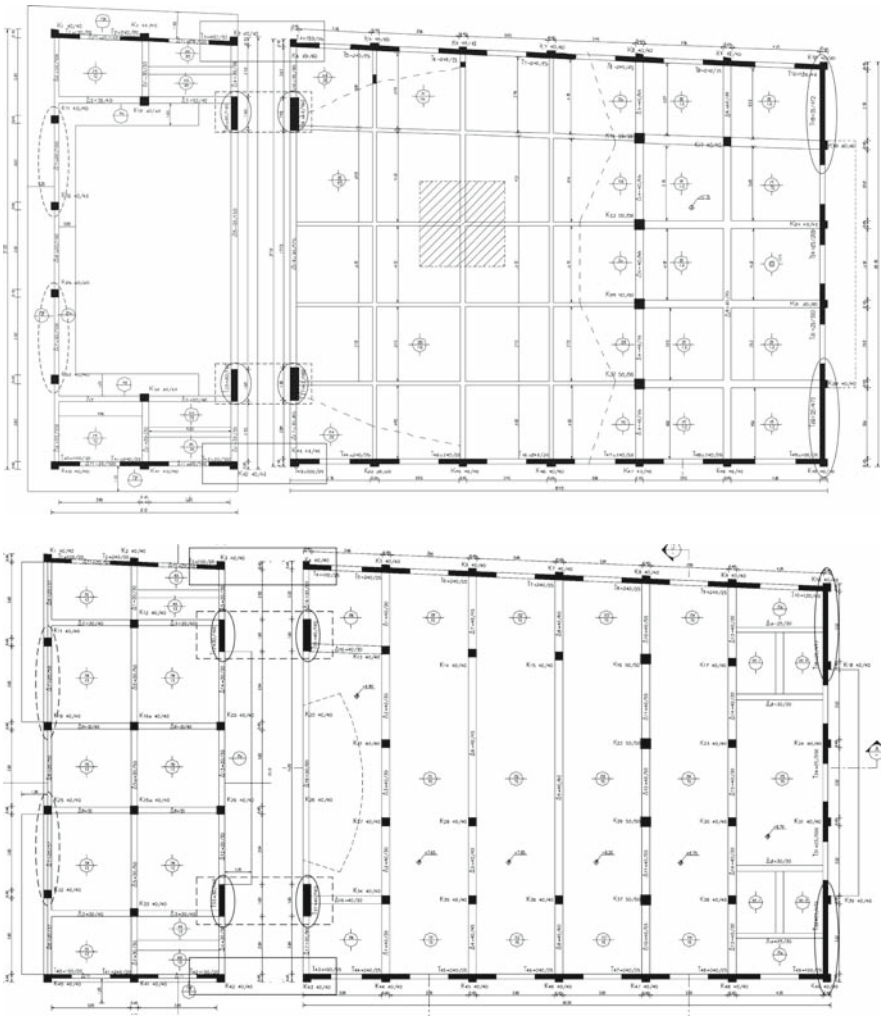

Fig. 4.18 Framing plan of the two-parts of the theatre facility. *Top*: roof; *bottom*: ground floor. *Left*: Stage part. *Right*: Theatre part (*Continuous-line ovals*: retrofitting with one-sided FRP; *dashed-line ovals*: added walls; *continuous-line rectangles*: jacketing into single wall across joint; *broken-line rectangles*: walls connceted with steel rods across joint; see Section 6.10.2)

motion is applied in the positive or in the negative sense, giving 8 orientations of the components of each bidirectional motion. So $7 \times 8 = 56$ nonlinear analyses have been carried out. The PGA level of 0.1 g has been chosen for the assessment of the as-built structure on the basis of pushover analyses with inverted triangular and 1st mode force patterns, which show that a seismic action with a PGA of 0.1 g in any of the two horizontal directions would cause violation of the limits specified in

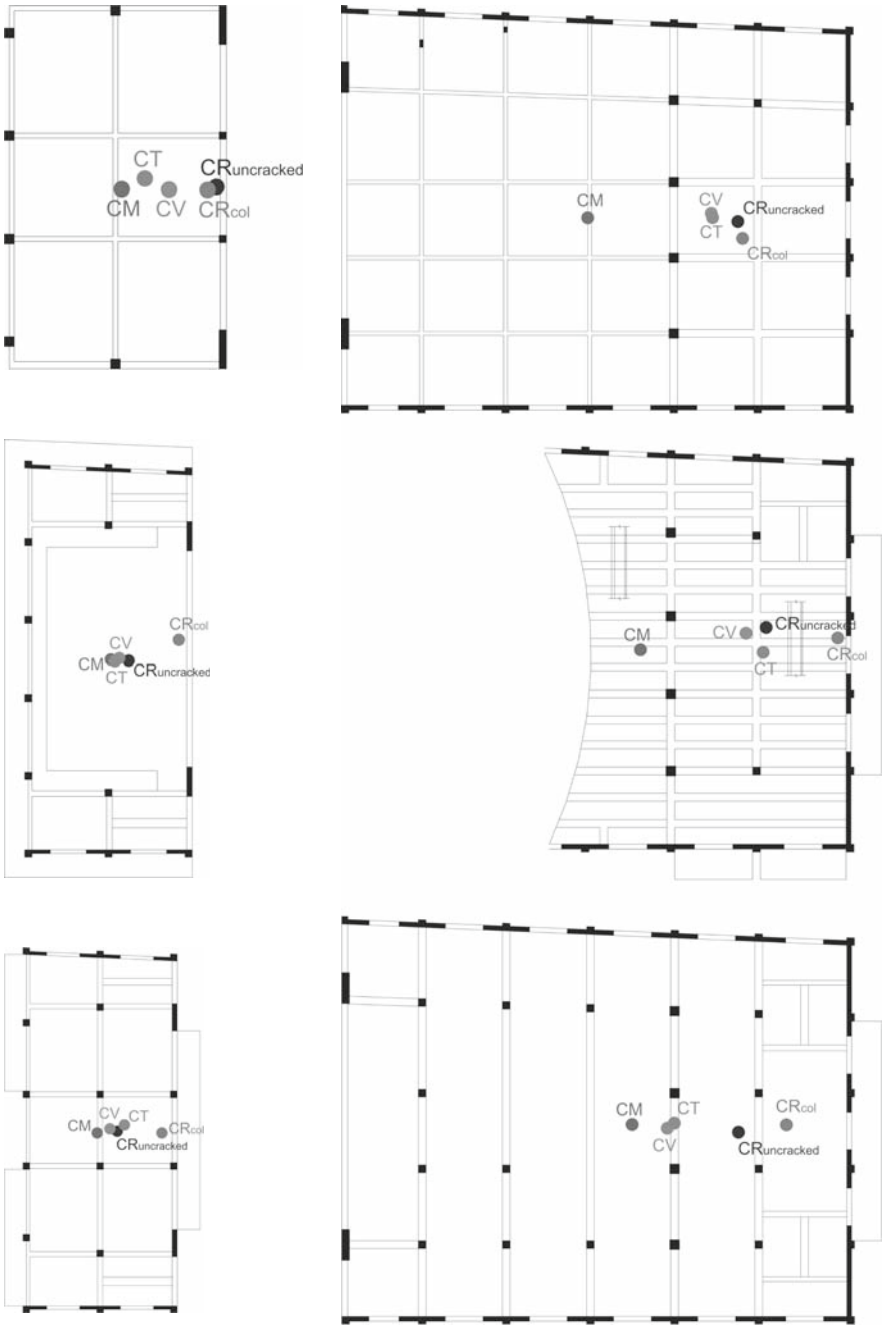

Fig. 4.19 Centres of mass (CM), stiffness (CR) or resistance (CV) and centre of twist (CT) at three levels of the stage (*left*) and the theatre (*right*) part of the theatre facility (Kosmopoulos and Fardis 2007)

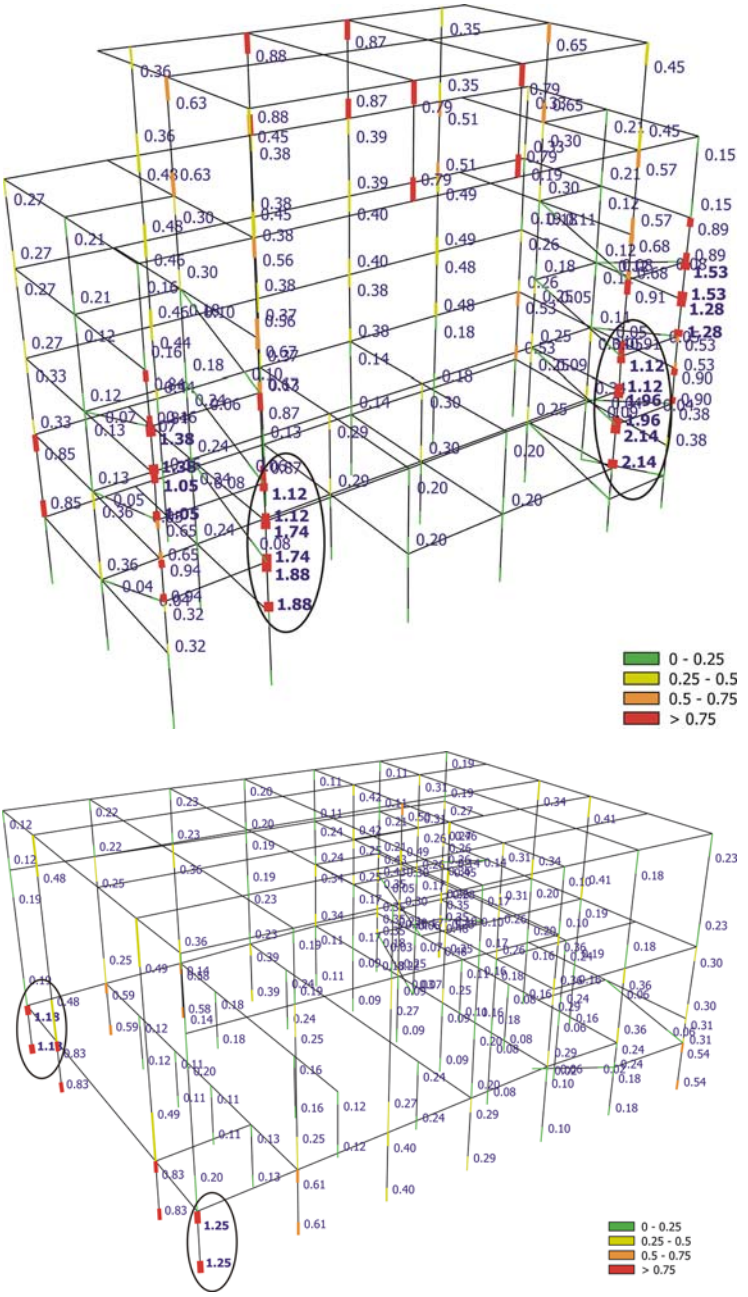

Fig. 4.20 Shear force demand-capacity-ratio (damage index) in vertical members of stage (*top*) and theatre (*bottom*) of as-built theatre facility (mean value over 56 bidirectional ground motions at PGA 0.1 g) (Kosmopoulos et al. 2007) (See also Colour Plate 14 on page 728)

Eurocode 8-Part 3 for Life Safety or Near Collapse in few members of both parts of the structure (Kosmopoulos et al. 2007).

The seismic response analyses follow the general modelling approach, points 1–11, of Section 4.10.5.1. Assumption no. 12 in Section 4.10.5.2 is also made. Vertical members are considered fixed at their connection with the foundation of the building (a two-way system of deep and heavy foundation beams for the theatre part, a basement-deep perimeter wall plus heavy two-way interior foundation beams at the stage part). Pounding between the two parts of the building at the vertical joint between them is neglected.

The shear force demand-capacity ratios (damage index) in Fig. 4.20 show that indeed a seismic action with a PGA of 0.1 g causes shear failures in two pairs of shear walls adjoining the expansion joint between the two parts of the building. The critical walls of the stage part are the two interior ones parallel to the joint. In the theatre part, critical are the two exterior walls at right angles to the joint. Twisting about a vertical axis near the side of the building opposite to the joint is one of the causes of shear failure at these locations. It is induced by the large eccentricity between the centres of stiffness (CR) or resistance (CV) or the centre of twist (CT) and the centre of overlying masses in the theatre part of the facility (Fig. 4.19, right).

Section 6.10.2 highlights the retrofitting of the building and the seismic response of the retrofitted structure.

4.11 Calculation of Displacement and Deformation Demands

4.11.1 Estimation of Inelastic Displacements and Deformations Through Linear Analysis

The prime role of seismic analysis for current force-based seismic design of new buildings is the estimation of seismic action effects in terms of internal forces, for use in force-based dimensioning or verification of members. As pointed out in Sections 1.2 and 4.1.2, linear-analysis, based on a 5%-damped elastic spectrum divided by the "behaviour factor" q of European codes or the "Force reduction" or "Response modification" factor R of US codes, is presently considered to serve well this end. Seismic displacement and deformation demands enter in member dimensioning and detailing only in an average sense and indirectly, via the ductility ratio, global or local, that determines the value of q (or R) for the estimation of seismic internal forces or the member detailing requirements, respectively. Their absolute magnitude is needed only for the calculation of P-Δ effects (see Section 4.9.7), the checks of interstorey drifts limits (e.g., for Eurocode 8 those listed in Section 1.1.3 under (i)–(iii)) and of the clearance between adjacent structures to avoid pounding, etc. These aspects are of secondary importance in force-based design of new buildings. So, an approximate estimation of seismic displacement demands seems sufficient.

In Eurocode 8 (CEN 2004a) the equal displacement rule suffices for the estimation of seismic displacements in the design of new buildings. In the period range where the design spectrum is not inversely proportional to q (notably up to the first corner period T_B, see Eq. (4.5a) in Section 4.2.2) the computed displacements are the elastic ones, as obtained from the elastic spectrum. For longer periods, displacement results of linear analysis for the 5%-damped elastic spectrum divided by the q-factor are back-multiplied by q. Eurocode 8 (CEN 2004a) allows National Annexes to refine the displacement calculation rules, e.g., through a q-μ-T relation, such as that of Eqs. (1.1) and (1.2) in Section 1.2.

In US codes for the design of new buildings displacements are calculated by back-multiplying the results of a linear analysis with the 5%-damped elastic spectrum divided by R, not by the full value of R but by $0.7R$ (SEAOC 1999), or by a value between about $0.7R$ (for systems with high R-values) and R (for low R-values) (BSSC 2003).[30]

The equal displacement rule, with variants such as Eqs. (1.1) and (1.2) in Section 1.2, is a well established approximation of the global displacement demand in a bilinear SDOF system, be it an equivalent one in the sense of Section 4.6.1.3 and Eqs. (4.13), (4.14) and (4.15) therein. However, its universal extension down to the level of nodal displacements and member deformations, just on grounds of their secondary importance in the context of force-based seismic design, may not be warranted. Implicit in this extension is the presumption of inelastic deformation demands spreading throughout the structural system. Indeed, codes for the seismic design of new buildings make every effort to prevent concentration of these demands in few members or locations (notably in a single "soft" storey): by providing a stiff and strong vertical spine over the full height of the building, by controlling the location of plastic hinges and the inelastic response mechanism through an imposed hierarchy of strengths and by guiding the designer towards a favourable structural layout. One of the returns is the permission to apply the equal displacement rule at the level of nodal displacements and member deformations. Indeed its applicability has been confirmed in Panagiotakos and Fardis (1999a) on the basis of over one thousand nonlinear dynamic response analyses of several planwise symmetric multistorey buildings designed in full accordance with the ENV-Eurocode 8.

The situation is very different in seismic assessment of existing substandard buildings. These buildings do not have an engineered hierarchy of strengths to spread inelastic deformation demands throughout the structure. Instead, their structural layout often promotes concentration of these demands in few members or locations. Moreover, in seismic assessment and retrofitting, which is nowadays fully displacement-based, member deformation demands are not anymore 2nd-class outcomes of the analysis but have the prime role in member verifications. So, they

[30]Except in the calculation of P-Δ effects, for which US codes use the displacements from the linear analysis with the 5%-damped elastic spectrum divided by R, without removing at all the effect of R (see Section 4.9.7).

should be estimated as reliably and accurately as practically feasible. For these reasons, recent codes for seismic assessment and retrofitting (ASCE 2007, CEN 2005a) are more prudent than those for new designs. They allow estimation of inelastic member deformation demands through linear analysis only when their variation between different members or locations is within certain limits:

- According to Part 3 of Eurocode 8 (CEN 2005a), linear analysis is applicable for the estimation of deformation demands in structural members, if the distribution of ductility demands over the *entire structure* is fairly uniform. A conveniently computed measure of the local ductility demand is employed: the demand-to-capacity ratio, D/C, in *flexure*, where D is the bending moment at the end of a member due to the seismic action and the concurrent gravity loads from elastic analysis and C the corresponding moment resistance. Note that, if the equal displacement rule indeed applies, D/C is about equal to the demand value of the chord-rotation ductility ratio, μ_θ. For linear analysis to be applicable, the maximum D/C-ratio in all "primary seismic" elements (defined and discussed in Section 4.12) should not exceed by more than a factor of about 2.5 its minimum value over those having $D/C > 1$.[31] D/C is taken not to exceed 1 (elastic response) at those sections around beam-column joints where the comparison of the sum of beam moment resistances, ΣM_{Rb}, to that of the columns, ΣM_{Rc}, precludes plastic hinging. No limit is set on the absolute magnitude of D/C for the applicability of linear analysis. However, there will always be an end section or two in the whole structure where plastic hinging will marginally be predicted, with a value of D/C a little over 1.0. So, the relative limit on the value of D/C is essentially an absolute one. In this respect the limitation on the basis of the D/C-ratio is quite restrictive for those Limit States where inelastic response is allowed. However, we will see in Section 4.11.2 that this restriction is not fully supported by hard evidence. Anyway, if this criterion is met (CEN 2005a) allows estimation of nodal displacements and member deformations through linear analysis with the 5%-damped elastic spectrum. If, in addition, both conditions (a) and (b) in Section 4.3.1 are met (CEN 2005a) allows using linear static analysis ("lateral force" procedure), instead of modal response spectrum analysis.
- The US Standard for seismic rehabilitation (ASCE 2007) uses as a criterion the maximum value of the elastic *internal force* demand (due to the seismic action and the concurrent gravity loads) to the corresponding capacity, *DCR*, throughout an "element". In this case an "element" is not just a single structural member, but a subsystem of the lateral-force resisting structure, such as a wall or plane frame. Estimation of deformation demands from linear analysis with the 5%-damped elastic spectrum is allowed, if the nonlinearity of the response is

[31] As a matter of fact, the value of this factor may be determined nationally within the range 2 to 3, as a Nationally Determined Parameter. 2.5 is the value recommended in Eurocode 8 (CEN 2005a).

either limited overall, or uniformly distributed throughout the structure. More specifically, either one of the following two conditions should be met:

(a) the maximum *DCR* value over the entire structure does not exceed 2.0, or
(b) all three of the following conditions are met:

1. all "primary" walls and plane frames of the building continue throughout its height, without out-of-plane offsets;
2. the weighted-average *DCR* of the "elements" in a storey, using as weight the (seismic) shear force of the "element", does not differ by more than 25% from that of an adjacent storey (to avoid a weak storey);
3. the "element" *DCR* does not increase from one side of the storey's centre of resistance to the other by more than 50% (for torsionally balanced strength).

The criteria in ASCE (2007) are harder to check or meet than those in CEN (2005a), as they use the demand-to-capacity ratio in the most critical internal force of a subsystem, which assumes more extreme values than the corresponding ratio in flexure alone.

4.11.2 Evaluation of the Capability of Linear Analysis to Predict Inelastic Deformation Demands

Panagiotakos and Fardis (1999a) have confirmed that linear analysis with the 5%-damped elastic spectrum provides indeed an acceptable approximation of inelastic chord rotation demands in planwise symmetric multistorey (and in most cases very regular in elevation) concrete buildings designed to the ENV-Eurocode 8, under unidirectional ground motions up to twice the design seimic action. However, what is at issue is the applicability of linear analysis for the prediction of inelastic deformation demands in existing buildings with poor structural layout, including strong irregularities in plan and/or elevation and subjected to bidirectional ground motions. This question has been addressed in Kosmopoulos and Fardis (2007) and Fardis and Kosmopoulos (2007), using as testcases the substandard and irregular buildings of Section 4.10.5, including as separate cases the unretrofitted and the partly concrete-jacketed versions of the SPEAR building and the two parts of the theatre facility. Like those in Panagiotakos and Fardis (1999a), these buildings are typical of multistorey concrete ones in that their 1st and 2nd mode periods are in the velocity-controlled part of the spectrum, $T_C < T < T_D$, where the equal displacement rule is considered to apply well for SDOF systems (see Eq. (1.1)). Nonlinear response-history analyses of these buildings have been carried out under the suite of 56 bidirectional ground motions described in Section 4.10.5.3 in connection with the theatre facility, with each component comforming to the smooth 5%-damped elastic response spectrum in Eurocode 8 for soil type C. The PGA of the motions

applied to the two versions of the SPEAR building increased from 0.15 to 0.3 g in steps of 0.05 g, to study the effect of motion intensity. The motions applied to the "Athens" building of Sections 2.4.2 and 4.10.5.3 and Figs. 2.21, 2.22 and 2.23 and to both parts of the theatre facility of Section 4.10.5.3 and Fig. 4.18 have a PGA of 0.15 and 0.1 g, respectively.

The results of the nonlinear response-history analyses of these buildings were compared to those of:

- linear static analysis according to Section 4.3, except that in Eq. (4.6) $m_{\text{eff},1}$ was taken equal to the full mass, m, and not reduced to $0.85m$, as allowed in CEN (2004a, 2005a), and
- modal response spectrum analysis in 3D according to Section 4.4, with CQC combination of peak modal responses (Eq. (4.11)).

Member stiffness in the linear analyses was equal to the corresponding elastic stiffness in the nonlinear ones (i.e., from Eq. (3.68)). The smooth 5%-damped Eurocode 8 elastic spectrum, to which the individual components of the suite of 56 bidirectional ground motions of the nonlinear response-history analysis are compatible, has been applied separately in horizontal directions X and Y. Member chord rotations from the separate analyses in X and Y were combined via the rigorous SRSS rule, Eq. (4.24). The oucome was added or subtracted from that due to the concurrent gravity loads, giving an elastic estimate of the chord rotation, θ_{el}, to be compared to the average over the 56 nonlinear response-history analyses of the peak inelastic chord rotation at the same member end, θ_{inel}. The conclusions of the comparison are the following:

- For elastic chord rotations estimated through modal response spectrum analysis, the average $\theta_{\text{inel}}/\theta_{\text{el}}$ ratio is overall very close to 1.0. When linear static analysis is used, the building-average $\theta_{\text{inel}}/\theta_{\text{el}}$ ratio is systematically less than 1.0; from a few percent to one-third in the different building cases, but giving an overall average value of 0.835 for $\theta_{\text{inel}}/\theta_{\text{el}}$ (very close to the factor of 0.85 given by CEN (2004a) for $m_{\text{eff},1}/m$ in Eq. (4.6), with only slight upwards deviations in the two out of the five buildings that indeed violated the Eurocode 8 condition of $T_1 < 2T_C$ for $m_{\text{eff},1}/m = 0.85$, see Section 4.3.2). Note, however, that the average $\theta_{\text{inel}}/\theta_{\text{el}}$ ratio in the various regular and fully symmetric multistorey buildings in Panagiotakos and Fardis (1999a) under unidirectional ground motions was equal to 1.07, both for modal response spectrum and linear static analysis. Provided, therefore, that the outcomes of separate linear analyses in X and Y are combined through the SRSS rule, Eq. (4.24), peak inelastic chord rotations are overall better estimated by their linear counterparts in real situations of geometry and loading in 3D than in rather idealised cases of near-perfectly regular and symmetric buildings under one-component seismic actions.

- The building-average inelastic-to-elastic-chord-rotation-ratio decreases with increasing PGA, despite the spreading of inelasticity and the increase of its magnitude, but the scatter of individual results increases.
- The storey-average $\theta_{inel}/\theta_{el}$ ratio does not systematically depend on elevation in the building. If elastic chord rotations are estimated via static analysis, there is a weak tendency of the storey-mean to increase on average from the base to the roof; but when modal response spectrum analysis is used instead, this tendency is weakened further or sometimes reversed.
- Linear static analysis does not produce as heightwise uniform a value of $\theta_{inel}/\theta_{el}$ as modal response spectrum analysis, especially when higher modes are important, as in the "Athens" building of Sections 2.4.2 and 4.10.5.3 and Figs. 2.21, 2.22 and 2.23. However, it gives more consistent results (i.e., with lower scatter within a storey) than modal response spectrum analysis for the beams and the two different axes of column bending. Only in the "Athens" building, for which higher modes are important, did modal response spectrum analysis produce lower scatter of individual $\theta_{inel}/\theta_{el}$ ratios in a storey than linear static analysis. In all other buildings linear static analysis gave much more uniform $\theta_{inel}/\theta_{el}$ ratios within a storey than modal response spectrum analysis. Note that this latter method is the only type of linear analysis allowed by Eurocode 8 for the "Athens" building and the two parts of the theatre facility, owing to their heightwise irregularity and for the "Athens" building to its long 1st and 2nd mode periods as well.
- Column $\theta_{inel}/\theta_{el}$ ratios are very consistent between top and bottom of the storey for the same axis of bending, regardless of the type of linear analysis.
- The pattern of deviations of individual $\theta_{inel}/\theta_{el}$ ratios in the various member types of each building, with respect to the storey-average for that member type, suggests a tendency of linear static analysis to overestimate inelastic torsional effects at the flexible side(s) and the central part of the torsionally flexible buildings (i.e., those violating Eq. (2.6)) and underestimate them at the stiff side(s). There is no clear trend in this respect for the torsionally stiff buildings. By contrast, the tendency of modal response spectrum analysis is to overestimate inelastic torsional effects at the stiff side(s) and the central part of the torsionally stiff buildings and underestimate them somewhat at the flexible side(s). This trend is less clear in the torsionally flexible buildings.
- In every single case the *D*/*C* (or *DCR*) values (with elastic demands, *D*, from the separate analyses in X and Y combined via the SRSS rule, Eq. (424)) violate the applicability criteria of ASCE (2007) or CEN (2005a) for the estimation of inelastic deformation demands at member ends through 5%-damped linear analysis.

The overall conclusion of the comparative analyses is that elastic modal response spectrum analysis with 5% damping gives on average unbiased and fairly accurate (within a few percent) estimates of member inelastic chord rotation demands

in multistorey concrete buildings typical of existing substandard construction. This might be taken to mean that there is room for revisiting and possibly relaxing the relevant criteria in ASCE (2007) or CEN (2005a), in order to allow wider use of 5%-damped elastic analysis for estimation of member inelastic chord rotation demands.

4.12 "Primary" V "Secondary Members" for Earthquake Resistance

4.12.1 Definition and Role of "Primary" and "Secondary Members"

Most current seismic codes recognise that certain structural members may have a secondary role and contribution to earthquake resistance. The main goal of the distinction of these "secondary members" from the rest, termed "primary", is to allow a certain simplification of the seismic design, assessment or retrofitting:

- In the design of new buildings, the contribution of "secondary members" to stiffness and resistance against seismic actions is not included in the structural model for the seismic analysis. The building structure is taken in design to rely for its earthquake resistance only on its "primary members". Only them are designed and detailed for earthquake resistance, in accordance with all the relevant rules in the seismic design code. "Secondary members" are fully considered and designed for the non-seismic actions and are subject to special verifications under the design seismic action and the concurrent gravity loads (see Section 4.12.3).
- In seismic assessment and retrofitting of existing buildings we accept more severe seismic damage in "secondary members", as they are less important for the performance and safety of the whole. Accordingly, their verification criteria for the seismic action are relaxed compared to those of "primary members". According to Eurocode 8 (CEN 2005a) in existing or retrofitted buildings the contribution of "secondary members" to stiffness and resistance against seismic actions should be neglected in the model for linear seismic analysis, like in new buildings, but should be included in a nonlinear analysis model.[32] Note, however, that, unless "secondary members" are fully included in the model for the seismic actions, it is not easy to check whether they meet their (relaxed) compliance criteria (see Section 4.12.5).

The classification of members into "primary" and "secondary" (as they are called in CEN 2004a, 2005a, ASCE 2007) is equivalent to the old-time distinction in US

[32] According to (ASCE 2007), cyclic degradation of strength and stiffness shoud be accounted for in the model of "secondary members" for a nonlinear analysis, while it may be disregarded for "primary members".

seismic design codes for new buildings (BSSC 2003, SEAOC 1999) of members which are part of the lateral- (or seismic) force-resisting system from those that are not. In Eurocode 8 (CEN 2004a, 2005a) the qualification "seismic" has been added to "primary" or "secondary", to make it clear that the differentiation applies only for the seismic action.

4.12.2 Constraints on the Designation of Members as "Secondary"

Besides the vague feature that it is not part of the lateral-load-resisting system, there is no precise definition of a "secondary member". It is up to the designer to decide which members, if any, he/she may consider as "secondary". To establish a limit to the discretion of the designer of a new building, Part 1 of Eurocode 8 (CEN 2004a) gives three conditions to be met:

1. The total contribution to lateral stiffness of all "secondary members" should not exceed 15% of that of all "primary" ones. Unless it is obvious that this condition is met (e.g., through back-of-the-envelope calculations on the basis of moments of inertia of vertical elements, or when the "secondary members" are few and/or truly secondary), to check it the designer should carry out two analyses per horizontal component of the seismic action. One including and another neglecting the contribution of "secondary members" to lateral stiffness (see Section 4.12.5). For the condition to be met, storey drifts computed from the latter analysis should be less than 1.15 times those from the first one.
2. The characterisation of some of the structural members as "secondary" should not change the classification of the structure from irregular to regular. As outlined in Sections 2.1.5, 2.1.6, 2.1.7 and 2.1.8, most Eurocode 8 regularity criteria – both in plan and in elevation – are qualitative and can be checked by inspection without analysis of the structural system for the seismic action. As far as regularity in elevation is concerned, this condition implies that (see Sections 2.1.7 and 2.1.8):

   (i). if a frame, column or wall does not continue throughout the full height of the relevant part of the building, it cannot be classified as "secondary"; and
   (ii). if in a frame buildings there is an abrupt change in the storey overstrength – as measured by the ratio of the sum of lateral force capacities of vertical elements and of masonry infills to the design storey shear – the overstrength variation cannot be smoothened out by classifying some vertical elements as "secondary".

As far as regularity in plan is concerned, this condition implies that, classification of some vertical elements as "secondary":

(i). does not reduce the eccentricity between any storey's centres of mass and stiffness from more than 30% of the storey torsional radius to less (see Section 2.1.5), and

(ii). will not increase the torsional radius in any direction from less than the radius of gyration of the masses to more (see Section 2.1.6).

3. "Secondary members" should meet the special requirements applying to them (see Section 4.12.3).

According to Part 3 of Eurocode 8 (CEN 2005a), seismic assessment and retrofitting of *existing buildings* is still subjected to the 2nd condition above, but not to the 1st one. Moreover, instead of the special requirements of Section 4.12.3, "secondary members" should meet the same verification criteria as "primary" ones, albeit with less conservative estimates of their capacities (see Section 6.5.6).

4.12.3 Special Design Requirements for "Secondary Members" in New Buildings

"Secondary members" of new buildings do not have to meet the rules and requirements of seismic design codes for dimensioning and detailing of structural members for earthquake resistance through energy dissipation and ductility. They only need to satisfy code rules for design for non-seismic actions and the additional requirement to maintain support of gravity loads under the most adverse displacements and deformations induced by the design seismic action applied together with the concurrent gravity loads. These seismic deformation demands are determined according to the equal displacement rule, on the basis of the results of normally two linear analyses per horizontal component of the design seismic action:

1. one neglecting the contribution of "secondary members" to lateral stiffness (see Section 4.12.5.1 for guidance), and
2. another including it.

The effect of the behaviour factor, q, is removed then according to Section 4.11.1 from the seismic deformations resulting from analysis no. 2 and the outcome is multiplied by the ratio of the interstorey drifts in the storey from analysis no. 1 to those of no. 2, to give our estimate for the seismic deformation demands in the "secondary members" when their contribution to lateral stiffness is ignored. If the value of the sensitivity ratio θ (from Eq. (4.45) in Section 4.9.7) exceeds 0.1, the 1st-order values should be divided by $(1–\theta)$ to account for 2nd-order (P–Δ) effects

According to Part 1 Eurocode 8 (CEN 2004a), internal forces (bending moments and shears) in "secondary members" calculated from their cracked stiffness (taken equal to the default value of 50% the gross, uncracked section stiffness) and the deformations induced by the design seismic action and computed according to the previous paragraph, should not exceed the design value of their flexural and shear resistance, M_{Rd} and V_{Rd}, respectively, when applied together with the concurrent gravity loads. This severely penalises "secondary members", as it requires them to remain elastic under the design seismic action. It amounts to an overstrength factor

of q in "secondary members" relative to the "primary" ones, if the strength of both is governed by the design seismic action and the concurrent gravity loads. Verification of "secondary members" on the basis of these requirements may not be feasible, unless:

- the global stiffness of the system of "primary members" and its connectivity to the "secondary" ones is such that seismic deformations imposed on the latter are low; or
- the lateral stiffness of "secondary members" is indeed very low.

4.12.4 Guidance on the Use of the Facility of "Secondary Members"

4.12.4.1 Seismic Design of New Buildings

A prime reason for the designer to consider as "secondary" some of the members of a new building designed for ductility, is when they are not within the scope of the rules for seismic design based on energy dissipation and ductility. For instance, flat slab frames and post-tensioned girders are not covered by seismic design codes. So, when using them, the designer may have to resist the full seismic action with walls or strong frames (usually at the perimeter), designating the flat slabs, the post-tensioned girders, as well as their supporting columns, as "secondary members". In a frame or frame-equivalent dual system, the columns supporting post-tensioned girders would better be taken as "secondary" anyway, because normally the large size of prestressed girders makes it unfeasible to satisfy Eq. (1.4). Moreover, such columns should have as small a cross-section as necessary for the support of gravity loads, to reduce the "parasitic" shears developing in them during post-tensioning at the expense of the axial force in the girder.

The designer may also want to consider as "secondary" those members of a new building that – owing to architectural constraints – cannot be made to conform to the seismic design rules for geometry, dimensioning or detailing for energy dissipation and ductility. Examples in DC M or H buildings designed according to Part 1 of Eurocode 8 (CEN 2004a) are beams which:

- are connected to a column at an eccentricity of the centroidal axes more than 25% of the largest cross-sectional dimension of the column at right angles to the beam, b_c, which is the limit specified in CEN (2004a);
- are supported on a column with cross-sectional depth, h_c, in the direction of the beam axis that cannot be made to satisfy the Eurocode 8 rule for bond and maximum diameter of the top bars of the beam within the joint (see Sections 3.3.2 and 5.4.1);
- have a width, b_w, greater than b_c plus the minimum of b_c or the depth of the beam, h_w, violating the relevant restriction in CEN (2004a);

– have top reinforcement (as governed by the combination of factored gravity loads) that cannot comply with the maximum allowed reinforcement ratio (see Section 5.3.2);
– connect two closely spaced columns, having a capacity-design shear from Eq. (1.9a) in Section 1.3.6.2 which is so large owing to the small clear span, L_{cl}, that the beam cannot be verified against the shear resistance for diagonal compression in the web, $V_{Rd,max}$; or, in a DC H building, the value of the ratio ζ_i in Eq. (1.10) of Section 1.3.6.2 is so close to –1, that the diagonal reinforcement required in the beam is too much to place.

Unlike the cases which are outside the scope of design rules for energy dissipation and ductility, those of the type above should preferably be accommodated through proper selection of the local structural layout, instead of resorting to the facility of "secondary members". There are two good reasons for doing so:

– The earthquake "sees" the structure as built, neither "knowing" much, nor "caring" about the considerations and assumptions made in its design calculations. So, the "primary members" may perform well thanks to their ductility, but the "secondary" ones may suffer serious damage.
– A structural system that cannot be utilised in its entirety for the engineered earthquake resistance of the building is a waste of resources. This is more so, given the conservatism of the special design requirements for "secondary members" (see Section 4.12.3).

That said, the option of designing the entire structural system for strength, instead of ductility (see Section 1.4.1) could be considered. In the framework of Eurocode 8, this means selecting DC L (Low) and $q = 1.5$. Then a distinction between "secondary" and "primary" members does not need to be made, as all members can be designed and detailed according to Eurocode 2 for non-seismic actions, without any regard to the special detailing and dimensioning rules of Eurocode 8 (CEN 2004a) for energy dissipation and ductility.

4.12.4.2 Seismic Assessment or Retrofitting

Unlike in the design of new buildings, where it may create more problems than it solves, the facility of "secondary members" can be used to advantage in seismic assessment and retrofitting of existing buildings. The designer may designate at the outset of the assessment (almost) all members as "primary" and, depending on the outcome of the verifications, consider whether few elements that (marginally) violate the verification criteria for "primary members" have reduced importance for seismic safety and performance to justify downgrading them to "secondary members", so that they can be checked with the relaxed pertinent criteria. In the framework of Part 3 of Eurocode 8 (CEN 2005a), the designer can do so free of constraints on the contribution of "secondary members" to the overall lateral stiffness (i.e., of condition no. 1 in Section 4.12.2, which applies only to new buildings). Besides, if

the structural model used from the outset is retained, there is no need to re-do the analysis with a new model either of the structure as a whole, or with its "primary members" alone.

The facility of "secondary members" is even more convenient for the retrofitting. It can be used to retrofit the structure by upgrading the earthquake resistance of only certain major existing elements and/or by adding a few new but large ones (e.g., concrete walls). The upgraded and/or the new elements may then be designed to take almost the full seismic action. They will be verified with the stricter criteria applying to "primary members", while the rest will be allowed to stay with their substandard detailing and poor earthquake resistance, if they meet the lax criteria for "secondary members". This may turn out to be a very cost-effective retrofitting strategy, as it allows limiting the disruption, including collection of information about the material properties and reinforcement of the as-built structure, to a small part of the building where the intervention takes place.

4.12.5 Modelling of "Secondary Members" in the Analysis

4.12.5.1 Modelling for the Design of New Buildings

In seismic design of new buildings based on linear analysis the strength and stiffness of "secondary members" against lateral loads is neglected in the analysis for the seismic action, but it may be considered in that for all other actions (e.g. gravity loads). Then, two different structural models may be used for the linear analysis (see also analysis types no. 1 and 2 in Section 4.12.3):

1. A model that completely neglects the contribution of "secondary members" to lateral stiffness.
2. Another which includes fully the "secondary members".

As pointed out in Section 4.12.3, the seismic deformation demands in the "secondary members" may then be obtained in a two-step procedure:

I. The elastic deformation demands in the "secondary members" due to the design seismic action are estimated from a linear seismic analysis using Model no. 2 (with the design spectrum, but removing afterwards the effect of the behaviour factor, q, from displacements and deformations according to Section 4.11.1).
II. The outcome of the Step I for storey i is multiplied by the ratio of interstorey drifts in that storey using Model no. 1 in the linear analysis for the design seismic action to those using Model no. 2.

Using two different structural models is not convenient, especially if linear analysis and design take place in an integrated computational environment. Among other problems, we have to use in the verifications:

- seismic action effects from an analysis with Model no. 1 (with seismic deformation demands in "secondary members" modified according to the paragraph above) and
- action effects of the concurrent gravity loads coming from an analysis with Model no. 2.

If we don't need to design the building for another lateral action, e.g., wind, it may be possible to use in some cases a single structural model for the seismic action and for gravity loads, namely one in which "secondary members" are included only with those properties that are essential for their gravity-load-bearing function. In such a model "secondary" columns and walls may be considered only with their axial stiffness and with zero flexural rigidity, or with moment releases (i.e., hinges) introduced between their ends and the joint they frame into. Such an approximation is acceptable, so long as the bending moments and shears induced in these members by gravity loads are negligible and their axial forces due to the seismic action also small. This precludes vertical elements on the perimeter of the building from such treatment. It is not good practice, anyway, to consider such members as "secondary".

If a single model is used for the seismic action and gravity loads according to the previous paragraph, "secondary" beams cannot in general be modelled with zero flexural rigidity or moment releases at the nodes, because this rigidity and the continuity of their spans are essential for their gravity-load bearing function. If they are not directly supported on vertical elements at all (e.g., when they are supported on girders), their seismic action effects will be negligible anyway, even when they are included in the model with their full flexural stiffness and connectivity. "Secondary" beams which are directly supported on vertical elements and continuous over two or more spans should be modelled with their full flexural stiffness. Their connectivity with the vertical elements depends on whether the latter are also "secondary" or not. If they are, zero flexural rigidity of these "secondary" vertical members, or moment releases at their connections with the beam-column joint are satisfactory also for the "secondary" beams they support. If the vertical elements are "primary", then two separate nodes can be introduced at the beam-column joint with pin connection between them: one node for the beam and another for the vertical element. The beam and the vertical element that continue past the joint will resist with their full flexural stiffness the gravity loads or the seismic action, respectively.

Note that, if a single structural model is used for the seismic action and for gravity loads along the lines of the two paragraphs above, internal forces in "secondary members"due to their seismic deformation demands can be estimated only by ad-hoc and approximate procedures for the verifications according to Section 4.12.3. For example, for a frame of "secondary" beams and/or columns, one may use the seismic interstorey drifts in the plane of the frame computed from the single model, remove from them the effect of the q-factor according to Section 4.11.1, use the corrected values as $\Delta\delta_i$ in Eq. (2.8) and solve for the column average seismic shear in that storey. If the columns of the frame have different moments of inertia, the total storey seismic shear in the frame is computed from the column average shear (with a weight of 0.5 on exterior columns) and back-distributed to the frame columns

in proportion to their moment of inertia. Individual column shears may then be multiplied by the clear column height to estimate the column end moments. The sum of these column seismic moments above and below a joint may then be distributed to the ends of the beams framing into the joint in inverse proportion to their span. The whole thing is as onerous as it sounds, especially as it is difficult to set it in a computational framework and most calculations may have to be done by hand or with spreadsheets.

It may be argued that, for damage limitation checks on the basis of interstorey drifts the contribution of "secondary members" to lateral stiffness may be considered in the linear analysis, as it is very unlikely that seismic deformations under the damage limitation seismic action will jeopardise their lateral stiffness and strength. However, seismic design codes do not differentiate the structural model to be applied in the analysis for the damage limitation seismic action from the one used for the design seismic action. Besides, for the designer's convenience, normally a single linear analysis is required for both levels of the seismic action. Analysis results for the damage limitation action are computed then by multiplying those for the design seismic action by the ratio of peak ground accelerations of the two actions. So, the contribution of "secondary members" to lateral stiffness should be neglected also at the damage limitation verifications.

4.12.5.2 Modelling for Seismic Assessment or Retrofitting

There is no real requirement to differentiate the modelling approach for "secondary members" from the normal one used for "primary" in seismic assessment and retrofitting. First of all, an analysis that neglects their contribution to stiffness against lateral loads (as Part 3 of Eurocode 8 allows doing for linear analysis) cannot determine the seismic deformation demands against which the capacities of "secondary members" should be verified (see Section 6.5.6). If the cyclic degradation of strength and stiffness is thought to be indeed much larger in "secondary members" than in "primary" ones,[33] it can be included in a nonlinear model. This can be done through a post-yield branch of the force-deformation curve in primary loading that is descending (with negative slope), instead of hardening or horizontal. If nonlinear dynamic analysis is used, the hysteresis rules may include degradation of strength with cycling, as in Park et al. (1987), Reinhorn et al. (1988), Coelho and Carvalho (1990), and Costa and Costa (1987).

[33]Note that, unless they are retrofitted, even the "primary members" of an existing substandard structure have larger cyclic degradation of strength and stiffness than a new member well designed and detailed for ductility.